UNIVERSITY OF ALBERTA

ANALYSIS OF TRANSIENT RESPONSES OF STEAM FLOW IN POWER PLANT PIPING NETWORKS

BY

MICHAEL W. KOHLENBERG ©

A thesis submitted to the Faculty of Graduate Studies and Research in partial fulfillment of the requirements for the degree of

MASTER OF SCIENCE

IN

PROCESS CONTROL

DEPARTMENT OF CHEMICAL ENGINEERING

Edmonton, Alberta

Spring, 1993

ISBN 0-315-82046-2

UNIVERSITY OF ALBERTA

RELEASE FORM

NAME OF AUTHOR: Michael W. Kohlenberg

TITLE OF THESIS: Analysis of Transient Responses of Steam Flow in Power Plant Piping Networks

DEGREE: Master of Science

YEAR THIS DEGREE GRANTED 1993

(SIGNED) M. Kohlenberg

PERMANENT ADDRESS:
Box 82
Bateman, Saskatchewan
SOH OEO

DATED April 15, 1993

UNIVERSITY OF ALBERTA

FACULTY OF GRADUATE STUDIES AND RESEARCH

The undersigned certify that they have read, and recommend to the Faculty of Graduate Studies and Research for acceptance, a thesis entitled **Analysis of Transient Responses of Steam Flow in Power Plant Piping Networks** submitted by **Michael W. Kohlenberg** in partial fulfillment of the requirements for the degree of **Master of Science** in **Process Control.**

Dr. R. K. Wood (Supervisor)

Dr. J. T. Ryan

W. Finlay

Dr. W. Finlay

Date March 18, 1993

To my parents.

Abstract

The development and numerical solution, utilizing the method of characteristics, of a dynamic mathematical model to describe the steam distribution network within the University of Alberta Heating Plant has been completed. This model consists of two first order partial differential equations to describe the pressure and flow characteristics of the steam. The steam distribution network consists of 5 boiler supply sources, 9 pressure reducing valves, 4 desuperheaters, and two exit nodes. Nineteen separate pipes with three nominal operating pressures of 6205, 2760, and 1035 kPag which connect the boilers, valves, desuperheaters, and exit nodes. These pipes have diameters ranging from 0.2 to 0.6 metres with equivalent lengths of 12 to 290 metres Results predicted by the simulator are verified through comparison with data collected in the Heating Plant steam line network and with published results. The simulator is then used to predict the transient pressures caused by a steam turbine trip.

Comparison of the simulator predictions with data collected from the Heating Plant steam line network showed that the pressure reducing valves were the dominant component in the model. The valve dynamics for certain valves in the system need to be included in the model. Simulator predictions were compared with published results for a steam turbine trip and from a transient occurring in a small natural gas pipeline network. The published results for the steam turbine trip utilized an adiabatic pipe model, while this work utilized an isothermal pipe model. Comparison with the published turbine trip results illustrated that the simpler isothermal pipe model was sufficient to model this type of transient. Simulator predictions compared with published results from transients occurring in the natural gas distribution network showed that using an average wave speed, obtained from averaging the wave speeds in each section of the network, was a valid simplification even when the wave speed within the individual sections within the network were highly variable.

Simulator predictions of the maximum pressure recorded during a steam turbine trip were made. It was found that for a constant boiler loading the maximum pressure in the network was a function of both turbine loading and the closing time of the stop valve. Higher loading of the turbine and quicker closing of the turbine stop valve produced larger pressure transients.

Acknowledgements

Many individuals assisted in the completion of this project. The supervision, guidance, and positive support provided by Dr. R. K. Wood proved to be very valuable during the completion of this thesis; Dr J. T. Ryan provided a review of the thesis and suggestions for improvement. Financial support from Dr. R. K. Wood and the Department of Chemical Engineering is gratefully acknowledged.

I would like to thank Terry Nonay for providing both a thesis project and employment with the Physical Plant, Utilities Department. This opportunity provided an excellent learning and working environment and is a very valuable stepping stone in my career. Ray Kjenner and the University of Alberta Heating Plant Staff have provided a large contribution. They have been very patient and helpful in providing answers to countless questions concerning the Heating Plant operations. I would also like to thank other members of the Physical Plant, Utilities staff, Stan Ostapowich, Clive Carter, Agnelo da Silva, and Tom Gryba, for their support.

My fellow graduate students have provided camaraderie and support throughout this project, especially Wellington Kwok, Paul Nowrocki, and Jean Corbin. Their positive support and comments were always welcome.

Table of Contents

List of Tables

List of Figures

Nomenclature

a	speed of sound, m/s
A	cross sectional area of a pipe section, m^2
Cv	valve flow coefficient from manufacturer's data
Cvm	valve flow coefficient based upon steady state plant data
D	diameter, m
f	friction factor
G_f	specific gravity of flowing fluid relative to water at 15.6° C
k	the ratio of specific heats
L	length, m
n	number of equally spaced reaches along a pipe length
N	number of pipes in a piping network
N_1	conversion constant used in valve sizing equation (6.309 e-5)
N_2	conversion constant used in valve sizing equation (6894.7)
P	static pressure, Pa
R	specific gas constant for steam, J/kg/K
step(f):	$f \leq 0$: step(f)=0
	$f > 0$: step(f)=1
t	time, s
T	temperature, K
V	velocity, m/s
wdel	specified exit fluid delivery flow rate at a pipe junction
w	mass flow rate, kg/s
x	distance along the horizontal axis of a pipe section, m
X	valve stem position, % of maximum travel
Z	compressibility factor

Greek

Δ	small increment
ρ	density, kg/m^3
τ	shear stress of the fluid acting on the pipe, Pa
ω	frequency of forcing function
θ	period of oscillation of pressure wave

Subscripts

U	upstream location
D	downstream location
i	pipe or header identification number in a pipe network illustrated in Figure 5-1 and 6-27
P	the point in the x-t plane at the location $(x, (t + \Delta t))$
R	the point in the x-t plane at the location $((x - \Delta x), t)$
S	the point in the x-t plane at the location $((x + \Delta x), t)$

Chapter 1 Introduction

Mathematical modeling plays an important part in the analysis of a process and its associated control system. The model can be based upon physical principles, empirical analysis, or a combination of both. Empirical dynamic models require an upset to the process to obtain data to develop the model parameters. This method may not be feasible or practical for certain processes. The model parameters can be obtained for the empirical dynamic model if it is permissible to upset the process; however, this type of model has problems associated with its general usage. If the plant configuration or process changes substantially then more process upsets need to be employed to update the model parameters. As an example consider an empirical model developed by a manufacturer to describe the pressure drop and flow characteristics associated with a control valve. The relationship published by the manufacturer applies only to steady state pressure and flow relationships. To include the dynamic component for this valve model a step change must be applied to the control signal to the valve and the resulting output from the control valve movement (valve position, flow, pressure) is observed. From the relationship of the input to the output an empirical dynamic model can be developed. If this valve is to be included in a different type of process, another step change must be applied to the valve to produce a new dynamic model of the control valve.

Dynamic mathematical models relying on the principles of physics and chemistry do not rely on process upsets for their development, although these upsets can be used to verify the model. This type of model can also be used to predict results that will enable the process engineer to develop or design changes to the process or to the process controls. The proposed improvement to the quality or safety of the process can be analyzed before the changes are actually physically implemented.

1.1 University of Alberta, Physical Plant, Utilities

The Physical Plant, Utilities department is a group operated by the University of Alberta for the purpose of supplying utility services (steam, chilled water, compressed air, demineralized water, electric power, natural gas, & domestic water) to all the buildings on the greater campus area. This department is a self contained utility company, like the City of Edmonton Utilities Department, operated by the University of Alberta. The customers of the Physical Plant, Utilities Department include the faculties associated with the University of Alberta, the Department of Public Works, and the University of Alberta Hospitals.

The Physical Plant Department consists of the following divisions: Electrical Utilities, Mechanical Utilities, Heating Plant, and Utilities Control and Monitoring Systems (UCMS). The UCMS and Heating Plant were closely involved in this work. A description of the services provided by these divisions will follow.

The UCMS group is responsible for the programming and maintenance of a large distributed control system (DCS) that serves the Utilities Department. The DCS system provides automatic control and monitoring of all the equipment within the Utilities Department. This includes control of chillers, boilers, circuit breakers, and pumps. This group is also responsible for metering of the steam and chilled water that is supplied to the customers.

The heating plant is a centrally located plant that provides steam to be used for heating buildings on the campus. Future expansion plans include the addition of a steam driven turbine to be used for cogeneration. Because of the critical nature of the service provided by this plant and the critical nature of some of the customers (U. of A. Hospital), large process upsets that could cause the plant to stop operating for an extended period of time cannot be tolerated. Plant disruptions to the process to obtain data for a complete empirical model are not practical. A model based largely on physical principles will be much more practical and safe to develop for use in analyzing the process and control system within this plant.

The addition of the steam driven turbine will require an analysis of the future operation of the plant with respect to the control of the turbine. The main concern with the addition of this turbine is the safety system.

The turbine safety system will utilize a stop valve to stop the flow of steam to the turbine if an unsafe condition occurs. An unsafe condition is one in which damage can occur to the machinery or injury could occur to human life. The manufacturer rates the closing time for this stop valve to be 0.2 seconds. The quick closing time of this valve will cause large unwanted transients in the heating plant steam line network. These transients could cause the plant to shut down because of a boiler going off line or at worst case it could rupture a pipe in the plant. A mathematical model is needed to try and predict the response that this transient will have on the plant. With this model it will be possible to develop a control strategy utilizing existing plant equipment to minimize the plant upset due to the closing of the stop valve.

1.2 Objectives of the Study

The objectives of this study were to:

1. collect transient data utilizing the distributed control system from the University of Alberta Heating Plant to investigate improvements to the current plant operation;

2. develop a mathematical model of the steam line network in the plant to describe the mass flow and pressure in the steam line distribution network within the plant;

3. solve the partial differential equations numerically to obtain predictions for the data collected;

4. compare the results of the predictions against the transient data collected from the Heating Plant;

5. use predictions from the mathematical model and the numerical solution to examine the effects on the process of the addition of a steam driven turbine.

1.3 Structure of the Thesis

Chapter 2 of this thesis presents a literature review of one dimensional transient compressible flow in circular pipes with specific interest to steam generating plants. This review covers the areas of the mathematical model development and numerical techniques used to obtain a solution to this model. The development of the mathematical model for the different model components is presented in Chapter 3. This will include all the assumptions used to develop the model, the model partial differential equations, and an integrated form of the equations to be used for the numerical solution. Chapter 4 contains a functional description of the heating plant steam line network and the distributed control system. Chapter 5 discusses the operation of the dynamic simulator. Included in this chapter is a technique to obtain the steady state hydraulic grade line and mass flow rates throughout the network. Simulation results are compared to two sets of transient data obtained from the heating plant steam line network in Chapter 6. This chapter also contains preliminary simulation results for the closing of a stop valve on a steam driven turbine within the steam line network. Chapter 7 contains concluding remarks and recommendations for future work.

Chapter 2 Literature Review

2.1 Introduction

A full review of the vast amount of published work concerned with experimental and simulation studies of transient compressible flow is beyond the scope of any thesis. This literature review will be limited to a consideration of those studies involving one dimensional representation of flow in closed circular pipes deemed to be relevant for application in power plants. Furthermore, the review of numerical solution techniques will be limited to the method of characteristics.

This literature review will cover two main areas in the simulation of transient compressible flow. These areas are model development and numerical methods. To develop the model various assumptions must be employed and model parameters must be developed. A numerical method must then be chosen to incorporate the model into a simulator.

Transient compressible flow can be modelled using either a lumped or distributed parameter system representation. In a lumped system model, a series of ordinary differential equations is used to describe the transient flow. Time is the only independent variable with variations in the spatial direction handled by the lumping process. Distributed systems are modelled using partial differential equations. These equations are then integrated directly by finite difference techniques or are converted to ordinary differential equations and integrated.

No strict guidelines exist to provide guidance as to the choice of using a lumped or distributed system model description. Fox (1978) states that for steady state flows, a compressible flow model may used for systems where Mach numbers (ratio of inertia to compressibility) are 0.3 or less. To model steady compressible oscillatory flow, Chaudry (1979) recommends that a lumped system representation may be used if $\frac{\omega L}{a} \leq 0.05$. The lumped system approach will produce good results if the transients in the system are oscillatory in nature with a low frequency of oscillation.

In the system in question severe transients can occur. These may be caused by boiler trips, pipe ruptures, and intentional and/or unintentional quick opening of a stop valve or a control valve. The lumped parameter approach will not be sufficient to model the system and a distributed parameter approach must be used.

The equations used to model the flow properties has been shown by Fox (1989), Wylie and Streeter (1983), and Zucrow and Hoffman (1976) to be described by coupled first order hyperbolic partial differential equations. The order of the system of equations will depend upon whether or not heat transfer and kinetic energy are negligible. If heat transfer and kinetic energy can be considered negligible then the system can be described through the use of the continuity and momentum equations. If these effects can not be ignored then the energy equation must be included. The system will then be described by three first order partial differential equations.

2.2 Numerical Techniques

From the literature review the author has identified four distinct methods for numerical integration of the hyperbolic partial differential model equations. These are the method of characteristics (MOC), the fully explicit finite difference methods, the fully implicit finite difference methods, and the method of lines (MOL). A subset of the MOL, the pseudo characteristic method of lines (PCMOL), has also been explored in the literature. Figure 2-1 provides an illustration of the possible choice of numerical methods that might be employed. This section will identify the advantages and the disadvantages of each method. It will also attempt to identify some of the decisions that need to be made within the different subdivisions of application of the MOC.

The finite element method is another numerical technique that has been employed to obtain the numerical solution for such a system of equations [Miner and Skop (1982)]. However, since the published literature only contains a few results for this method no review is provided.

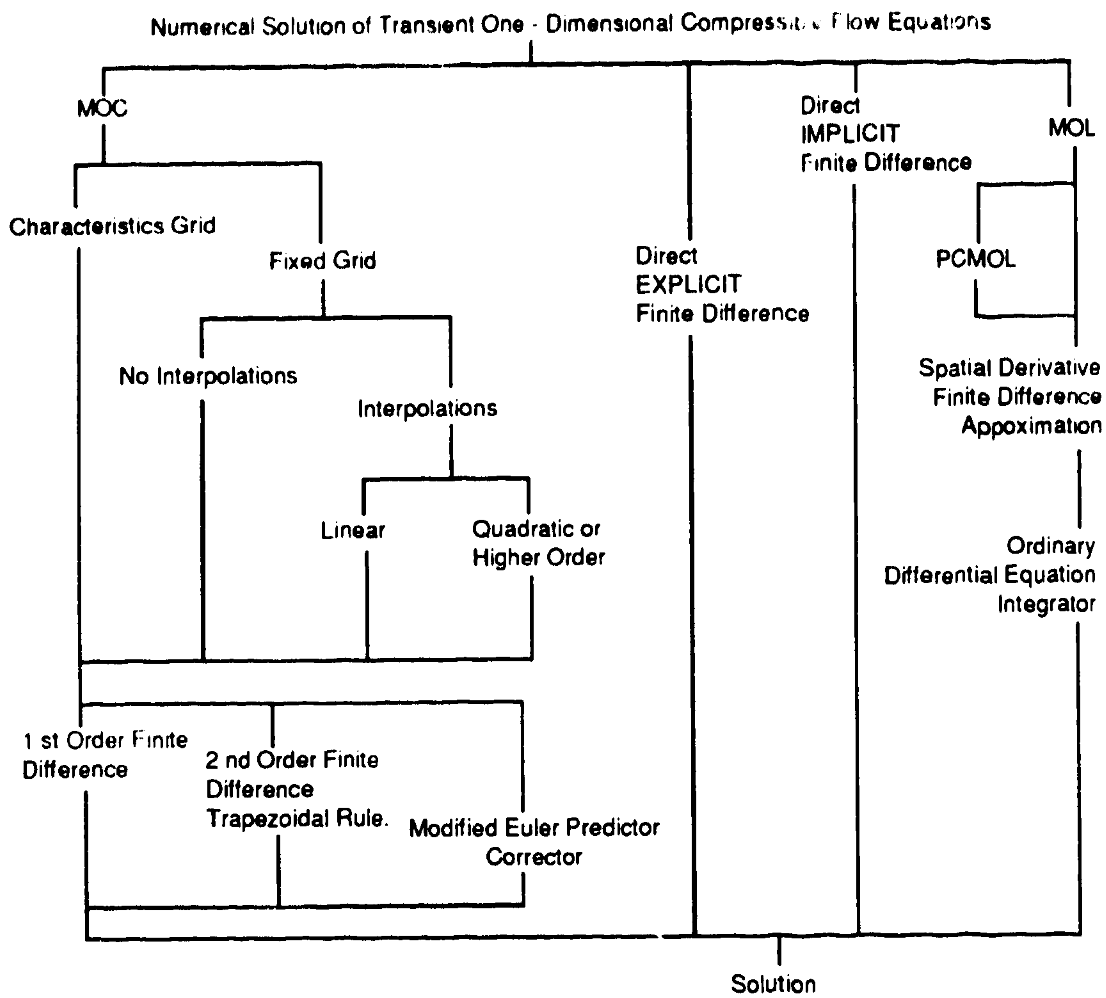

Figure 2-1 Flow Chart of Numerical Methods for the Solution of One Dimensional Transient Compressible Flow Equations

Once the model equations have been established, it is then necessary to select a suitable numerical method to solve the equations to predict the transient behavior. Table 2-1 provides a selected list of publications which provide a valuable review/comparison of one or more of the numerical techniques listed in Figure 2-1. Table 2-2 summarizes the main advantages and disadvantages of each of the principal methods shown in Figure 2-1. Although the information provided in Figure 2-1 and Tables 2-1 and 2-2 was utilized to select the numerical solution technique used in this work, consulting this material should allow any worker to select a suitable numerical technique for their particular model.

Table 2-1 List of selected Publications that provide a Detailed Description of Suitable Numerical Techniques for the Solution of One Dimensional Transient Compressible Flow Equations

Reference	Numerical Technique	Type of Integration
Carver (1980)	PCMOL	Various order finite difference approximations for spatial derivatives with a multi-step integrator, GEAR (Hindmarsh (1974)).
Carver (1981)	MOL	Various order finite difference approximations for spatial derivatives with a multi-step integrator GEAR (Hindmarsh (1974)).
Chaudry (1979)	MOC IMPLICIT Finite Difference	1st and 2nd order finite difference and a modified predictor corrector on a fixed grid. Simultaneous solution of a system of nonlinear equations.
Fox (1989)	MOC	1st order finite difference on a fixed grid.
Hancox and Banerjee (1977)	MOC IMPLICIT Finite Difference	1st order finite difference approximations on a characteristics grid. Spatial derivatives are biased according to the sign of the eigenvalues. Requires the simultaneous solution of a system of nonlinear equations.
Modisette et al. (1984)	MOC EXPLICIT Finite Difference IMPLICIT Finite Difference	1st order finite difference on a fixed grid. 1st order finite difference. Utilizes the "Box" form of the implicit finite difference algorithm. Requires the simultaneous solution of a system of nonlinear equations.
Sod (1978)	EXPLICIT Finite Difference	Various single step and two step finite difference algorithms (Godunov, Lax-Wendroff, MacCormack and Rusanov).
Wang (1987)	PCMOL	Spatial derivatives approximated by fourth order finite difference algorithm with a multi-step integration package, ODEPACK (Hindmarsh (1982)), for temporal derivatives.
Wylie and Streeter (1983)	MOC	1st and 2nd order finite difference on a fixed and on a characteristics grid.
Yow (1971)	MOC	2 nd order trapezoidal rule on a fixed grid.
Zucrow and Hoffman (1976)	MOC	Modified predictor corrector algorithm on a fixed grid and characteristics grid.

Table 2-2 Comparison of Numerical Methods for Solution of One Dimensional Unsteady Compressible Transient Flow Equations.

Numerical Method	Advantages	Disadvantages
Method of characteristics with characteristic grid (wave tracing method, direct marching method).	1. More accurate than the MOC with a fixed grid because numerical interpolations are not needed for a system with two dependent variables. 2. The Courant stability condition is always satisfied. 3. Large step lengths are possible because the stability condition is satisfied. 4. The method is exact in the constant coefficient case with two dependent variables.	1. A solution at a specified point in space and time is not guaranteed so boundary conditions are difficult to incorporate and require interpolations. 2. For solutions involving more than two dependent variables the complexity of the method is greatly increased. 3. Good initial steady state starting values are needed because this technique is slow to reach steady state.
Method of characteristics with a fixed grid (method of specified time intervals, inverse marching method)	1. The best of all the methods for incorporating boundary conditions (junctions, networks, valves, nonlinear...) because each section is handled separately. 2. A solution at a specified time and spatial point are obtained. 3. Easier to obtain a solution for more than two dependent variables than when using the characteristics grid. 4. Easy to incorporate minor terms such as friction effects and heat transfer effects. 5. Program is easy to debug because transient solution satisfies steady state equations.	1. Stability and thus the magnitude of the time step are bounded by Courant's stability criterion resulting in a long computational time. 2. If interpolations are needed then smearing of the solution can occur. 3. Good initial steady state starting values are needed because this technique is slow to reach steady state.

Table 2-2 (continued) Comparison of Numerical Methods for Solution of One Dimensional Unsteady Compressible Transient Flow Equations.

Numerical Method	Advantages	Disadvantages
Direct explicit finite difference methods	1. The original partial differential equations can be discretized directly without manipulation of the original governing partial differential equations. 2. No solution to linear or nonlinear equations is required.	1. Stability and thus the magnitude of the time step are bounded by Courant's stability criterion resulting in a long computational time. 2. Difficult to handle complex boundary conditions. 3. For methods higher than first order, numerical overshoot occurs and must be overcome by supplying an artificial damping coefficient.
Direct implicit finite difference methods	1. Unconditionally stable for all magnitudes of time and spatial increments. Time step will only be limited by the resolution required to simulate the transient response.	1. Requires the simultaneous solution of a complete set of equations describing the system. Large and complex systems become difficult to handle. 2. Difficult to handle complex boundary conditions.
Method of lines	1. Easy to implement. 2. Allows the user to take advantage of the highly developed software used to solve ordinary differential equations.	1. Difficult to handle complex boundary conditions.
Pseudo characteristic method of lines (biased upwind formulas)	1. Easy to implement. 2. Allows the user to take advantage of the highly developed software used to solve ordinary differential equations. 3. More accurate than the normal MOL by making use of higher order discretization formulas biased in the upwind or downwind direction based upon the sign of the characteristic for calculating the spatial derivatives.	1. Difficult to handle complex boundary conditions.

2.2.1 Method of Characteristics

The main idea behind the method of characteristics is to convert the partial differential equations into ordinary differential equations. The actual steps to do this are given in Chapter 3 and Appendix A as well as by the texts and papers cited in Table 2-1. This method is one of the most widely used methods for the solution of the type of model equations employed in this work. Many authors use this numerical solution technique for the bench marking the performance of newer or different numerical methods [Hancox and Banerjee (1977), Gorton (1976), Modisette et al. (1984), Yow (1971)].

2.2.2 Direct Explicit Finite Difference Methods

The main advantage of this method is that no linear or nonlinear equations need to be solved. Direct explicit methods do not require mathematical transformations like the method of characteristics and thus maintain a good resemblance to the original equations. A minimum of effort is required in converting these equations into a discrete form suitable for programming. A good review of these methods is provided by Sod (1978).

2.2.3 Implicit Finite Difference Numerical Methods

It can be seen from Table 2-2 that this method has the advantage of being unconditionally stable so that large time steps and large spatial divisions are possible. The only limiting factor in the decision of selecting the time step is that too large a time step will produce loss of resolution of the transient response. Because of this fact, for systems with rapid dynamics smaller time steps are required so no advantage is gained from this method over the other methods that have a restriction on the time step for stability reasons [Niessner (1980)]. This method would, however, be appropriate for the simulation of long slow transients such as occur in natural gas pipelines.

The main disadvantage of this method, that is the difficulty of handling the boundary conditions can be overcome with a little bit of ingenuity. For example, Chaudry (1979) suggests utilizing the combination of the method of characteristics at the boundary conditions and the implicit method for the interior points.

2.2.4 Method of Lines

The method of lines is a very general technique used to discretize the partial differential equations into a system of ordinary differential equations. This system of equations is then integrated using standard ordinary differential equation solution algorithms such as explicit or implicit Runge Kutta and multistep integration routines.

Method of lines packages are generally split into two modules [Carver (1982)]. The first module contains routines for discretizing the spatial derivatives. Some piece wise approximation polynomials (Lagrange, Legendre, and Hermite) are used to represent the spatial derivative. The second module contains the integrator for the system of ordinary differential equations. Ordinary differential equation integrator software packages such as GEAR (Hindmarsh (1974)) and ODEPACK (Hindmarsh (1982)) are readily available.

As seen in Figure 2-1 there is a subset of the method of lines called pseudo characteristic method of lines (PCMOL). This method, as described by Carver (1980) and Wang (1987) utilizes the sign of the eigenvalues of the partial differential equations to compute the direction for biasing spatial derivatives. This method has the property of being able to produce a stable solution for flows with higher Mach numbers where the simple method of lines could not. This method has been shown to be superior to the normal method of lines by Wang (1987). It is also very similar in nature to a group of numerical techniques who use "upwind biasing" of the spatial derivatives.

2.3 Important Model Assumptions and Parameters

The pertinent literature as would be expected contains a wide variety of different models depending on the various assumptions that are employed. The important assumptions relate to aspects such as heat transfer effects, frictional effects, convective acceleration, pipe elasticity, etc.

Furthermore, the choice of model parameters generally reflects on the assumptions used in establishing the model. These parameters include the working fluid, number of phases, the size of the system being simulated, boundary conditions, and the procedure used for evaluation of the model coefficients.

A summary of the pertinent literature concerning model assumptions and system parameters is given in Table 2-3. Table 2-3 also provides a description of the key elements of the system being simulated. Table 2-4 provides a brief description of each of these publications. The material that follows is based on the publications documented in Tables 2-3 and 2-4.

Table 2-3: Summary of Model Assumptions and Parameters Employed in Pipeline Studies

Reference	Heat Transfer Effects	Friction	Convective Acceleration	Pipe Elasticity or Area Changes	Pipe Length	Working Fluid / Number of Phases	Experimental /Simulation Work	Type of Boundary Conditions	Location of Evaluation of Coefficients
Brown (1987)	AD	ND	N	N	S	W / 1	S	Check Valve	CT
Chaudry (1979)	ISO	CON	N	Y	M, L	W / 1	E/S	Junction, Valve, Turbine, Pump	CT
Cheng (1978)	AD	ND	Y	Y	ND	S / 1	S	Junction, Orifice, Valve	ND
Elansary (1990)	ISO	CON	N	Y	M	W / 1	S	Valve	CT
Flatt (1985)	ND	ND	Y	ND	L	NG / 1	S	ND	AVE
Fox (1989)	ISO, HT	VAR	Y	N	ND	W, NG / 1	N	Turbine, Valve, Junction	CT
Gorton (1976)	AD	CON	Y	N	S	S / 1	E/S	Valve, Boiler Drum	CT
Hancox (1977)	HT	VAR	Y	N	S	W / 2	E/S	Blowdown	AVE
Lee (1976)	ND	ND	ND	ND	ND	S / 1	E	Valve	ND
Luk (1975)	AD	ND	Y	Y	ND	S / 1	S	Valve	ND
Modisette (1984)	ALL	VAR, LIN	N	N	L	NG / 1	S	Compressor	CT
Moody (1973)	AD	CON	N	N	ND	W, A/ 2	E/S	Valve	ND
Nicholas (1990)	HT	ND	Y	Y	L	NG / 1	S	ND	ND
Picard (1988)	AD, HT	CON	Y	N	S	NG / 1, 2	E/S	ND	CT

Table 2-3 (continued): Summary of Model Assumptions and Parameters Employed in Pipeline Studies

Reference	Heat Transfer Effects	Friction	Convective Acceleration	Pipe Elasticity or Area Changes	Pipe Length	Working Fluid / Number of Phases	Experimental /Simulation Work	Type of Boundary Conditions	Location of Evaluation of Coefficients
Samra (1978)	ISO	ND	N	N	L	W / 1	S	ND	ND
Strong (1978)	ND	CON	ND	Y	S	W / 2	S	Steam Generator, Valve	ND
Wang (1987)	AD	INV	Y	N	S	A, A and S/ 1, 2	E/S	Nozzle, Blower	CT
Watton (1983)	AD	CON	N	N	S	ND / 1	S	Pump, Valve, Resistive Load	CT
Wylie and Streeter (1983)	ALL	CON	Y	BOTH	M, L	W, NG / 1	E/S	Valve, Pump, Turbine, Junctions	CT, AVE
Ying (1978)	AD	ND	Y	N	S	S / 1	E	Turbine Stop Valve, Boiler Outlet	ND
Yow (1971)	ISO	CON	N	N	L	NG / 1	E/S	Regulator, Junction, Compressor	AVE
Zucrow (1976)	AD, HT	INV	Y	N	S	PG	S	Nozzle	AVE

ND=Not Documented, Y = Yes, N = No
Heat Transfer Effects: HT = Full Heat Transfer, AD = Adiabatic, ISO = Isothermal
Friction: CON = Constant Friction Factor, VAR = Variable Friction Factor, INV = Inviscid Flow
Pipe Lengths: S = Small (<500 m), M = Medium (500m - 1000m), L = Large (>1000m)
Working Fluid: W = Water, S = Steam, A = Air, NG = Natural Gas, PG = Perfect Gas, RG = Real Gas
Location of Evaluation of Coefficients: CT = Current Time, AVE = Average of Current Time and Future

Table 2-4 Description of Pipeline Flow Studies cited in Table 2-3

Author	Purpose
Brown (1987)	A pipe model was developed to study the effects of a check valve on the transient flow in the pipe.
Chaudry (1979)	A text presenting methods for solution for hydraulic transients for hydroelectric projects, pumped-storage schemes, water-supply systems, nuclear power plants, oil pipelines, and industrial piping systems. Case studies of working systems are presented.
Cheng (1978)	A general purpose computer code to model unsteady compressible fluid flow was developed. The numerical method consists of an explicit two step Lax Wendroff with an implicit artificial viscosity term for the interior points and the method of characteristics and a finite difference technique for complex boundary conditions.
Elansary (1990)	A numerical simulation was conducted to predict the flow, pressures and pipe stresses in a pipe wall for a given valve closure history. An optimal search technique is then used to predict a valve closure path to minimize stresses in the pipe rather than minimizing the pressure developed in the pipe.
Flatt (1985)	Presents a second order technique for integration of the equations used to describe unsteady flow in long natural gas pipelines. This technique is used in conjunction with the method of characteristics.
Fox (1989)	A text primarily concerned with the transient flow of liquids, although a chapter on natural gas pipelines is included. The primary numerical method used is the method of characteristics with first order finite difference integration on a fixed grid. The book does not contain any simulation or case studies but does contain computer programs to implement the methods described.
Gorton (1978)	Predicted the transients in power plant piping using the method of characteristics and the explicit finite difference method to determine fluid and flow properties. Tests include closing a turbine stop valve and opening of a safety relief valve.
Hancox (1977)	Used the method of characteristics to develop a standard solution technique for use as a benchmark solution. Developed a finite difference technique which is computationally more efficient than the method of characteristics. The accuracy of the solution was tested using the benchmark solution obtained using the method of characteristics.
Lee (1978)	Experimental data for a steam turbine trip are presented to be used to validate simulation results.
Luk (1975)	The fluid and flow properties during the trip of a steam turbine are simulated. The results are used to analyze the pipe stresses in the system.
Modissete (1984)	Compared three different numerical methods (method of characteristics, explicit, implicit) used to model dynamic flow in a pipeline. Compare the effect of different physical approximations on the model (isothermal, adiabatic, heat transfer).
Moody (1973)	Used the method of characteristics to predict fluid-mechanical properties which can then be employed to predict associated pipe loads.
Nicolas (1990)	Presented an unsteady flow mathematical model for pipeline flow for use in leak detection. Details of the numerical method used to solve the model are not presented.

Table 2-4 (continued) Description of Pipeline Flow Studies cited in Table 2-3

Author	Purpose
Picard (1988)	Developed a model to investigate the effects of nonisentropic decompression in a pipeline rupture. The simulation result of this model is compared with real fluid isentropic and perfect fluid isentropic model simulations as well as with experimental test results.
Samra (1978)	Used the method of characteristics to calculate the flow and fluid properties to observe the different effects of design and design materials on power plant piping systems.
Strong (1978)	Used integral procedures rather than differential and finite difference procedures such as the method of characteristics to predict fluid and force behavior in nuclear power plant piping systems.
Wang (1987)	Utilized the pseudo characteristic method of lines to predict flow properties in a pneumatic conveyer system.
Watton (1983)	Examined the effect of transmission line losses in fluid hydraulic systems using various techniques. The methods examined were the method of characteristics and implicit finite difference methods.
Wylie and Streeter (1983)	A text presenting methods to solve transient and oscillatory flow problems. Time domain solutions are presented using exclusively the method of characteristics solution method. A thorough presentation of boundary conditions and assumptions is presented. Examples include analysis of flow in natural gas pipelines.
Ying (1978)	Developed a model to predict transient pressures in a power plant steam piping system caused by steam turbine trips. The model includes a variable pressure boundary condition at the boiler superheater outlet. Experimental results are provided.
Yow (1971)	Developed and numerically solved a mathematical model to describe fluid and flow characteristics in a natural gas pipeline. The limitation on line length and discretization error are investigated. Also since inertial effects are small compared to frictional effects, an inertial multiplier is introduced to speed up the transient calculation.
Zucrow (1976)	A text presenting a thorough study of steady and unsteady compressible flow of perfect gases. The material is geared more toward gas flow with high subsonic flows, transonic flows, and supersonic flows.

2.3.1 Model Assumptions

• Heat Transfer Effects

If heat transfer effects are not negligible, then the energy equation must be introduced into the model along with the continuity and momentum equations [Chaudry (1979)]. Modisette et al. (1984) provides a good comparison of the effect of different heat transfer scenarios on the simulation of a natural gas pipeline.

Under isothermal conditions the model will include only the continuity and energy equation. In the case of the transient isothermal model the heat flow is enough to equal the enthalpy change brought about by the flow work. If this heat transfer did not take place the temperature of the fluid would change due to compression or expansion. Thus in this case the energy equation can be ignored. For simulation of systems involving liquids as the working fluid and for long natural gas pipelines this is the most common assumption to be used [Fox (1989), Chaudry (1979), Wylie and Streeter (1983)].

The next most common assumption is to assume adiabatic or isentropic conditions. While this will require the use of the energy equation it avoids the necessity of producing a correlation for the heat transfer in the first case and correlation's for the frictional and heat transfer effects in the second case. These are the most common assumptions used where gas is the working fluid in shorter well insulated pipes. An all purpose model to cover heat transfer effects is developed in Zucrow and Hoffman (1976).

•FRICTION

The choice of whether or not to include friction loss or to assume inviscid flow depends on the magnitude of the viscous forces to the inertial forces. In general, the assumption of inviscid flow can only be assumed for shorter length pipes with quick transients. Zucrow and Hoffman (1976) provides a thorough presentation of the modelling and numerical solution approach that applies under these conditions.

When friction is included it is first necessary to decide upon the nature of the type of representation for the friction term that is to be employed. The majority of the texts and papers use a steady state approximation for the friction term. The Darcy Weisbach and the Fanning equation are employed to represent the shear stress set up by friction. Once the representation has been decided upon it is then necessary to decide if the friction factor will be maintained constant or to re-evaluate at certain time intervals. This choice is influenced by the desired accuracy of the solution and the magnitude of the effect of the friction term. Chaudry (1979) and Wylie and Streeter (1983) both elect to keep the friction factor constant during simulations while Fox (1989) and Zucrow and Hoffman (1976) provide formulas for re-evaluating the friction coefficients based on the Reynolds number and pipe relative roughness.

•CONVECTIVE ACCELERATION

The decision to include a convective acceleration term depends upon the bulk velocity of the fluid relative to the speed of sound in the fluid. Just as in the choice of the friction term, the more compressible the fluid and the more severe the transient, the more necessary it is to include the convective acceleration term. Wylie and Streeter (1983) provides a derivation to prove that this term can be ignored for natural gas pipelines.

•PIPE ELASTICITY

Unless very flexible tubing is being used or the purpose of the model is to analyze pipe stresses such as in Elansary and Contractor (1990), pipe elasticity is ignored.

2.3.2 Model Parameters

•PIPE LENGTHS

The pipe lengths noted in Table 2-3 provide an indication of the size of the system involved in the simulation / experimental work. For longer pipes the frictional effects become important.

•WORKING FLUIDS/NUMBER OF PHASES IN WORKING FLUID

For liquids, fluid compressibility is not a concern but for gases it is necessary to decide if the gas can be treated as a perfect gas or as a real gas. The number of phases is also important. If more than one phase exists then the decision has to be made to treat the phases as homogeneous or separated flow.

•EXPERIMENTAL WORK/SIMULATION WORK

This entry in Table 2-3 denotes if the results of experimental studies are included. Obviously a comparison of the simulated responses with the experimental behavior allows for an assessment of the validity of the choice of model assumptions and model parameters.

•BOUNDARY CONDITIONS

Boundary conditions are an essential and an important feature of all of the simulation studies so the table documents the conditions that are employed.

•EVALUATION OF COEFFICIENTS

The wave speed and the friction term are examples of coefficients that are adapted during the simulation. It is important to decide on how and at what locations these terms will be evaluated. In the case of the friction terms the square of the flow rate is involved. To evaluate this term the flow rate at the current time step or the average flow rate at the current time step and the new time step is used. This amounts to a first or second order evaluation of the friction term. Wylie and Streeter (1983) recommends a first order evaluation for most liquid pipeline systems of short to medium length, while a second order evaluation is needed for longer lines.

Chapter 3 Steam Line Network Modelling

3.1 Introduction

A dynamic model of the steam line network in the heating plant is needed. With this model it will be possible to review the current control strategy and a control strategy that can be designed to handle the future addition of a steam driven turbine to be used for cogeneration.

The model of the steam line network in the heating plant consists of a number of different components:

1. Flow through a single pipe element.
2. A simple pressure or flow boundary for the end point of single pipe.
3. A common node or header where two or more pipes meet with a boundary condition of either a pressure specified at the node or a given flow delivery at the node.
4. Flow through pressure reducing valves (control valves).

The model equations used to describe steam flow through the piping network are the equation of state and two coupled hyperbolic partial differential equations representing the conservation of mass and momentum. This form of model has been used to model transient isothermal flow in natural gas pipelines [Wiley and Streeter (1982), Yow (1971), Fox (1989), Modisette et al. (1976)].

Flow through the headers is modelled with a simple continuity equation assuming no capacitance in the header. The pressure reducing valves are modelled using manufacturer's steady state valve sizing equations.

3.2 Single Pipe Model

Wylie and Streeter (1982), Fox (1989), and Yow (1971) have developed models for describing transient flow in a natural gas pipeline. Each model contains a few minor differences that will be discussed. This type of model was chosen because of the utilization of only two dependent variables: pressure and mass flow rate. The development of this model relating to high pressure steam flow will now be presented.

The model is based on the following assumptions:

1. The flow is assumed to be one dimensional.

2. The change in kinetic energy (velocity head) is neglected.

3. Pipe is horizontal (no effect of gravity).

4. The cross sectional area of the pipe is constant along a given section of single pipe.

5. The flow of the steam in the pipe is assumed to be isothermal and the steam properties can be modelled using an equation of state.

6. The wave speed is calculated as an average for the whole network and is assumed to be constant for the current time step calculation.

7. The compressibility factor for the steam is assumed to be constant throughout the section.

8. The transient friction losses are described using the steady state Darcy-Weisbach equation. The friction factor in this equation will be assumed constant through the section.

9. Other losses due to elbows, tees, expansions, and contractions are represented by use of equivalent length loss as given by Avallone and Baumeister (1986).

3.2.1 Equation of State

The equation of state for the steam flowing through the line can be given by

$$\frac{P}{\rho} = R\,T\,Z \tag{3-1}$$

The propagation of a sound wave in a perfect gas is given by

$$a^2 = k\frac{P}{\rho} \tag{3-2}$$

Under the assumption of isothermal flow equation (3-2) reduces to

$$a^2 = \frac{P}{\rho} = R\,T\,Z = \text{constant} \tag{3-3}$$

3.2.2 Equation of Continuity

The continuity equation for a control volume states that the time rate of change of mass within the control volume must equal the mass flux from the control volume surface. For a small segment of pipe this is expressed as

$$-\frac{\partial w}{\partial x} = \frac{\partial(\rho\,A)}{\partial t} \tag{3-4}$$

If we substitute equation (3-3) for ρ into equation (3-4) and expand the partial differentials we obtain

$$\frac{\partial P}{\partial t} + \frac{a^2}{A}\frac{\partial w}{\partial x} = 0 \tag{3-5}$$

3.2.3. Equation of Motion

From Newton's second law the equation of motion can be stated as the time rate of change of momentum must equal the summation of forces on a body. For a control volume over a short segment of pipe this can be represented as

$$-\frac{\partial P}{\partial x}A - \tau\,\pi\,D = \rho\,A\frac{DV}{Dt} \tag{3-6}$$

The substantial derivative of the velocity is then given by

$$\frac{DV}{Dt} = V\frac{\partial V}{\partial x} + \frac{\partial V}{\partial t} \tag{3-7}$$

If we ignore changes in kinetic energy or velocity head as being negligible compared to the pressure head over the length of the pipe, equation (3-7) reduces to

$$\frac{DV}{Dt} = \frac{\partial V}{\partial t} \qquad (3\text{-}8)$$

An expression is needed to relate the fluid velocity to the dependent variables of mass flow and pressure. This is given by

$$V = \frac{w}{A\rho} \qquad (3\text{-}9)$$

Taking the partial differential of both sides of equation (3-9) with respect to time and substituting equation (3-3) for ρ we obtain

$$\frac{\partial V}{\partial t} = \frac{a^2}{A}\frac{\partial\left(\frac{w}{P}\right)}{\partial t} = \frac{a^2}{AP}\left(\frac{\partial w}{\partial t} - \frac{w}{P}\frac{\partial P}{\partial t}\right) \qquad (3\text{-}10)$$

Following the method outlined in Wylie and Streeter (1982), the last term in the bracket in equation (3-10) can be shown to be small compared to the first term in the bracket. Using equation (3-5), the last term in the brackets can be rearranged to

$$-\frac{w}{P}\frac{\partial P}{\partial t} = \frac{w}{P}\frac{a^2}{A}\frac{\partial w}{\partial x} \qquad (3\text{-}11)$$

Substitution for the wave speed using equation (3-3) gives

$$\frac{w}{\rho A}\frac{\partial w}{\partial x} = V\frac{\partial w}{\partial x} \approx \frac{V}{a}\frac{\partial w}{\partial t} \qquad (3\text{-}12)$$

where it is assumed that

$$\frac{\partial w}{\partial x} - \frac{1}{a}\frac{\partial w}{\partial t} = 0 \qquad (3\text{-}13)$$

If we substitute (3-12) back into the right hand side of (3-10) we obtain

$$\frac{a^2}{AP}\left(\frac{\partial w}{\partial t} - \frac{w}{P}\frac{\partial P}{\partial t}\right) = \frac{a^2}{AP}\left(\frac{\partial w}{\partial t} + \frac{V}{a}\frac{\partial w}{\partial t}\right) = \frac{a^2}{AP}\frac{\partial w}{\partial t}\left(1 + \frac{V}{a}\right) \qquad (3\text{-}14)$$

For our system the term V/a is less than 0.1 therefore it can be neglected and the partial derivative of velocity with respect to time can be represented as

$$\frac{\partial V}{\partial t} = \frac{a^2}{AP}\frac{\partial w}{\partial t} \qquad (3\text{-}15)$$

An expression for the shear stress in terms of the dependent variables is found from steady state Darcy Weisbach equation

$$\Delta P = \frac{f L \rho}{D}\frac{V^2}{2} \qquad (3\text{-}16)$$

If we do a force balance at steady state on a section of length L we obtain

$$\Delta P \frac{\pi D^2}{4} = \tau \pi D L \qquad (3\text{-}17)$$

If we substitute for ΔP from (3-17) into (3-16) we obtain an expression for the shear stress as

$$\tau = \frac{\rho f V^2}{8} \qquad (3\text{-}18)$$

To obtain an equation in terms of our dependent variables we substitute equation (3-9) and (3-3) into (3-18) and obtain

$$\tau = \frac{\rho f w^2 a^4}{8 P^2 A^2} \qquad (3\text{-}19)$$

If we substitute equations (3-8), (3-15), and (3-19) into equation (3-6) we obtain

$$-\frac{\partial P}{\partial x} A - \frac{\rho\, f\, w^2 a^4}{8\, P^2 A^2} \pi D = \rho\, A \frac{a^2}{A\, P} \frac{\partial w}{\partial t} \qquad (3\text{-}20)$$

Simplifying this expression we obtain

$$\frac{1}{A} \frac{\partial w}{\partial t} + \frac{\partial P}{\partial x} + \frac{f\, w^2 a^2}{2\, P\, D\, A^2} = 0 \qquad (3\text{-}21)$$

3.2.4 Characteristic Formulation

Equations (3-5) and (3-6) are coupled hyperbolic partial differential equations that describe the dynamic flow characteristics of the steam flow. As an analytical solution for these equations is not available, special techniques must be used to numerically integrate these equations. To put them in a form suitable for integration, the method of characteristics is used to convert the partial differential equations to ordinary differential equations. Appendix A provides the details of this transformation. The converted ordinary differential equations are given as

$$\frac{1}{A} \frac{dw}{dt} + \frac{1}{a} \frac{dP}{dt} + \frac{f\, a^2 w^2}{2\, D\, A^2\, P} = 0 \qquad (3\text{-}22)$$

$$dx = a\, dt \qquad (3\text{-}23)$$

$$\frac{1}{A} \frac{dw}{dt} - \frac{1}{a} \frac{dP}{dt} + \frac{f\, a^2 w^2}{2\, D\, A^2\, P} = 0 \qquad (3\text{-}24)$$

$$dx = -\, a\, dt \qquad (3\text{-}25)$$

where (3-23) and (3-25) represent the characteristic equations and (3-22) and (3-24) are the associated compatibility equations.

To numerically integrate the above four ordinary differential equations, there are basically two approaches to take: 1. fixed grid (method of specified time intervals) 2. characteristic grid (wave tracing method). Wylie and Streeter (1982),Zucrow and Hoffman (1976), and Fox (1989) all contain examples of both methods. The fixed grid method will be used here because it allows for the prediction of dependent variables at given internal points or nodes while the characteristic grid does not guarantee a solution at any of the internal nodes.

The method of specified time intervals consists of forming a grid of rectangles in the x-t plane as shown in Figure 3-1. The grid spacing is determined by discretizing the characteristic equations to be

$$\Delta x = a\,\Delta t \tag{3-26}$$

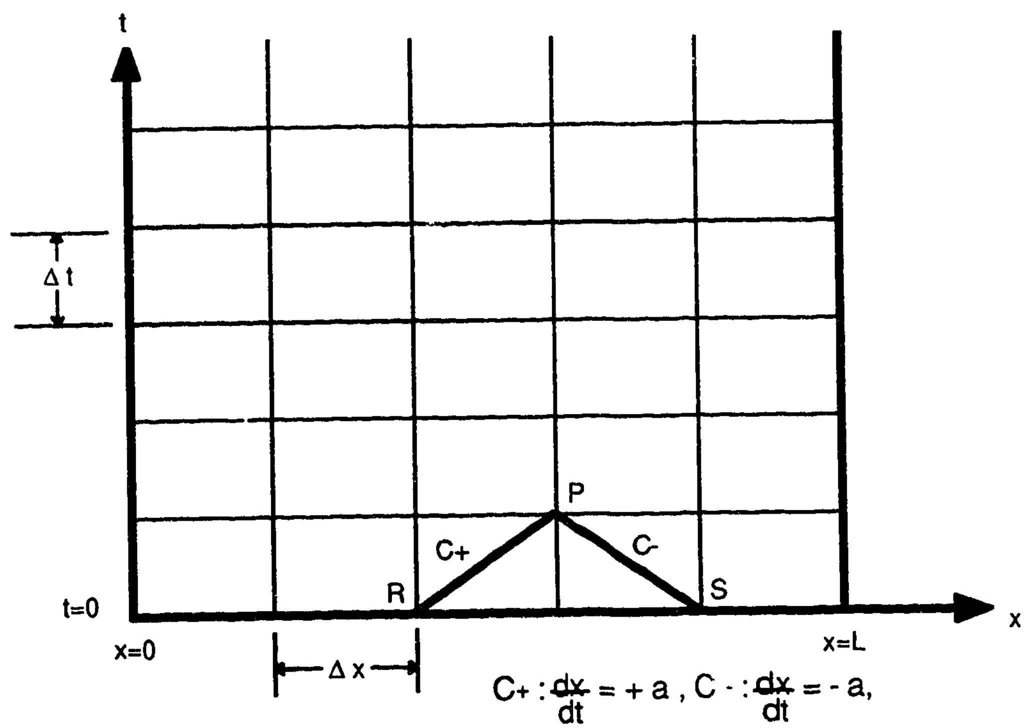

Figure 3-1: Illustration of the method of specified time intervals.

Selecting a value for either Δx or Δt, the other independent variable is then fixed according to equation (3-26).

To obtain equations suitable to put into a finite difference form, equations (3-22) and (3-24) are multiplied by dt. Equations (3-23) and (3-25) are used to substitute for dt. The equations can then be integrated as shown below

$$\int_{w_R}^{w_P} \frac{a}{A}\, dw + \int_{P_R}^{P_P} dP + \int_{x_R}^{x_P} \frac{f\, a^2\, w^2}{2\, D\, A^2\, P}\, dx = 0 \qquad (3\text{-}27)$$

$$\int_{w_S}^{w_P} \frac{a}{A}\, dw - \int_{P_S}^{P_P} dP + \int_{x_P}^{x_S} \frac{f\, a^2\, w^2}{2\, D\, A^2\, P}\, dx = 0 \qquad (3\text{-}28)$$

where the subscripts refer to the locations in Figure 3-1.

Before integrating equations (3-27) and (3-28), an approximation for the evaluation of w and P must be made. Wylie and Streeter (1982) take an average of the two at points R and P or S and P. Fox (1989) and Modisette et al.(1984) simply use the values at either points R or S. This is a simpler method because an explicit solution can then be obtained while the method employed by Wylie requires an iterative solution. The method employed by Wylie and Streeter (1982) will be the method used in the simulation.

The integrated equation for the positive characteristic (3-23) is given by

$$\frac{a}{A}(w_P-w_R)+(P_P-P_R)+\frac{f\, a^2\, (x_P-x_R)}{DA^2\, (P_P+P_R)}\left(\frac{w_P+w_R}{2}\right)\left|\frac{w_P+w_R}{2}\right| = 0 \qquad (3\text{-}30)$$

and the integrated equation for the negative characteristic (3-25) is given by

$$\frac{a}{A}(w_P- w_S)-(P_P-P_S)+\frac{f\, a^2\, (x_S-x_P)}{DA^2\, (P_P+P_S)}\left(\frac{w_P+ w_S}{2}\right)\left|\frac{w_P+w_S}{2}\right| = 0 \qquad (3\text{-}31)$$

Equations (3-30) and (3-31) represent a second order finite difference form utilizing the method of characteristics formulation to convert the partial differential equations to ordinary differential equations.

The propagation of the solution can be understood by reference to Figure 3-1. At steady state (t=0), all the dependent variables are known at each x interval. To advance the solution to point P, the information at the previous time step and upstream and downstream of point P (points R and S) must be known. From this it can be seen that the information travels along these characteristic lines at a rate equal to the wave speed to obtain the solution at the interior point P. The boundary conditions involve a similar transfer of information and will be discussed in the next section.

An important point needs to be made concerning two assumptions employed in this solution approach. The numerical solution of these equations has been simplified by neglecting the change in kinetic energy and assuming that the wave speed is constant throughout the simulation. If the change in kinetic energy is not negligible it is shown in Wylie and Streeter (1982), Zucrow and Hoffman (1976), and Fox (1989) that the characteristics are given by

$$\frac{dx}{dt} = V \pm a \qquad (3\text{-}32)$$

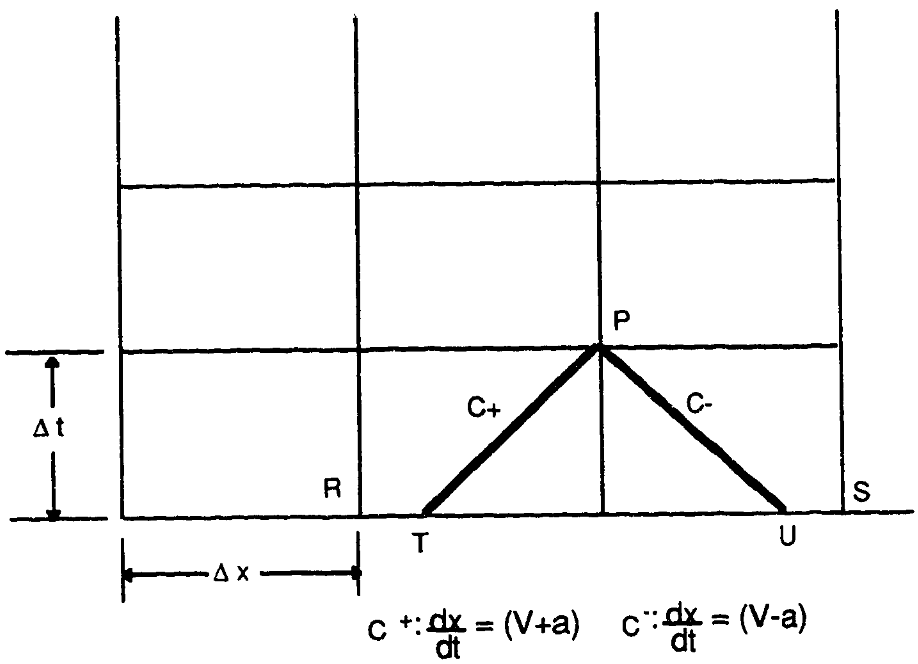

Figure 3-2: Method of Specified Time Intervals with Interpolations.

If the kinetic energy is not negligible and the wave speed is not constant, then the characteristic lines are no longer constant throughout the simulation. If this is the case then the Courant stability criterion must then be employed in the selection of the grid on the x-t plane. This criterion is given by

$$\frac{\Delta x}{\Delta t} \geq \max(V + a) \tag{3-33}$$

Reasons for this criterion are outlined in Zucrow and Hoffman (1976), and Wang (1987).

Referring to Figure 3-2, the solution at point P needs to be calculated with the dependent variables known at points R and S. Interpolations are now needed to obtain the values at points T and U. Instead of solving two equations for two unknowns, it is necessary to solve six equations for six unknowns (both pressure and mass flow rates have to be calculated at T and U).

3.2.5 Steady State Model.

Before beginning a dynamic solution of a steam line network, a steady state solution of the network must be obtained. Typically a flow or pressure is given at two of the boundaries and the flows and the pressures at the intermediate nodes must be solved for. To do this, a steady state solution of equation (3-21) is needed. It should be noted that the transient solution give by equations (3-30) and (3-31) must satisfy this steady state solution.

At steady state the mass flow term is constant, therefore the only independent variable in equation (3-21) is pressure and the equation can be written as

$$P\,dP + \frac{f\,w^2\,a^2}{2\,D\,A^2}\,dx = 0 \tag{3-34}$$

If equation (3-34) is integrated along a section of pipe of length L from the upstream boundary to the downstream boundary the result is given by

$$\frac{(P_U^2 - P_D^2)}{2} + \frac{f\,w^2\,a^2}{2\,D\,A^2}\,L = 0 \tag{3-35}$$

By letting $w_P = w_R$ and $w_P = w_S$ in equations (3-30) and (3-31), it can be seen that they satisfy equation (3-35) during steady state conditions.

3.3 Boundary Conditions

The boundary conditions in the steam line network all utilize the basic finite difference formulation given by equations (3-30) and (3-31). There are essentially two basic types of boundary conditions involved. This first type constrains and guides the system at either an input point or an exit point of the pipe network. For this simulation, this consists of supplying a pressure or flow entering/exiting a single pipe which is connected to the network. This can also be extended to a junction or header where two or more pipes meet and a delivery flow (either entry or exit) is specified.

The second type of boundary condition exists to connect the nodes or the pipes of the network together. This can be described as split boundary type of problem. The two types of boundaries dealt with here incluae a header with no delivery at the junction, and a valve which is used in this system for the purposes of controlling the pressure.

3.3.1 Left/Right Pipe Ends with Pressure/Flow Specified

This boundary condition will be used to simulate either a pressure or flow supply into a single pipe such as a boiler or else an exit pressure or flow condition out of a single pipe network such as delivery into the system.

The known values are the pressures and flows at point S and R. The unknowns can be either the pressures or flows at the point P with the subscript referring to either the left side (entry into the pipe) or the right side (exit from the pipe) as shown in Figure 3-3. The decision to use either equation (3-30) or (3-31) will depend upon the assumption of the direction of flow. If the flow is into the pipe then equation (3-31) which corresponds to the C^- characteristic will be used. If the flow is exiting the pipe then equation (3-30) which corresponds to the C^+ characteristic will be used.

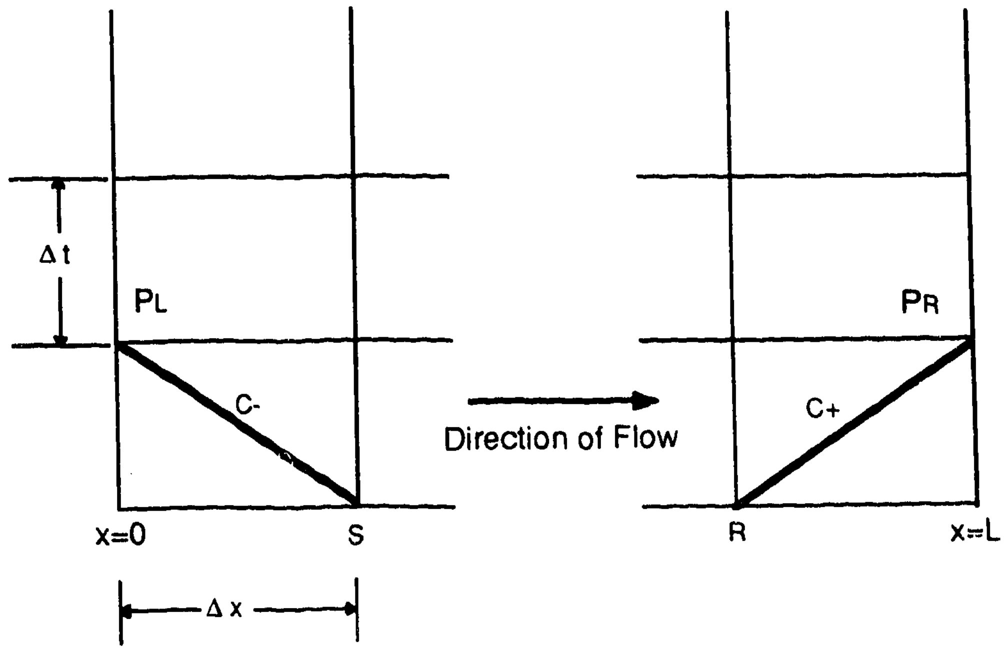

Figure 3-3: Simple Boundary Conditions for a single pipe

This solution leaves us with one equation and one unknown. It does not matter whether a pressure or flow boundary is the unknown as neither of the two can be obtained directly from (3-30) or (3-31) so an iterative solution must be used. A Newton-Raphson solution converges very quickly and is used to solve for the unknown in this boundary condition.

3.3.2 Header: Pressure or a Delivery Flow Rate Specified at Node

The basic requirement of this boundary condition is that the net mass flow at the junction must be equal to zero. In other words, the fluid capacitance of the header is considered negligible.

A junction of three pipes, with the flow directions indicated in Figure 3-4. The knowns include the flows and pressures at the previous time step at the x interval represented by R_1, R_2, and S_3 where the subscripts refer to the pipe numbers. Three unknowns include the flows into the header from pipes 1 and 2 and the flow exiting the header into pipe 3 at the new time step. The fourth unknown will be given depending upon the user requiring a specified delivery flow or a specified pressure at the node. Either one can be specified leaving the other to be calculated. Because of the assumption of no header capacitance, the pressure at the header is common to all three pipes. This then leaves four unknowns to be solved.

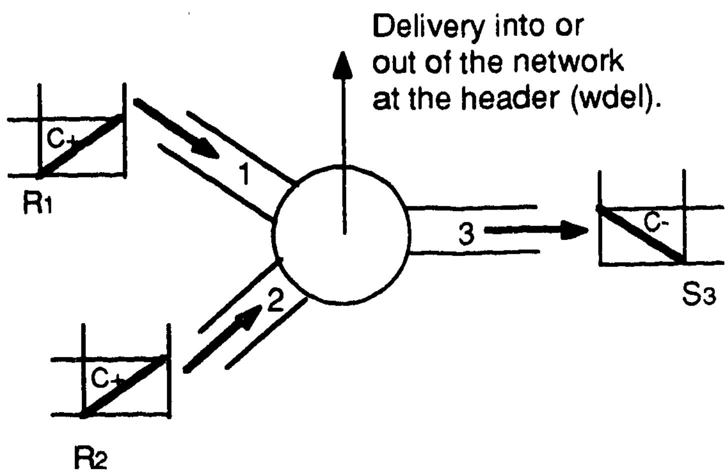

Figure 3-4: Schematic representation of a header.

The results from the single pipe case can be utilized in this boundary condition. If flow is leaving from a pipe and entering into the header then the C^+ characteristic or equation (3-30) can be used and applied to that particular pipe. A similar situation exists for the flow exiting the header and entering a pipe; the C^- characteristic or equation (3-31) can be applied to the boundary of that particular pipe. For the particular case illustrated in Figure 3-4, this results in three equations; one for each pipe. The fourth equation is obtained from the application of the steady state continuity equation given by

$$w_1 + w_2 - w_3 - wdel = 0 \tag{3-36}$$

When building a network solution the direction of flow is not always known to the user. In this method a direction of flow is assumed for the solution so if the guessed flow direction is incorrect the flow is negative.

This then gives us a system of four non-linear equations which need to be solved iteratively. For the purpose of this simulator two subroutines were written. One subroutine handles the case of a specified delivery flow at the node while the other subroutine handles the case of a specified pressure condition at the node. Each subroutine can handle up to five pipes meeting at a header. The solution for the flows/pressure utilizes another subroutine from the IMSL Math Library (1989) called DNEQNJ, which utilizes a modified Newton's method to solve for the unknowns.

3.3.3 Valves

To completely analyze the steam line network, a valve boundary condition must be developed. To incorporate automatic control of the system, this model must be capable of relating the valve stem position to modulated flow rate.

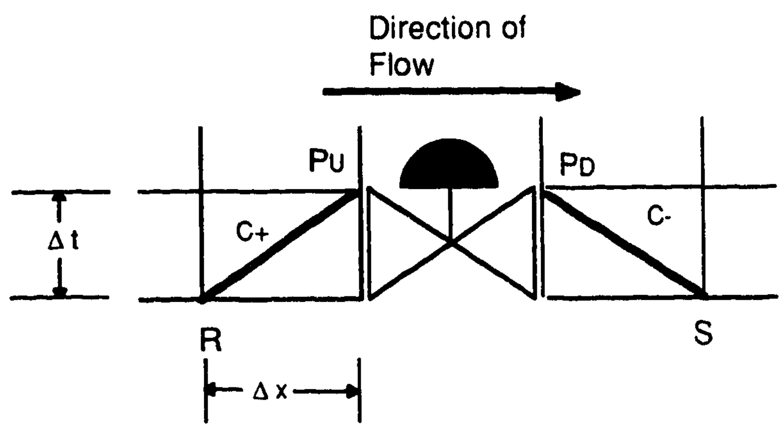

Figure 3-5: Illustration of Flow Through a Control Valve.

Once again equations (3-30) and (3-31) are incorporated into this boundary condition with the pressures and flows known at points R and S. The unknowns include the pressure at the upstream and downstream side of the valve and the flow through the valve. The third relationship used to solve for the three unknowns is the steady state valve sizing equation obtained from either the manufacturer's literature or from steady state plant operating data. Again an iterative type procedure is required to solve the system of three nonlinear equations. As was the case in the header subroutine, the IMSL (1989) subroutine DNEQNJ is used to obtain the solution for the upstream and downstream pressures and the flow through the valve.

In the heating plant steam line network the type of valve being used to throttle the steam is a globe valve. Of the nine pressure reducing valves in use in the network, two of the valves are manufactured by **Valtek** and the remaining valves are manufactured by **Fisher Controls**. The design equations for the valves can be found in Anon (1978), Instrument Society of America (1985), and Fisher Controls (1977).

3.3.3.1 Standard Valve Sizing Equation

The following equation is the standard equation used by control valve manufacturers for describing the flow, pressure, and valve stem position for control valves operating with incompressible fluids

$$w = C_v \rho N_1 \sqrt{\frac{P_U - P_D}{N_2 G_f}} \tag{3-37}$$

This equation assumes that the flow through the valve is turbulent and not choked. The density included in this equation will be calculated using the ideal gas law (3-1) and will take care of any changes in compressibility encountered in the steam during the simulation. Equations which are designed for use with compressible fluids are slightly more complex and essentially integrate the ideal gas law directly into the valve sizing equations [Anon (1978), Instrument Society of America (1985), and Fisher Controls (1977)].

The valve coefficient C_v is related to the valve stem position. The stem position and the pressure drop across the valve govern the flow through the valve. This relationship will depend upon the valve flow characteristic. The valve flow characteristic describes the relationship between a change in valve stem position to the change encountered in the flow through the valve with a constant pressure drop across the valve. The valve coefficients vs. valve openings used in this work are contained in Appendix B.

The valve coefficients are determined experimentally using water at standard conditions as the test fluid. It is numerically equal to the number of U.S gallons of water at 15.6° C that will flow through the valve in one minute when the pressure differential across the valve is one pound per square inch [Fisher Controls (1977)]. Since, the flow and pressure units used for the simulation are expressed in units of kg/s and Pa, conversion factors N_1 and N_2 are utilized to convert the equation for use with these units.

3.3.3.2 Generic Valve Equation

If the valve flow characteristics are not available from the manufacturer, then a more generic form of the valve equation can be used. This equation can be used to develop a valve coefficient correlation based upon steady state operating data from the process.

$$w = C_{vm} \sqrt{\frac{P_U - P_D}{\rho}} \qquad (3\text{-}38)$$

The generic valve coefficients used in this work can be found in Appendix B.

Chapter 4 Control System Configuration and Description of Heating Plant Steam Line Network

4.1 Introduction

In this chapter a functional description of the heating plant steam line network and the associated control systems will be given. This will include an illustration and description of the points where data were collected.

The steam line network and control system configuration in the heating plant, can be described by dividing the system into three distinct sections. These sections are based upon the nominal steady state operating pressures for the steam line within each specific section. The first section is based upon the operating pressure of 6205 kPa. This section includes both Boiler 4 and 5 which operate at this pressure. The second section, based on an operating pressure of 2760 kPa, includes Boilers 1,2, and 3 which all operate at this pressure. The boiler capacities are given in Table 4-1. The third section operates at 1035 kPa, which is the supply pressure to the tunnel system.

4.2 Functional Description of Heating Plant Steam Line Network

A schematic diagram of the main steam flow path ,including the boilers and pressure reducing valves in the heating plant, is given in Figure 4-1. Steam flows from Boilers 4 and 5 at a pressure of 6205 kPag into High Pressure Header No. 2. The steam from these two boilers is throttled to a pressure of 2760 kPag. Pressure reducing valves PY-7040A/B reduce the pressure for Boiler 4 while PY-7040C/D reduce the pressure for Boiler 5. The PY-7040A/B valves are globe valves with linear trim, manufactured by Fisher Controls, while the PY-7040C/D valves are also globe valves with linear trim but manufactured by Valtek Valves. Further information on these valves is provided in Appendix B.

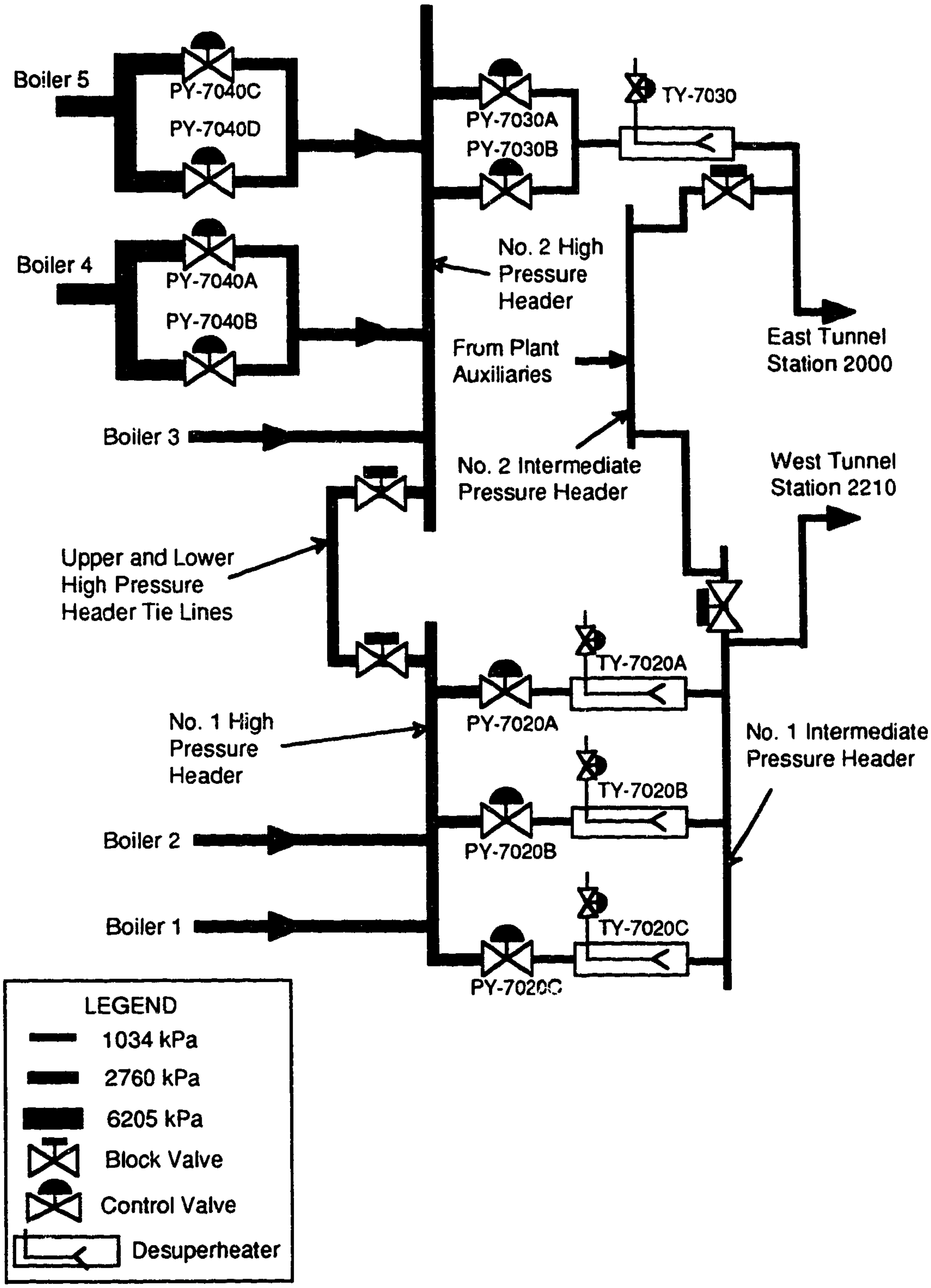

Figure 4-1 Schematic Diagram of the Steam Line Network of the University of Alberta

Boiler 3 feeds directly into the High Pressure Header No. 2 with no pressure reduction. Boilers 1 and 2 feed directly into High Pressure Header No. 1 at the same pressure as Boiler 3 and as can be seen, the No. 1 and 2 High Pressure Headers are connected by two tie lines, which is kept open during normal plant operations regardless of which set of boilers is operating. The block valves on the tie lines are only closed when there is a need to isolate one of the headers in a case of maintenance or pipe failure in the opposing header.

Table 4-1: Heating Plant Boiler Capacities

BOILER	MAXIMUM FLOW (kg/h)	OPERATING TEMPERATURE (°C)	OPERATING PRESSURE (kPag)
1	66,000	400	2760
2	66,000	400	2760
3	110,000	400	2760
4	165,000	400	6205
5	145,000	400	6205

As shown in Figure 4-1, the steam from the high pressure header system flows through another set of pressure reducing valves and into the tunnel system. The pressure of the steam is reduced from 2760 kPag to 1035 kPag by PY-7030A/B and 7020A/B/C. During normal operation, one set of valves is usually put in the manual mode and base loaded while the other set of valves is in the automatic mode to control supply pressure to the tunnel at 1035 kPag.

Associated with these two valve sets are the desuperheating stations which perform the final conditioning of the steam. A mixture of water and high pressure steam is injected into the steam after PY-7020A/B/C and 7030A/B to reduce the temperature of the steam to 210 °C as required by the design specifications for distribution to the utilities corridor.

4.3 Control System Configuration

The control system configuration can be described in a similar fashion as the steam line layout by dividing the control loops into the three sections based upon the operating pressures of the system. The instrumentation and point tag designations for the material that will follow are given in Table 4-2. The complete point tag description for the relevant control loops and measurement points in the heating plant steam flow network is given in Table 4-3. The points are all grouped according to the pressure divisions of the network.

Table 4-2: Instrumentation and Control System Designations

ITEM	DESIGNATION
Pressure Indicating Controller	PIC
Temperature Indicating Controller	TIC
Flow Recording Controller	FRC
Pressure Transmitter	PT
Temperature Transmitter	TT
Flow Transmitter	FT
Flow Recorder	FR
Pressure Relay (Signal from controller to and including Final Control Element)	PY
Temperature Relay	TY
Flow Relay	FY

The output relays will include all hardware from the output from the controller to including the final control elements.

Figure 4-2 to 4-8 provide a block diagram description of the signal flows for the control points. Figures 4-9 to 4-12 provide a graphic representation of the physical layout of the measurement points used for feedback signals to the controllers and for monitoring purposes.

Table 4-3: Controller and Measurement Point Descriptions

Operating Pressure (kPa)	Point Tag	Description
6205	PIC-5000	Boiler 5 Master Pressure Controller
	FT-5000	Boiler 5 Steam Flow
	TT-5017	Boiler 5 Superheater Steam Exit Temperature
	FRC-5001	Boiler 5 Gas Controller
	FRC-5002	Boiler 5 Air Controller
	PIC-4000	Boiler 4 Master Pressure Controller
	FT-4000	Boiler 4 Steam Flow
	TT-4010	Boiler 4 Superheater Steam Exit Temperature
2760	PIC-7040	Boiler 4 & 5 Master Pressure Reducing Controller
	PCV-7040A	PIC-7040 Slave Control for Valve A.
	PCV-7040B	PIC-7040 Slave Control for Valve B.
	PCV-7040C	PIC-7040 Slave Control for Valve C.
	PCV-7040D	PIC-7040 Slave Control for Valve D.
	PIC-6200	Boiler 1,2, & 3 Master Pressure Controller
	PIC-1000	Boiler 1 Pressure Controller
	FT-1000	Boiler 1 Steam Flow
	TT-1010	Boiler 1 Superheater Exit Temperature
	PIC-2000	Boiler 2 Pressure Controller
	FT-2000	Boiler 2 Steam Flow
	TT-2010	Boiler 2 Superheater Exit Temperature
	PIC-3000	Boiler 3 Pressure Controller
	FT-3000	Boiler 3 Steam Flow
	TT-3010	Boiler 3 Superheater Exit Temperature
1035	PIC-7020	Master Pressure Reducing Controller for High Pressure Header No. 1
	PCV-7020A	PIC-7020 Slave Control for Valve A.
	PCV-7020B	PIC-7020 Slave Control for Valve B.
	PCV-7020C	PIC-7020 Slave Control for Valve C.
	TIC-7020A	Temperature Control for Valve A.
	TIC-7020B	Temperature Control for Valve B.
	TIC-7020C	Temperature Control for Valve C.
	PIC-7030	Master Pressure Reducing Controller for High Pressure Header No. 2
	PCV-7030A	PIC-7030 Slave Control for Valve A.
	PCV-7030B	PIC-7030 Slave Control for Valve B.
	TIC-7030	Temperature Control.

The firing control system for Boiler 5 is controlled by the master pressure controller PIC-5000 as can be observed from Figure 4-2. This controller tries to maintain the exit pressure of Boiler 5 at a set point of 6205 kPag. The pressure transmitter PT-5000 senses the steam pressure at the exit of the superheater on Boiler 5 which is used as a feedback signal to pressure controller PIC-5000. This controller is the master controller of a cross limiting firing control loop. The PIC-5000 controller provides a remote set point to the slaves in the loop. The slaves in this loop are the gas and air controllers labelled FRC-5001 and FRC-5002 respectively. Each have their own transmitter for feedback as illustrated in Figure 4-2.

The firing control system for Boiler 4 is an exact duplicate of the system used for Boiler 5. The master controller, PIC-4000 provides set point signals to FRC-4001 and FRC-4002. These air and gas controllers are also in a cross limiting firing control configuration.

Boilers 1 and 2 are the original boilers installed when the south heating plant was constructed. These two boilers which supply steam at 2760 kPag feed into High Pressure Header No. 1. In 1966 Boiler 3 with a working pressure of 2760 kPag was added to increase the capacity of the plant. This boiler feeds into High Pressure Header No. 2.

During the mid seventies, due to increasing steam demands from the greater campus area, Boiler 4 was added. Due to the advances in technology, Boiler 4 was designed to operate at a much higher pressure (6205 kPag) than Boilers 1,2, and 3 so to tie Boiler 4 in to the existing plant supply headers, the steam supply pressure from Boiler 4 had to be reduced to 2760 kPag. This pressure reduction is handled by PY-7040. The station consisted of two globe valves (PY-7040A & PY-7040B) operating in parallel to step down the operating pressure from 6205 kPag to 2760 kPag. The steam flow after these valves is then piped into High Pressure Header No. 2.

In 1988 the heating plant was again expanded. Boiler 5 was added on the basis that eventually the two original Boilers would be replaced and also to give the plant a larger capacity at the higher operating pressure of Boiler 4. Furthermore, this increased capacity at the higher pressure would allow the addition of a steam driven turbine to be used for cogeneration purposes.

To meet the existing process requirements, the pressure from Boiler 5 also had to be stepped down. The logical way to do this was to add another parallel set of globe valves to the exit line of Boiler 5. These globe valves, PY-7040C/D, became two more slaves of pressure control loop PIC-7040.

Figure 4-3 shows the block diagram for PIC-7040. The pressure transmitter PT-7040 provides the operating steam pressure a few metres before entry into High Pressure Header No. 2. This pressure is used as a feedback to the distributed control system and allows PIC-7040 to control the flow from Boiler 5 to maintain the operating pressure of High Pressure Header No. 2 at 2760 kPag.

The two intermediate points in the control diagram warrant some discussion. When the main controller PIC-7040 is set in the automatic mode, it calculates a control action based upon the set point and the feedback signal from the transmitter PT-7040. This signal is then passed through software to two intermediate or "dummy" controllers labeled PCV-7040C and PCV-7040D. These two controllers are termed "dummy" controllers because they simply pass the calculated control signal to the valve positioner on each of the valves with the option of biasing the signal. These two points do not provide control action since the positioner is a simple mechanical mechanism that ensures that the valve stem moves to the desired position based on the signal from the controller.

The biasing option allows the operator to have more flow through one valve than the other. If the master controller calls for a valve opening of 25% and one valve has a bias of -5%, that valve will only be open 20% while the valve without the bias will be open to 25%.

This controller can be operated in either an automatic or a manual mode. The mode of operation will depend on which combination of boilers is on line. This will be discussed further after pressure control for boilers 1,2, and 3 are discussed.

The master pressure controller PIC-6200 shown in Figure 4-4 operates in a similar manner as PIC-7040. The purpose of this controller is to maintain the operating pressure in the high pressure header system at a set point of 2760 kPag. It accomplishes this task by regulating the firing controls, and thus regulating the steam flow from Boilers 1, 2, and 3.

The pressure transmitter PT-6200 can sense the pressure in either High Pressure Header No. 1 or High Pressure Header No. 2. This option exists so that if there is required maintenance or a failure on one of the headers, operations can be continued by isolating the header through block valves in the header tie line and sensing the pressure in the other header.

If the PIC-6200 controller is in the automatic mode, it will calculate a control action based upon the difference between the set point and the measured pressure. In a manner similar to PIC-7040, this control action is then passed to the dummy controllers PIC-1000, PIC-2000, and PIC-3000. As explained these controllers simply act as a transfer of the control signal and can only bias the signal up or down by a certain percentage. The control signal from these 3 intermediate controllers is used as a remote set point to the gas and air controllers for each of the respective boilers. Each of these boilers has a parallel cross limited firing control system similar to that on Boilers 4 and 5.

Based upon operating experience, the operational modes, automatic and manual, of PIC-6200 and the three intermediate control points (PIC-1000, PIC-2000, and PIC-3000) will vary depending upon the combination of boilers that are in operation. If PIC-6200 is in the automatic mode and more than one of the boilers is in operation, the normal operational sequence would be to have one of the intermediate controllers in auto and the others in manual. As an example consider both Boilers 1 and 3 being on line with PIC-6200 in the automatic mode. In this case, the PIC-1000 controller will arbitrarily selected to be in the manual operating mode and a desired output (0-100%)will be set by the operator. This action "base loads" the boiler at a constant flow rate and the back pressure from the header will keep the boiler at its operating pressure. Meanwhile PIC-3000 will be in automatic mode. This controller will be passed its control action from PIC-6200. Boiler 3 will then be maintaining the header pressure by increasing or decreasing the firing rate of Boiler 3. This method of base loading one boiler while putting the other boiler on automatic firing control is used so that the boilers don't "fight" each other. If both boilers were put in the automatic mode, similarities in the boiler dynamics would cause a less stable or possibly an unstable operation of the boilers.

It is to be noted that the operational modes of PIC-7040 and PIC-6200 also are selected so that only one of the controllers is in the automatic mode. The purpose of these controllers is to maintain an operating pressure of 2760 kPag in the high pressure header system. Boilers 4 and 5 can be considered as one supply source to maintain this pressure, while Boilers 1,2, and 3 are the second supply source. If one of the boilers from one source is being operated while one of the boilers from the other source is also being operated, then either PIC-7040 or PIC-6200 will be in the automatic mode and the other controller in the manual mode. This technique of operation is used so that one supply source gets base loaded to operate at a constant flow rate and the other source takes up the swing in the system pressure.

The final two pressure control loops in the steam line network are, PIC-7020 and PIC-7030, are shown in Figure 4-5 and 4-6. The purpose of these two controllers is to maintain a supply pressure to the tunnel system of 1035 kPag. The operation of these two control loops is identical to the PIC-7040 control loop. The only differences between PIC-7020 and PIC-7030 loops is that a PIC-7030 has two globe style control valves operating in parallel while PIC-7020 has 3 globe control valves operating in parallel.

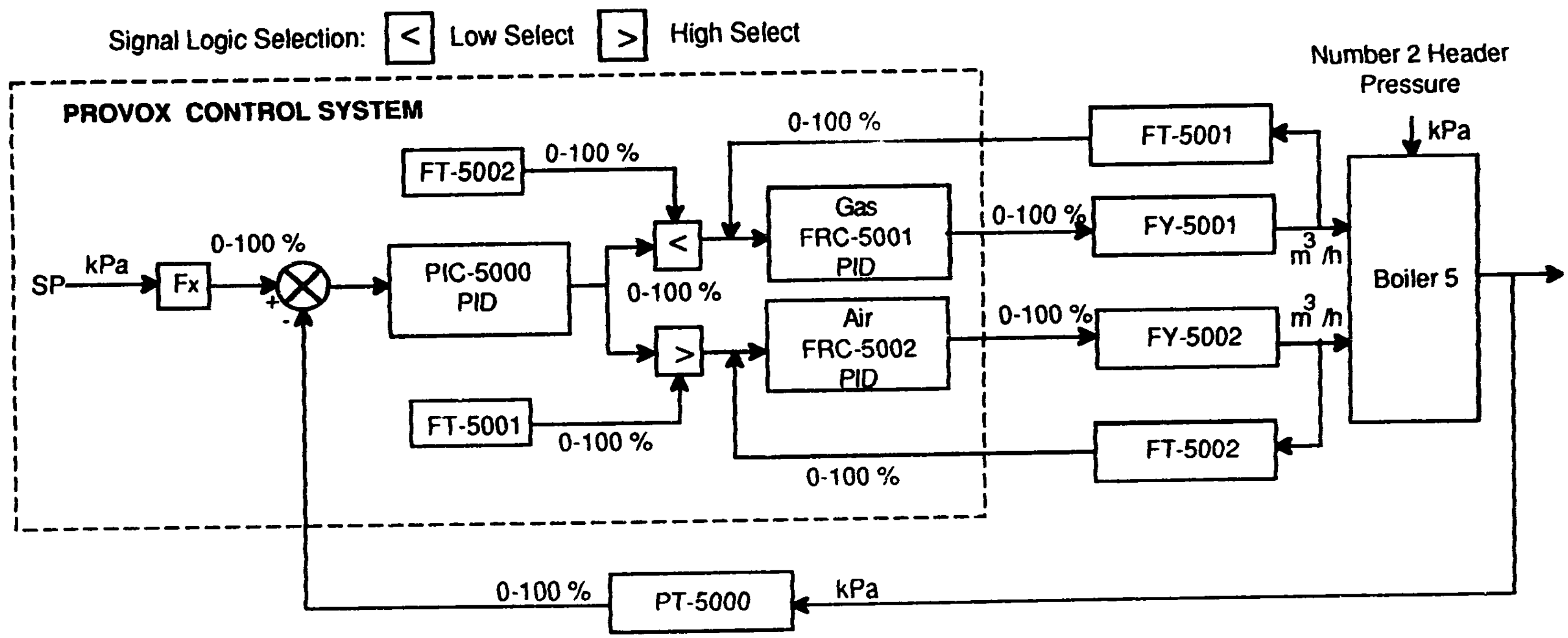

Figure 4-2 Block Diagram for Pressure Control Loop PIC-5000

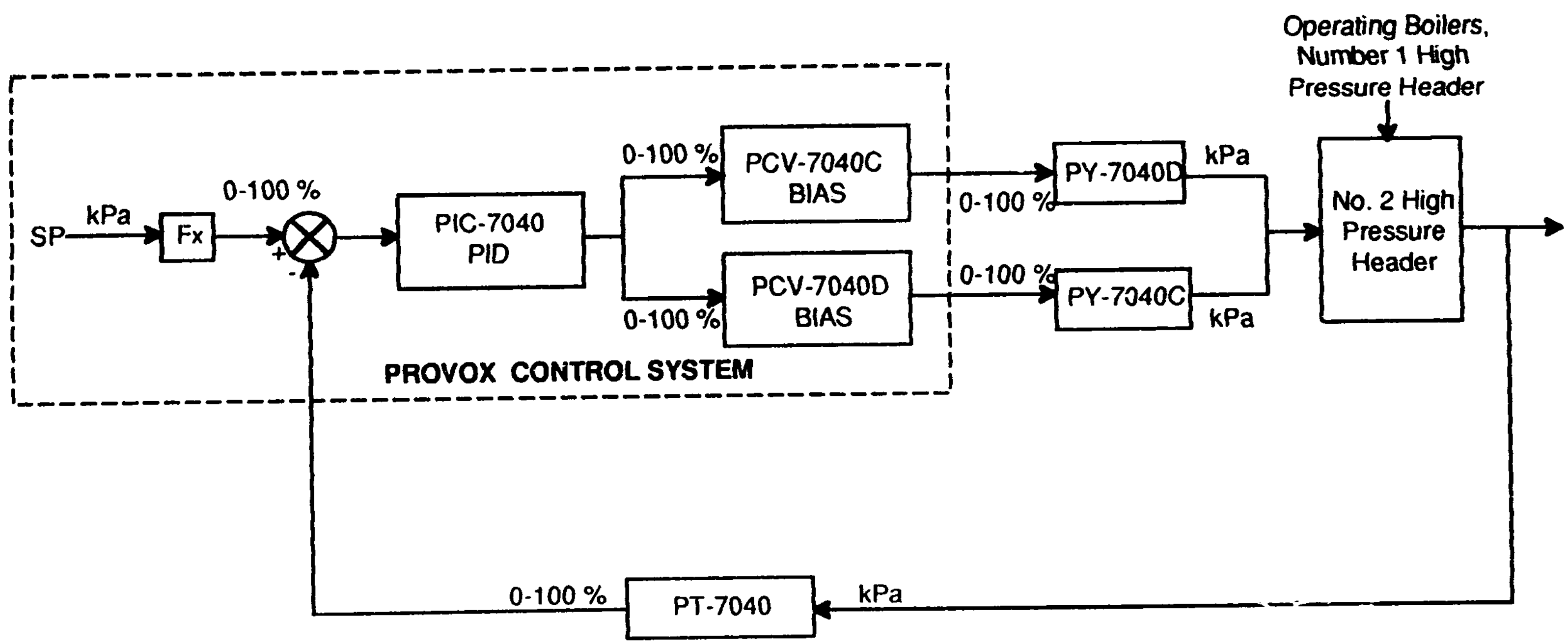

Figure 4-3 Block Diagram for Control Loop PIC-7040

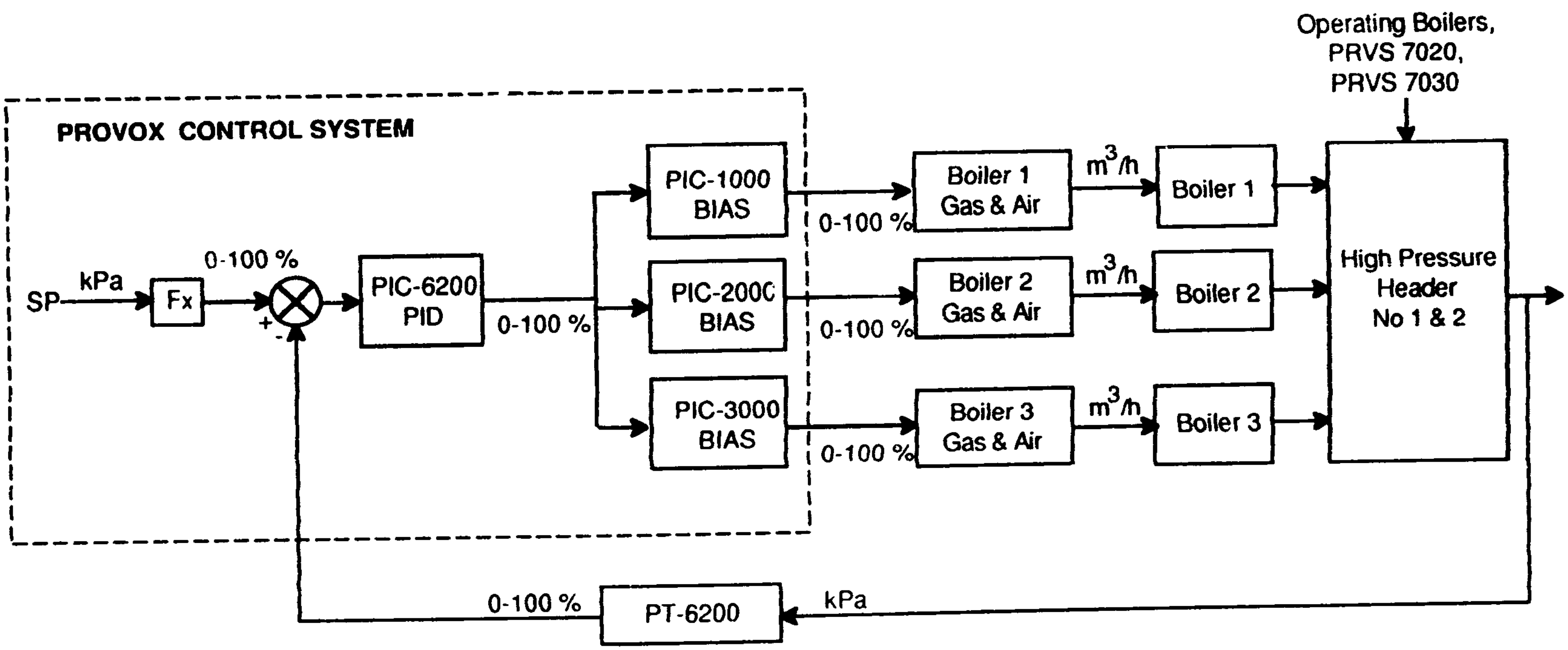

Figure 4-4 Block Diagram of Pressure Control Loop PIC-6200

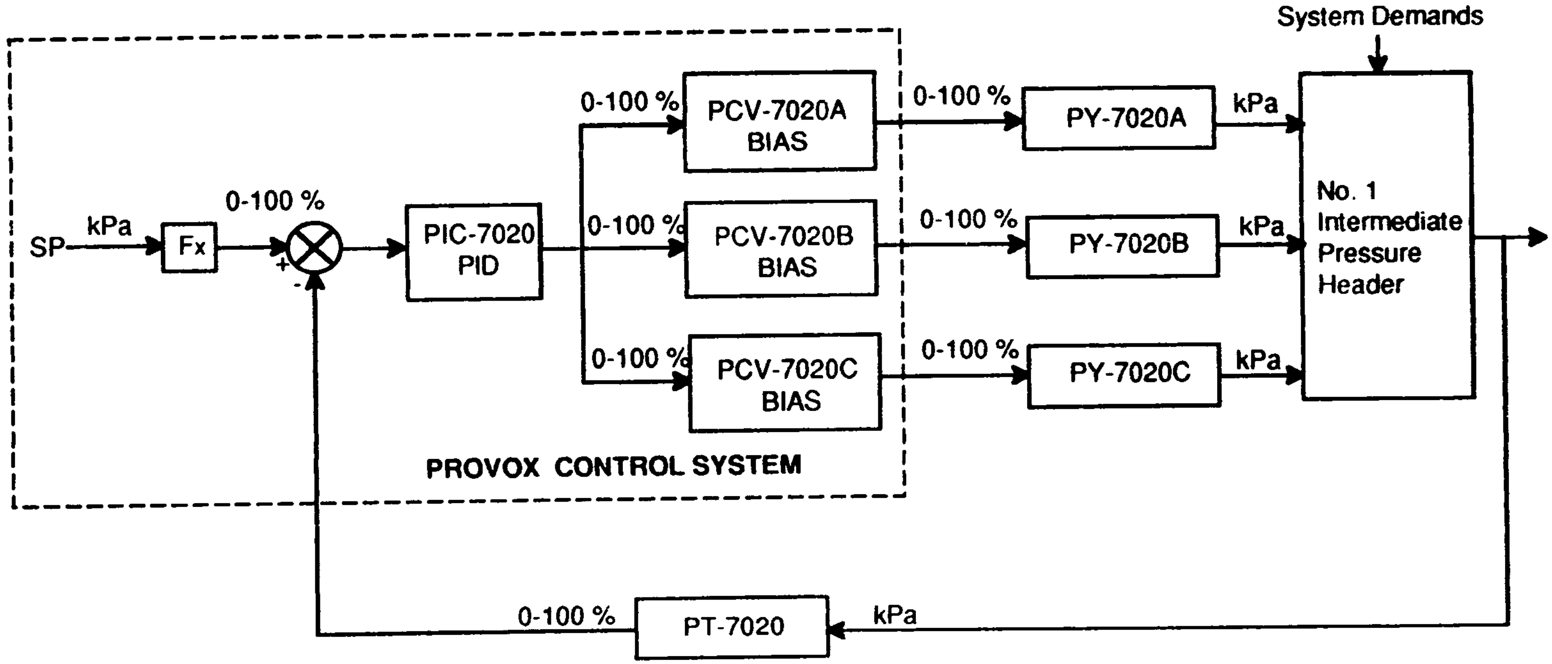

Figure 4-5 Block Diagram of Pressure Control Loop PIC-7020

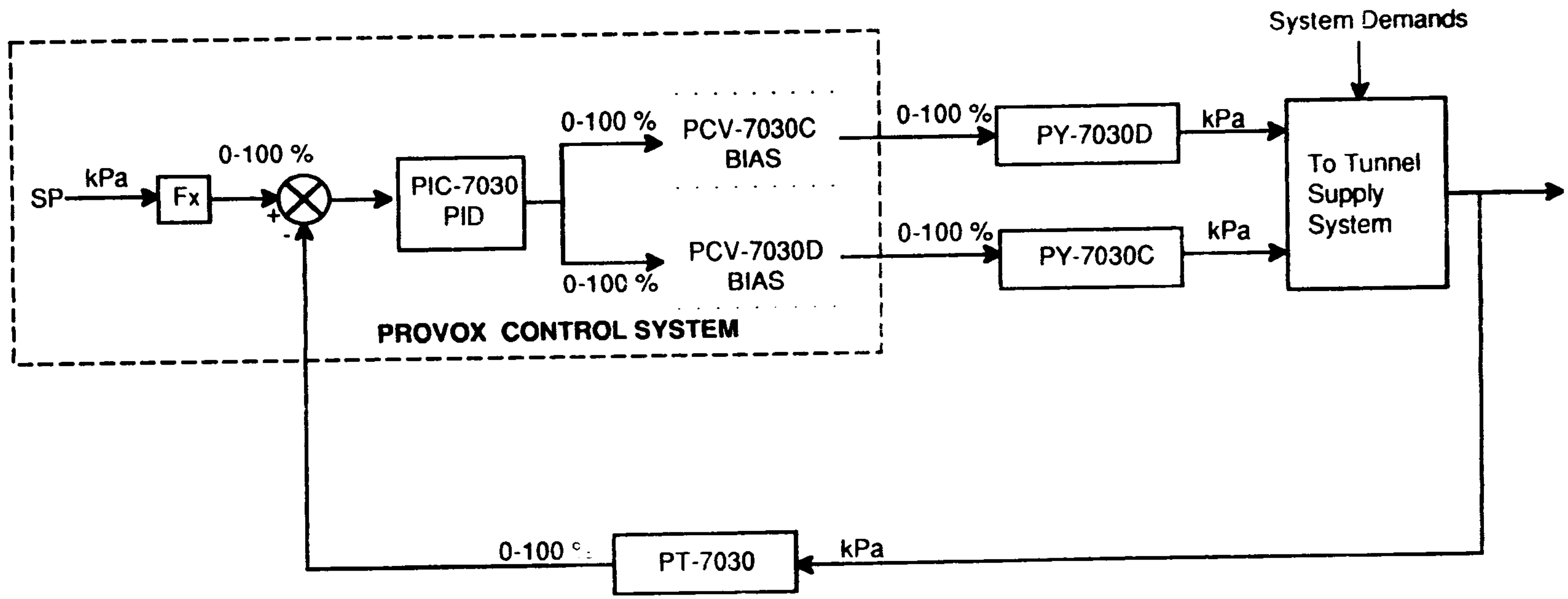

Figure 4-6 Block Diagram for Pressure Control Loop PIC-7030

**NOTE: Similar configurations exist for TIC-7020B and TIC-7020C.

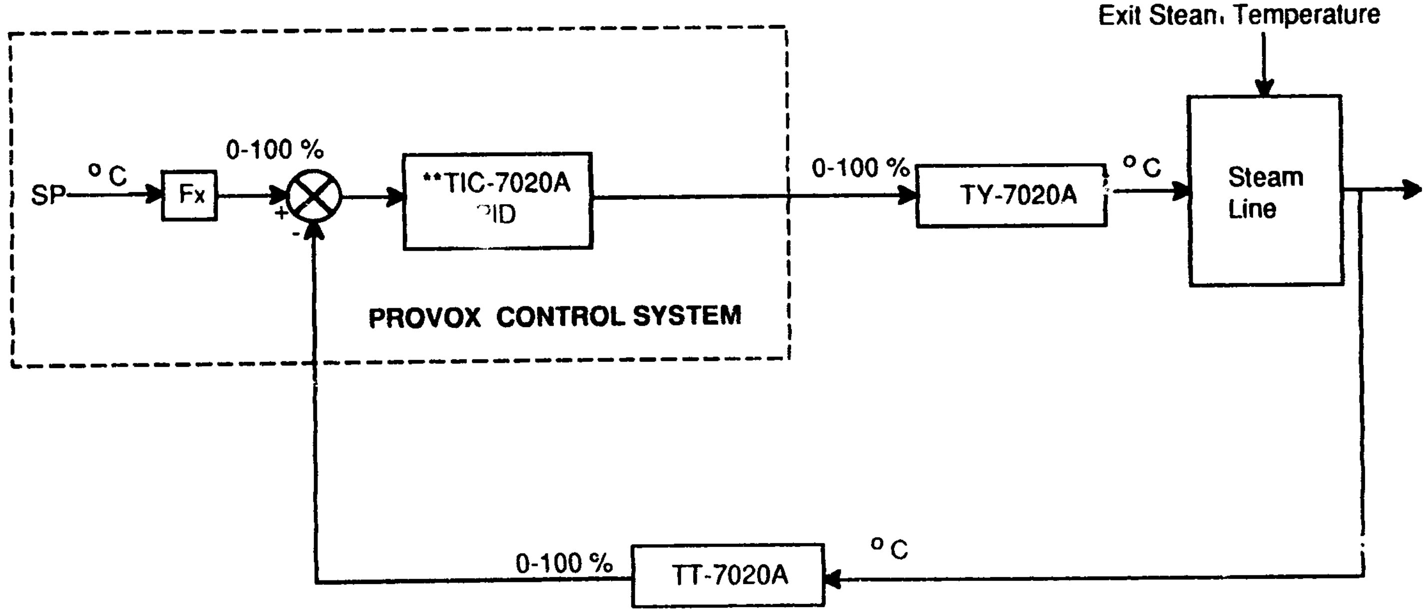

Figure 4-7 Block Diagram for Desuperheating Temperature Control Loop TIC-7020A

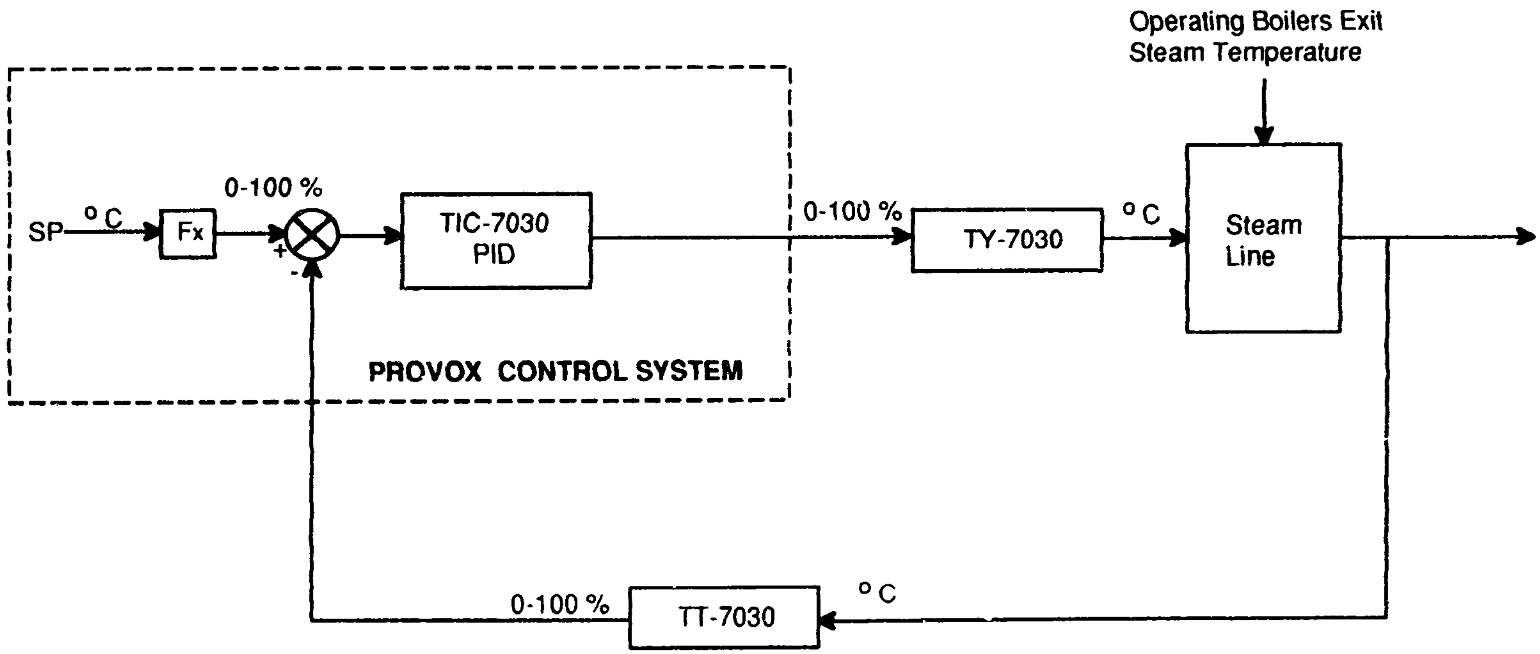

Figure 4-8 Block Diagram for Desuperheating Temperature Control Loop TIC-7030

The feedback for PIC-7020 is located on Intermediate Pressure Header No. 1. The feedback for PIC-7030 is located just before the tie line from No. 1 Intermediate Pressure Header intersects the exhaust side line of PY-7030A/B. For the purposes of this thesis this junction will then be referred to as No 2 Intermediate Pressure Header.

A similar operating analogy can be drawn between PIC-7020 and PIC-7030 as can be drawn between PIC-7040 and PIC-6200. Because of the parallel supply and the connection of the downstream headers through a tie line to the two stations, normal operations are to base load either PIC-7020 or PIC-7030 by putting either controller in manual and let the other controller be in automatic mode to take the swings.

Figures 4-7 and 4-8 illustrate the block diagrams for the control loops of the desuperheating stations. The temperature transmitter for these desuperheaters is located downstream of the injection point of the desuperheating spray. If the PRV station is in operation, the temperature controller will always be operating in the automatic mode.

4.4 Data Collection Points

Data were collected from the boilers and the steam line network in the heating plant from the fall of 1991 through to the spring of 1992. Figures 4-9 to 4-12 provides a schematic illustration of the actual location of the transmitters and valves from which the data were collected. The number of boilers operating during the winter season will vary with the steam demand, but typically one of the larger boilers (4 or 5) will be operating in conjunction with one or two of the smaller boilers (1, 2, or 3). This was the case when the data were collected.

As Boiler 5 was in a startup and testing phase during data collection, it ran for the majority of the winter. During the cold temperature periods when the data were collected, Boiler 3, and sometimes Boiler 1 were on line.

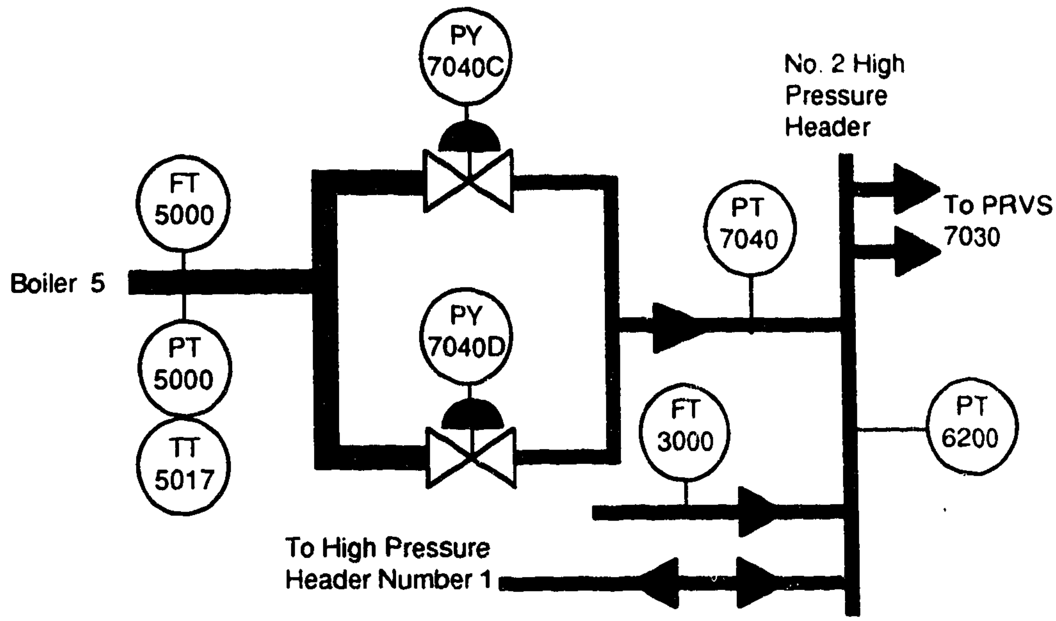

Figure 4-9 Point Tag Location for Data Collection for Pressure Control Loop PIC-5000 and PIC-7040.

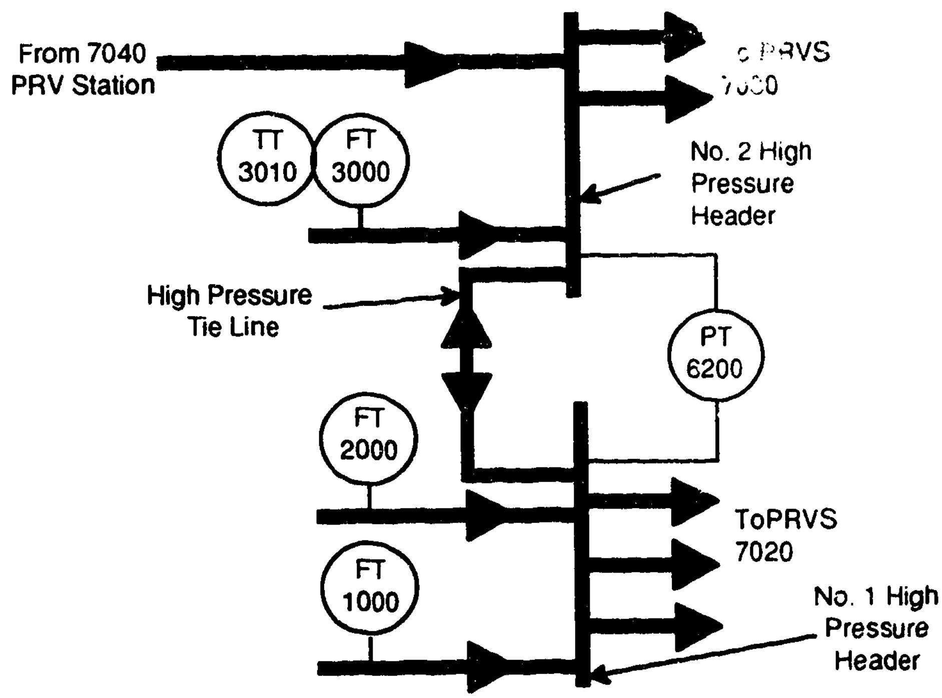

Figure 4-10 Point Tag Location for Data Collection Points for Pressure Control Loop PIC-6200.

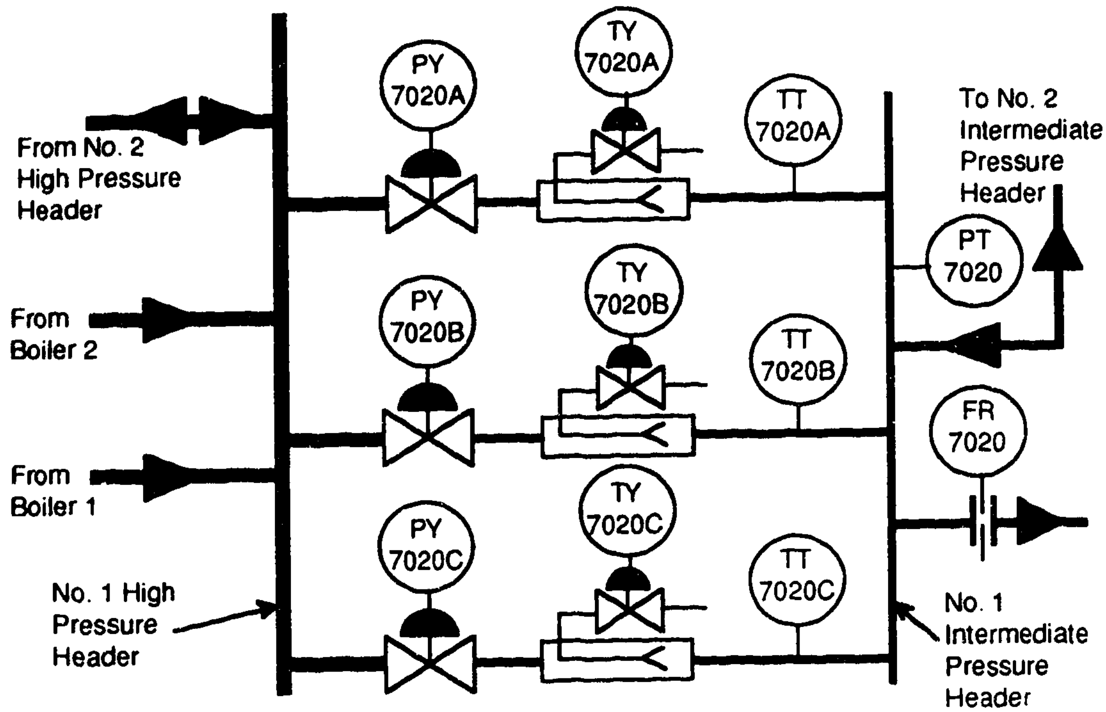

Figure 4-11 Point Tag Location for Data Collection for Control Loops PIC-7020 AND TIC-7020A, B, and C.

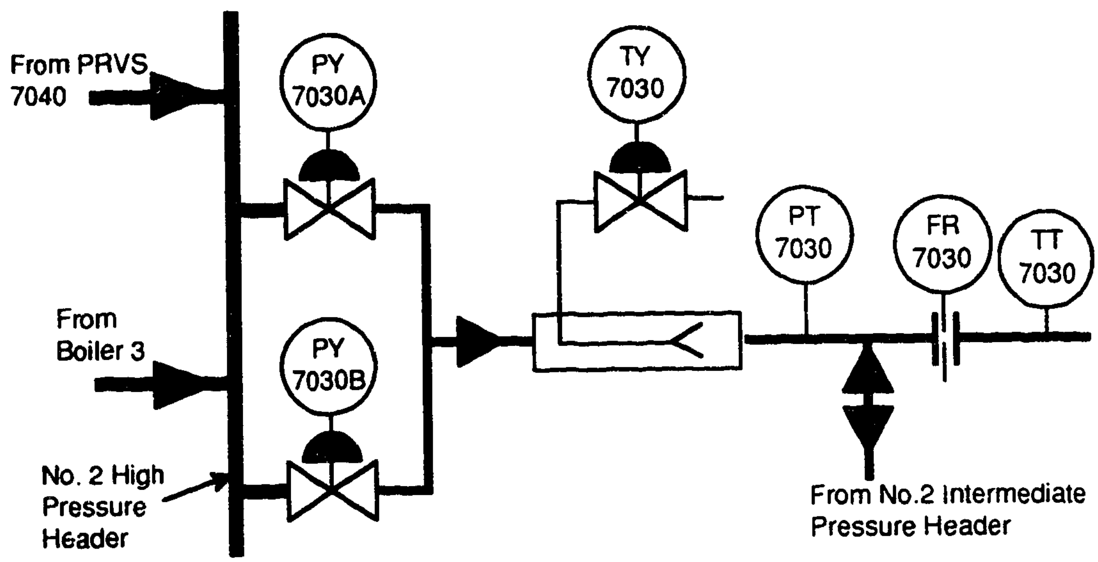

Figure 4-12 Point Tag Location for Data Collection for Pressure Control Loop PIC-7030 and Desuperheating Temperature Control Loop TIC-7030.

4.5 Data Collection System

The control and measurement points described in the previous section are part of a large distributed control system (DCS) that is used by the University of Alberta Utilities Department. This section will contain a brief description of the different components of this distributed control system.

The DCS operated by the Utilities department consists of four main components:

1. control computers;
2. console computers;
3. communication computers;
4. computer highway interface package (CHIP) computers.

The control computers provide the interface between the DCS and the field components. The measured values of flow, pressure, temperature, etc. are transmitted to the control computer to be used as a process variable. If this measurement is associated with a control loop, the control computer compares this process variable with the required setpoint and computes an error signal. This signal is then used in a control algorithm located in the control computers memory to compute a change in the control signal. This computed control signal is then converted to a current output and sent out to the final control element (valve, vanes...).

The console computers provide the operators with an interface to the control computers along with alarm handling capabilities and a platform for integrating and accumulating various measurements. The interface provides the operator with a visual display of the various components associated with a control loop such as the setpoint, process variable, and the control signal to the final control element. The operator can also use this console computer to change the values of the setpoint, control output, or operational mode of the control computer (automatic control, manual control...).

In a DCS there will be a large number of console computers and control computers. The Utilities Department has five console computers and twenty six control computers. Information needs to be shared between the various control and console computers in the DCS. The smooth flow of information between these devices is controlled by the communications computer.

The CHIP computer contains software that allows a host computer (mini or micro) to gain access to the information on all the other devices (control and console computers) on a distributed control system. Figure 4-13 is a schematic diagram of the various components contained within the CHIP computer. The main components consist of the CHIP kernel, a real time database, and CHIP programming library.

The CHIP kernel provides the communication software interface between the host computer and the DCS data highway. The software converts information from the native format of the host computer to a common communications format that is used by the other devices on the DCS data highway.

The real time database located on the CHIP computer is similar to real time databases contained on the console and control computers. This database can store information concerning all data parameters of a control point that exists on any of the control computers. This database can also be used to store information for the result of a calculation programmed into the CHIP computer. This information computed using the CHIP computer can be displayed on a console computer for use by plant personnel.

The software library is a group of user called subroutines that can be accessed by user written programs utilizing FORTRAN, Pascal, and C programming languages. These subroutines allow the programmer to access information from the real time database on the CHIP computer or access information directly from a real time database located on a control or console computer.

This CHIP computer was used to collect the transient data presented in Chapter 6. All the necessary measurement and control information from the field computers was routed to the real time database located on the CHIP computer. A FORTRAN program was then written utilizing the CHIP programming library to read the data located in the CHIP real time database at regular intervals. The data were then stored in ASCII files on the CHIP computer and subsequently downloaded to a micro computer for use in this work.

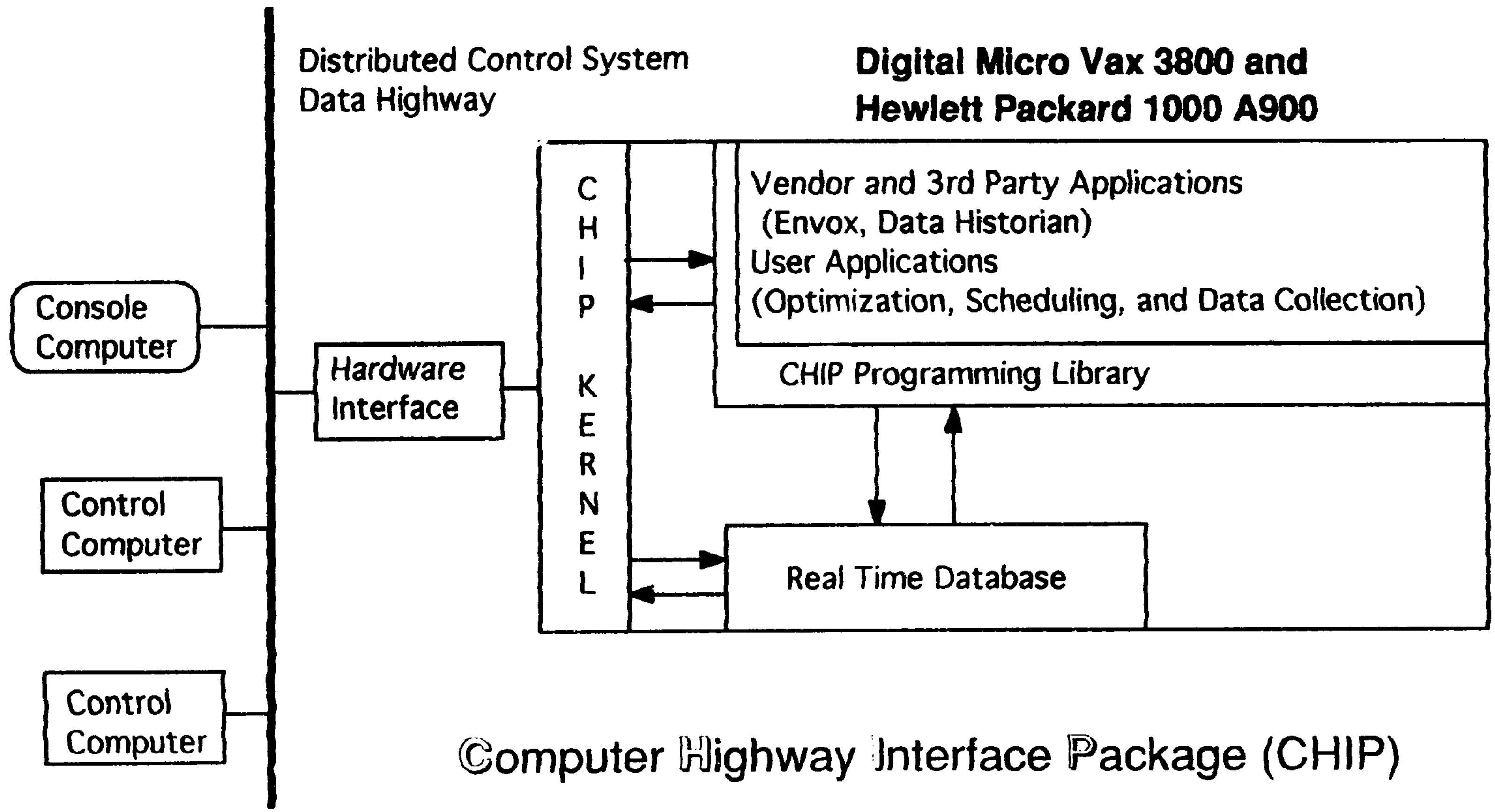

Figure 4-13 Computer Highway Interface Package Diagram

Chapter 5 Simulator

5.1 Introduction

To obtain a dynamic network solution, a three part process was used. The first step was to simplify the steam line network and identify the steam line components and boundary conditions. The second step involved designing and implementing a technique to obtain the steady state pressures at the nodes and the flows in the pipes. The third step was to incorporate the unsteady state equations developed in Chapter 3 into a dynamic simulator.

5.2 Simplification and Identification of the Steam Line Network

Figure 5-1 represents a schematic diagram of the simplified network used by the simulator. The simplification reflects the equipment operating in the plant during the collection of the data and assumptions used to simplify the solution. This simplified network then needed to have its components and boundary conditions labeled and identified to enable easy design and troubleshooting of the simulator code.

In order to begin with model verification, the data had to be analyzed and a decision made on where to start with the model verification. It was decided that the best transient data set would be used. This happened during two different trips of Boiler 5. One trip occurred when Boiler 5 was operating at its peak capacity. The second occurred when Boiler 5 was operating at approximately at one third capacity. During this transient period Boiler 2 and Boiler 4 were not operating. Since Boiler 4 was not operating the PY-7040A/B pressure reducing valves were not in service. Valves PY-7020B/C were also shut down during the data collection period so these equipment items are not shown in Figure 5-1.

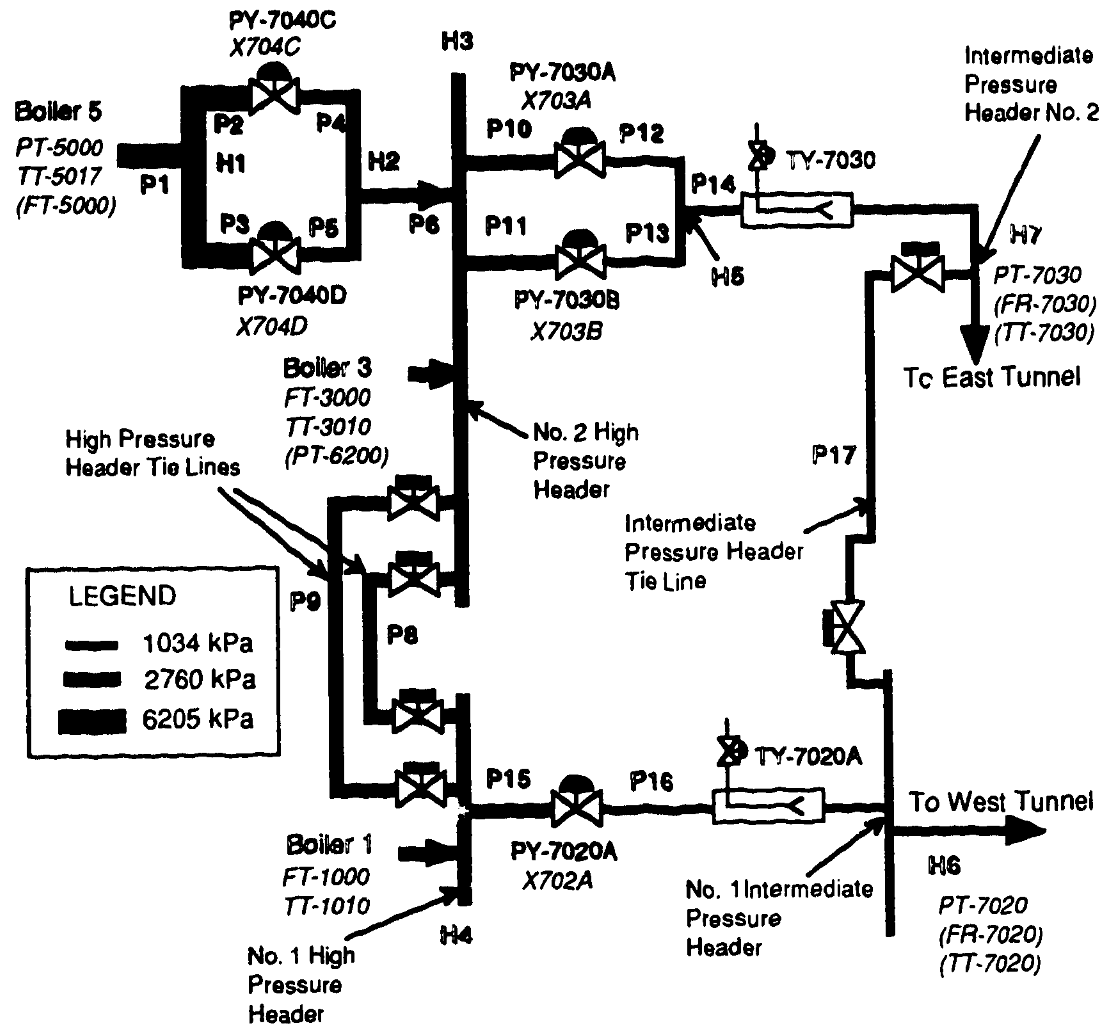

Figure 5-1 Modified Heating Plant Steam Line Network for Simulation.

A second simplification of the actual network, as represented by Figure 5-1, involves shifting Intermediate Pressure Header No. 2 and ignoring the flow from the plant auxiliaries into this header. This header can be considered as being directly connected to pipe 14. Physically the distance between Intermediate Pressure Header No. 2 and pipe 14 is very short so that the head losses due to this short section can be considered negligible. The flow from the plant auxiliaries is small compared to the rest of the flows and can thus be considered negligible.

To properly design and troubleshoot the simulator, the components and boundary conditions of the network need to be identified. The outlined lettering in Figure 5-1 represents the components of the network that were operating during data collection. The designation P# and H# number represent identification of a pipe and a header respectively. The point tag designations of the data collected appears in italicized letters on Figure 5-1. The point tags without brackets denote collected data for input boundary conditions to the simulator while the tags with brackets denote collected data that will be compared with simulator predictions.

5.3 Simulator Design

The steam line simulator for the heating plant is comprised of two main sections; it has a steady state section and a dynamic section. In order to begin the transient solution utilizing the method of characteristics, a steady state solution is required. Due to the complexity of the steam line network an explicit exact steady state solution can not be found from the direct application of the steady state continuity and momentum equations. This exact steady state solution is required because the method of characteristics is extremely sensitive to any perturbation of the boundary conditions. If an exact steady state solution is not available at the start of the dynamic simulation an artificial transient will be introduced which will propagate within the dynamic solution. A significant amount of computing time is required for any artificially induced transient to decay because of the small time increment required by the method of characteristics. For example for a pipe increment length, $\Delta x = 5$ metres at a given wave speed in the high pressure steam of 512 m/s, the time step is calculated from equation (3-26) to be approximately 0.0097 of a second.

The dynamic portion of the simulator can be executed once the steady state hydraulic profile and flow rates are determined. The purpose of the dynamic portion of the simulator is to calculate one of the dependent variables of pressure or flow given the other dependent variable as the boundary condition at the entry or exit of the flow into the network. The input to the simulator will also require the valve stem positions (percentage open) for the control valves.

5.3.1 Steady State

The steady state flow rates through each of the piping sections in the network and the corresponding pressures at all the intermediate nodes in the network are required as a basis for studying the unsteady state behavior. These nodes include pressures at the junctions where two or more different pipes meet and the pressures upstream and downstream of the pressure reducing valve. Once the pressures at the nodes and flows through each pipe are known, the steady state hydraulic gradient can be calculated along the discretized intervals of the pipe.

Figure 5-2 illustrates the process used to determine the steady state solution. The first step is to obtain an approximate solution. This approximate solution is needed as an initial guess to obtain an exact solution. The exact or final steady state solution calculation requires an iterative approach so the starting values input to this calculation must be close to the final solution or the solution will not converge to the proper values. The approximate solution is obtained by breaking the system into smaller parts and utilizing certain assumptions and intermediate steady state data from the data files to obtain an explicit solution. This calculation is made easier with the use of a spreadsheet.

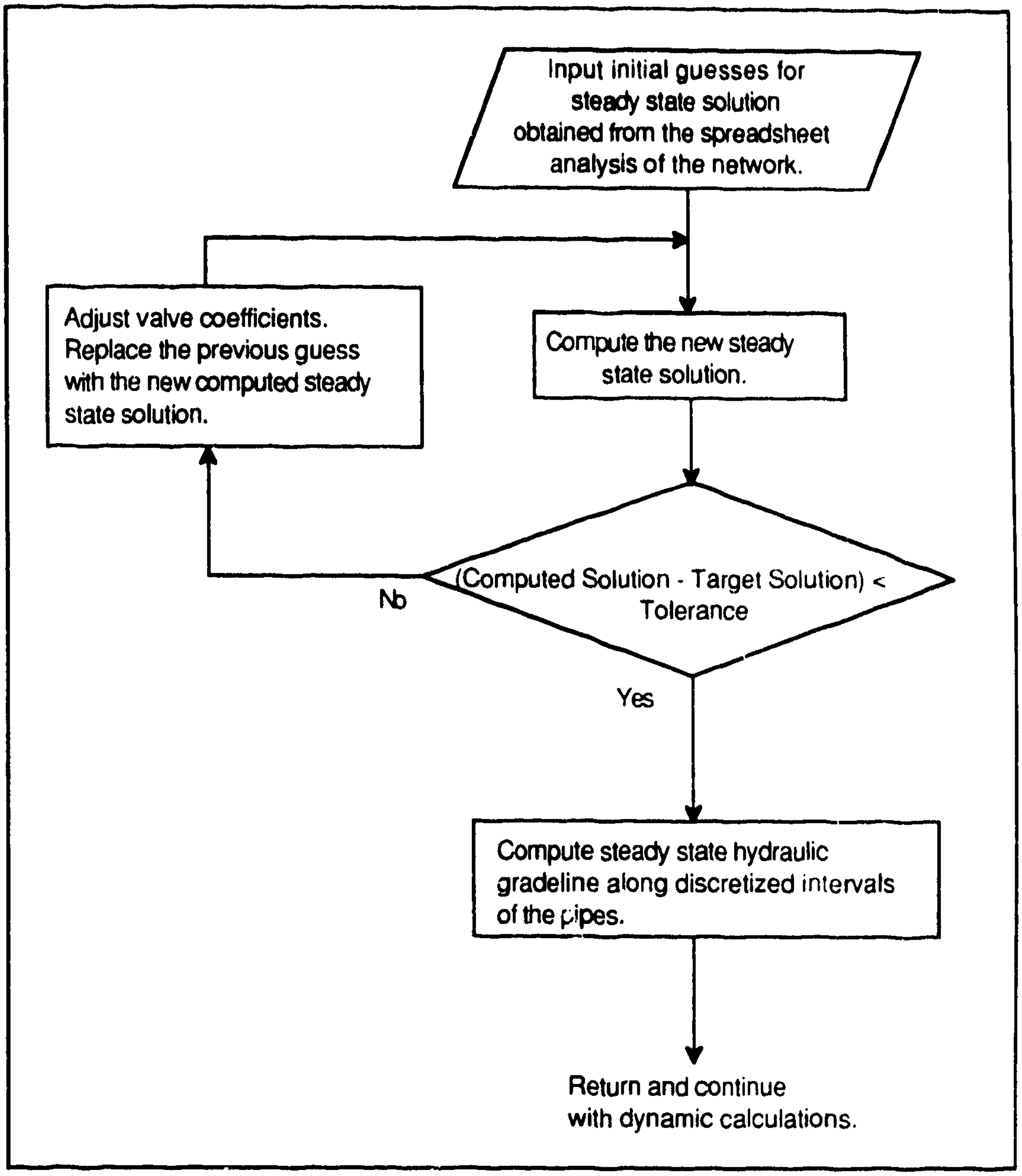

Figure 5-2 Steady State Steam Line Network Flow Chart

An identification must be made of all the unknown flow rates in the pipes and the unknown pressures at the nodes. Table 5-1 provides identification of these parameters.

Table 5-1: Identification of Unknown Pressures at Nodes and Unknown Flows in Pipes.

SYMBOL	DESCRIPTION
FT-5000	Exit flow from boiler 5 into pipe 1.
P_{H1}	Pressure at header 1.
w_2	Flow in Pipe 2.
w_3	Flow in Pipe 3.
P_{2U}	Pressure upstream of valve 7040C
P_{3U}	Pressure upstream of valve 7040D
w_4	Flow in Pipe 4.
w_5	Flow in Pipe 5.
P_{4D}	Pressure downstream of valve 704C
P_{5D}	Pressure downstream of valve 704D
w_6	Flow in Pipe 6.
P_{H2}	Pressure at header 2.
w_8	Flow in Pipe 8.
w_9	Flow in Pipe 9.
w_{10}	Flow in Pipe 10.
w_{11}	Flow in Pipe 11.
P_{H3}	Pressure at header 3.(PT-6200)
P_{H4}	Pressure at header 4.
P_{10U}	Pressure upstream of valve 7030A
P_{11U}	Pressure upstream of valve 7030B
w_{15}	Flow in Pipe 15.
P_{15U}	Pressure upstream of valve 7020A
w_{12}	Flow in pipe 12.
w_{13}	Flow in pipe 13.
P_{12D}	Pressure downstream of valve 7030A
P_{13D}	Pressure downstream of valve 7030B
w_{16}	Flow in pipe 16.
P_{16D}	Pressure downstream of valve 7020A
w_{14}	Flow in Pipe 14.
P_{H5}	Pressure at header 5.
w_{17}	Flow in pipe 17.
FR-7020	Delivery flow rate at header 6.
FR-7030	Delivery flow rate at header 7.

Once the unknowns are identified the steady state starting data from the data files are obtained. The data for the first simulation run are given in Table 5-2.

Table 5-2: Steady State Operating Conditions.

Point Tag	Steady State Value from Data
PT-5000	6190 kPa
TT-5017	392.45 °C
FT-3000	8.65 kg/s
TT-3010	349.3 °C
FT-1000	0.0 kg/s
TT-1010	N/A
PT-7030	1020 kPa
PT-7020	1058 kPa
FT-5000	39.83 kg/s
FR-7030	38.15 kg/s
FR-7020	10.40 kg/s
PT-6200	2700 kPa
X702	42%
X703	64.56%
X704	50.4 %

The actual spreadsheet calculations used to obtain the approximate steady state solution are given in Figures 5-3 to 5-7. These figures will be used as an aid to explain the procedure used to arrive at the initial unknown pressures and flows given in Table 5-1. The first part of the spreadsheet given in Figure 5-3 is an identification of the properties and constants used in subsequent calculations. The compressibility factors are obtained from Table 3-173 located in Perry and Green (1984). The density is calculated from equation (3-1) and the wave speed is calculated from equation (3-3). The wave speed is calculated based upon the exit steam conditions of Boiler 5. For the purposes of this initial calculation, this wave speed will be assumed to be the same for all sections of the network.

1. Identification of Properties and Constants.			
ZH=	0.89		-compressibility factor of steam for PRVS 7040.
RHOH=	23.0	(kg/m^3)	-density of steam for PRVS 7040.
ZM=	0.94		-compressibility factor of steam for PRVS 7020 and 7030.
RHOM=	9.8	(kg/m^3)	-density of steam for PRVS 7020 and 7030.
a=	508.0	(m/s)	-speed of sound
f=	0.015		-Darcy friction factor
N1=	6.31E-05		-conversion constants for
N2=	6.8947		valve equation for PRVS 7020 and 7030.
D#=			-diameter of pipe #.
A#=			-cross sectional area of pipe #.
L#=			-length of pipe #.

Figure 5-3 Identification of Properties and Constants for Steady State Spreadsheet Calculations.

Figure 5-4 illustrates the next part of the calculation. This calculation refers to the network section from the exit of Boiler 5 to the High Pressure Header 2 (Section 1). The purpose of the calculation will be to apply the steady state momentum equation (3-35) to pipe sections, a steady state continuity equation (3-36) to the header sections, and the valve equation (3-37) to the valves. From Table 5-2 we obtain the pressure (PT-5000) and the flow (FT-5000) of the steam exiting Boiler 5. The flow given by point tag FT-5000 will be the steady state flow in Pipe 1. Equation (3-35) is then applied to the pipe to obtain the pressure at Header #1 (P_{H1}). At this point it will be assumed that the flow into Header 1 will split in half. This assumption is based upon the fact that the resistance caused by pipes 2 and 3 and the valves 7040 C and D are approximately equal because their line lengths are similar and the valves are the same size and are open the same amount. With this assumption the upstream pressure at PY-7040 C (P_{2U}) can be calculated by applying equation (3-35). To obtain the downstream pressure at this valve (P_{4D}), equation (3-37) is applied. This equation requires the valve coefficient (CV704). This coefficient is obtained by using the percent opening of the valve (X704) obtained from Table 5-2. This percentage opening can then be converted into a valve coefficient using a correlation obtained experimentally or from manufacturer's data. In the case of PY-7040C this correlation was obtained experimentally. The results of which are contained in Appendix B. With the downstream pressure calculated, the pressure at Header 2 and Header 3 can be calculated. At steady state operating conditions the flow in Pipe 6 will be equal to the flow in Pipe 1.

```
2. Steady State Calculation for Section 1.

   PT-5000=  6187.5E+03  (Pa)
   FT-5000=  39.83       (kg/s)
    CV704=  0.0531      -valve coefficient for PRVS 7040 A

       PH1=  SQRT(PT-5000^2-a*f*L1/D1/A1*FT-5000^2)
             6114.0E+03  (Pa)

       P2U=  SQRT(PH1^2-a*f*L2/D2/A2^2*(FT-5000/2)^2)
             6105.1E+03  (Pa)

       P4D=  (P2U/RHOH-(FT-5000/2/CV704)^2)*RHOH
             2869.9E+03  (Pa)

       PH2=  SQRT(P4D^2+a*f*L4/D4/A4^2*(FT-5000/2)^2)
             2837.6E+03  (Pa)

       PH3=  SQRT(PH2^2+a*f*L6/D6/A6^2*(FT-5000/2)^2)
             2704.4E+03  (Pa)
```

Figure 5-4 Spreadsheet Calculation for Section 1.

The value calculated for P_{H3} from the spreadsheet is then compared to the steady state value of PT-6200 from Table 5-2. Since PT-6200 is the pressure measurement in this header, the values should be equal. Due to mismatches in the model parameters these values will differ. This can be caused by improper estimates of line losses, improper calibration of valve positioners, etc. If these values differ by a significant amount, then adjustment needs to made to the steady state model parameters. It has been found by experience, that the most sensitive model parameter is the valve coefficient. By adjusting this coefficient the error in model parameters can be compensated. When this coefficient has been adjusted properly an estimate of all the pressures at the nodes and the steady state flows in the pipes will have been obtained.

Figure 5-5 illustrates the calculation for the steady state flow rate in Pipe 17. Equation (3-35) is applied between Header 6 and 7 to determine this flow rate. The pressures represented by point tags PT-7020 and PT-7030 are used as boundary conditions.

```
3. Steady State Calculation to Determine Flow Rate in Pipe 17.

   PT-7020=  1056.2E+03  (Pa)
   PT-7030=  1018.7E+03  (Pa)

       w17=  SQRT((PT-7020^2-PT-7030^2)*D17*A17^2/a/f/L17)
             3.87         (kg/s)
```

Figure 5-5 Spreadsheet Calculation for Determining Flow Rate in Pipe 17.

Figure 5-6 shows the calculations from Header 6 through Pipe 14 and PY-7030A/B valves back to Header 3 (Section 2). The procedure followed here is the same as for part 2 (cf. Figure 5-4) of the spreadsheet except that this time the calculation proceeds back against the flow rather than following the flow. The valve coefficient (CV703) is obtained from the valve position (X703) given in Table 5-2 and the manufacturer's data given in Appendix B.

```
4. Steady State Calculation for Section 2.
   FR-7030=  38.15        (kg/s)
     CV703=  179.7        -valve coefficient for PRVS 7040 A
       w14=  FR-7030 - w17
             34.28        (kg/s)

       PH5=  SQRT( PT-7030^2 + a * f * L14 / D14 / A14^2 * w14^2 )
              1022.7E+03  (Pa)

      P12D=  SQRT( PH5^2 + a * f * L12 / D12 / A12^2 * ( w14 / 2 )^2 )
              1062.0E+03  (Pa)

      P10U=  ( P12D / RHOM / C2 + ( w14 / 2 / CV703 / RHOM / C1 )^2 ) * RHOM * C2
              2670.4E+03  (Pa)

       PH3=  SQRT( P10U^2 + a * f * L10 / D10 / A10^2 * ( w14 / 2 )^2 )
              2700.9E+03  (Pa)
```

Figure 5-6: Spreadsheet Calculation for Determining Flow Rates and Pressures in Section 2.

The steady state flow rates and pressures in Pipes 8, 9, 15, 16, PY-7020, and Header 4 are determined by using the calculations outlined in Figure 5-7. As with part 4 of the spreadsheet calculations (cf. Figure 5-6), the calculation proceeds back against the flow and CV702 is adjusted to correct for model inaccuracies. The only difference between these spreadsheet calculation expressions and those in Figure 5-4 and 5-6 is the calculation to determine the flows in Pipe 8 and 9. Because these pipes are of a different size and length, their resistance are not equal.

```
5. Steady State Calculation for Section 3.
  FR-7020=  10.4        (kg/s)
    CV702=  150         -valve coefficient for PRVS 7020 A
      w16=  FR-7020 + w17
            14.27       (kg/s)

     P16D=  SQRT( PT-7020^2 + a * f * L16 / D16 / A16^2 * w16^2 )
            1076.1E+03  (Pa)

     P15U=  ( P16D / RHOM / C2 + ( w16 / CV702 / RHOM / C1 )^2 ) * RHOM * C2
            2674.8E+03  (Pa)

      PH4=  SQRT( P15U^2 + a * f * L15 / D15 / A15^2 * w16^2 )
            2699.5E+03  (Pa)

        A=  1 - ( a * f * L9 / D9 / A9^2 ) / ( a * f * L8 / D8 / A8^2 )
            0.8680

        B=  - w16 * 2
            -28.5318

        C=  w16^2
            203.5166

       w9=  ( -B - SQRT( B^2 - 4 * A * C )) / 2 / A
            10.46       (kg/s)
            ( -B + SQRT( B^2 - 4 * A * C )) / 2 / A
            22.41       (kg/s)

       w8=  SQRT( W9^2 * ( a * f * L9 / D9 / A9^2 ) / ( a * f * L8 / D8 / A8^2 ))
            3.80        (kg/s)
            SQRT( w9^2 * ( a * f * L9 / D9 / A9^2 ) / ( a * f * L8 / D8 / A8^2 ))
            8.14        (kg/s)

      PH3=  SQRT( PH4^2 + a * f * L9 / D9 / A9^2 * U9^2 )
            2701.6E+03  (Pa)
```

Figure 5-7: Spreadsheet Calculation for Determining Flow Rates and Pressures in Section 3.

To obtain these flows, equation (3-35) is applied between Header 3 and Header 4 for both Pipe 8 and 9 as

$$P_{H3}^2 = P_{H4}^2 - a * f * L_9 / D_9 / A_9^2 * w_9^2 \qquad (5\text{-}1)$$

$$P_{H3}^2 = P_{H4}^2 - a * f * L_8 / D_8 / A_8^2 * w_8^2 \qquad (5\text{-}2)$$

Equating Equations (5-1) and (5-2) and rearranging yields

$$w_8^2 = \frac{a * f * L_9 / D_9 / A_9^2}{a * f * L_8 / D_8 / A_8^2} * w_9^2 \qquad (5\text{-}3)$$

Applying a steady state continuity equation to Header 4 we obtain

$$w_8 = w_{16} - w_9 \qquad (5\text{-}4)$$

If we square both sides of Equation (5-4) and equate to Equation (5-3) it follows that

$$0 = w_9^2 * (1.0 - \frac{a * f * L_9 / D_9 / A_9^2}{a * f * L_8 / D_8 / A_8^2}) - 2.0 * w_{16} * w_9 + w_{16}^2 \qquad (5\text{-}5)$$

which is a quadratic equation in terms of w_9 (w_{16} is known from a mass balance calculation on Header 6). The coefficients of this quadratic equation are referred to as A, B, and C in Figure 5-7. The solution of this quadratic equation yields two different values for w_9 and subsequently w_8. Performing a mass balance on Header 4 we see that there is only one solution that satisfies this equation.

The spreadsheet calculation results in reasonably accurate steady state conditions but the values can be refined even further to eliminate certain assumptions such as equal resistance between the lines containing PY-7040C/D and compensate for constant densities used in the valve equations.

Equations for the 33 unknowns given in Table 5-1 can be developed through the application of the steady state momentum equation (3-35), continuity equation (3-36), and valve equation (3-37). An IMSL

Math Library subroutine called DNEQNF is then utilized to obtain a simultaneous solution of the system of nonlinear equations. This subroutine utilizes a Newton type of solution. The user only need supply the function and an initial guess of the solution. The subroutine estimates the Jacobian for the solution so the derivatives of the functions do not need to be supplied.

It is important that the appropriate unknown be associated with the appropriate equation. If this ordering is not proper, then the solution of the system of equations will not converge. This will be caused by an ill-conditioned Jacobian in the subroutine that performs the solution. A map of this ordering is provided in table 5-3.

Table 5-3: Correspondence between Unknowns and Equations for Simultaneous Solution of Steady State Network Pressures and Flows.

SYMBOL	NETWORK COMPONENT	STEADY STATE EQUATION
FT-5000	Header 1	Continuity
P_{H1}	Pipe 1	Momentum
w_2	PY-7040 C	Valve
w_3	PY-7040 D	Valve
P_{2U}	Pipe 2	Momentum
P_{3U}	Pipe 3	Momentum
w_4	PY-7040 C	Continuity
w_5	PY-7040 D	Continuity
P_{4D}	Pipe 4	Momentum
P_{5D}	Pipe 5	Momentum
w_6	Header 2	Continuity
P_{H2}	Pipe 6	Momentum
w_8	Header 3	Continuity
w_9	Header 4	Continuity
w_{10}	PY-7030 A	Valve
w_{11}	PY-7030 B	Valve
P_{H3}	Pipe 8	Momentum
P_{H4}	Pipe 9	Momentum
P_{10U}	Pipe 10	Momentum
P_{11U}	Pipe 11	Momentum
w_{15}	PY-7020 A	Valve
P_{15U}	Pipe 15	Momentum
w_{12}	PY-7030 A	Continuity
w_{13}	PY-7030 B	Continuity
P_{12D}	Pipe 12	Momentum
P_{13D}	Pipe 13	Momentum

Table 5-3 (continued): Correspondence between Unknowns and Equations for Simultaneous Solution of Steady State Network Pressures and Flows.

SYMBOL	NETWORK COMPONENT	STEADY STATE EQUATION
w_{16}	PY-7020 A	Valve
P_{16D}	Pipe 16	Momentum
w_{14}	Header 5	Continuity
P_{H5}	Pipe 14	Momentum
w_{17}	Pipe 17	Momentum
FR-7020	Header 6	Continuity
FR-7030	Header 7	Continuity

The same type of approach used for the spreadsheet calculations to adjust for model inaccuracies is used in this portion of the simulator. The major difference is that the valve coefficients use a comparison of the boundary flows for adjustment rather than the pressure in High Pressure Header 3. The CV704 coefficient is adjusted based upon the error between the value calculated by the simulator and the value obtained from the data file. Similarly CV702 and CV703 are adjusted based upon the error in flow rates given by FR-7020 and FR-7030.

The above solution yields results that are accurate enough not to cause artificial transients in the initial dynamic responses predicted by the simulator. The results are then applied along discretized intervals of the network to obtain the hydraulic profile.

5.3 2 Dynamic Simulator

Once the steady state solution has been found, the dynamic portion of the simulation can begin. Figure 5-8 contains a flow chart used to describe the dynamic portion of the simulator.

Initially the simulator reads in the boundary conditions from the data file. The boundary conditions, described by their point tag designations, are PT-5000, X7040C, X7040D, FT-1000, FT-3000, X7030A, X7030B, X7020A, PT-7020, PT-7030, TT-5017,TT-3010, TT-1010. The initial values for these boundary conditions are fed to the steady state portion of the simulator.

The valve coefficients are adjusted in the steady state portion of the simulator to obtain the steady state pressures and flows. To keep utilizing the relationships between the valve openings used as boundary conditions and the valve coefficients that are needed in the equations, a percentage offset must be computed. This offset will then be subtracted from each new percent valve opening obtained from boundary conditions for each new time step before the correlations are used to compute new valve coefficients.

The remainder of the dynamic portion of the simulator consists of specialized subroutines used to handle each specific type of equipment in the steam line. They all utilize a Newton type of solution to solve for the unknowns. The dynamic equations used in each of the subroutines are described in Chapter 3.

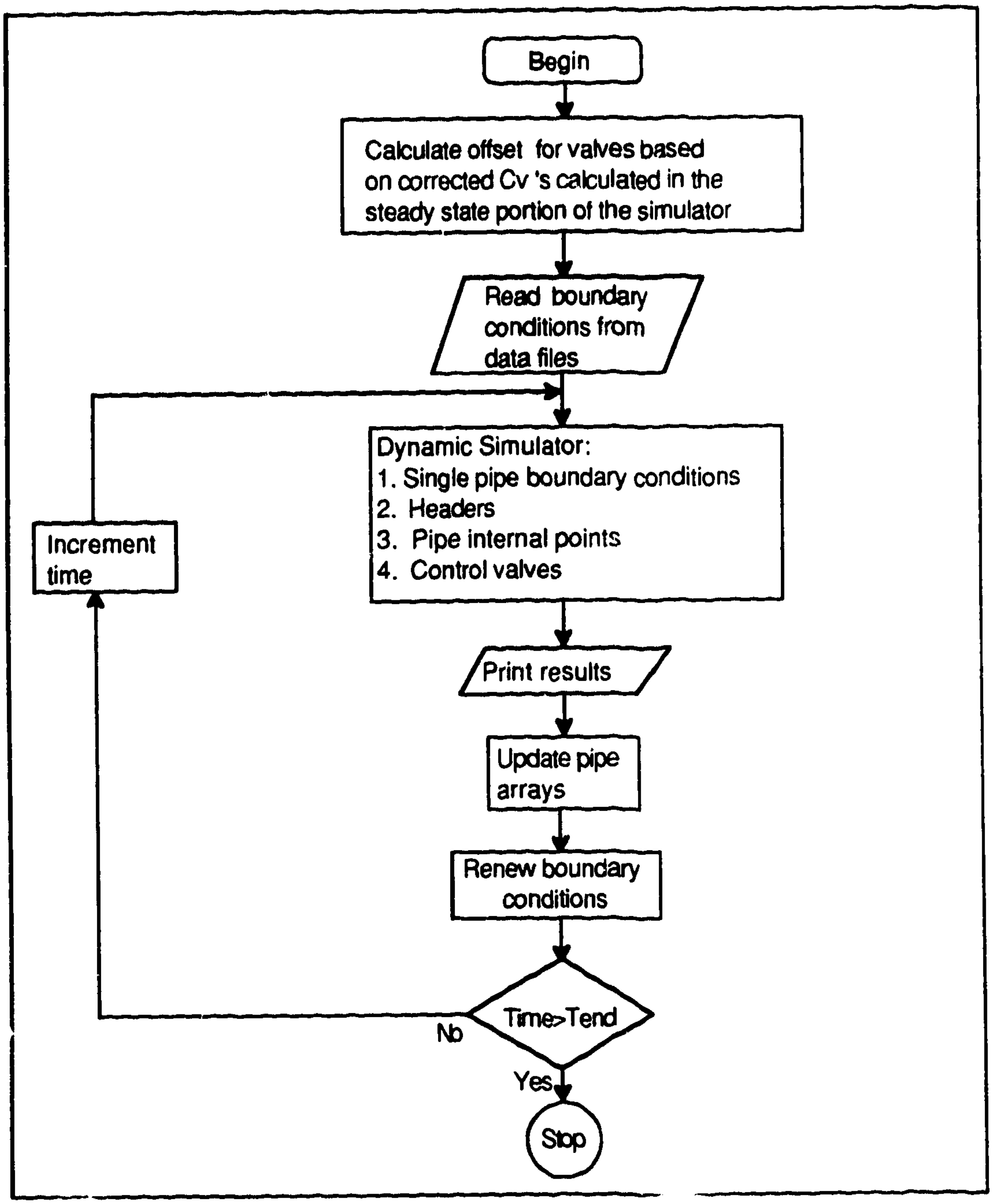

Figure 5-8 Flow Chart for Dynamic Steam Line Network Simulator.

Chapter 6 Simulation Results

6.1 Introduction

The reliability of the dynamic predictions of the different components of the simulator was assessed by comparison with previously published results. These tests were done not only to verify that the program was correct, but also to evaluate the assumption of isothermal flow employed in the heating plant model.

The first system considered was the single pipe results of Gorton (1978). The next system that was simulated was a small natural gas pipeline network studied by Yow (1971). This system was studied to test the junction or header boundary conditions. The third test of the simulator was the validation of the mathematical model of the heating plant steam line network. This was done by utilizing data collected from the heating plant during the winter of 1991.

Based on the testing procedure described above, the simulator was modified as necessary and then used to predict the transient response of the heating plant steam line network to a steam turbine trip. These results are given in the final portion of this chapter.

6.2 Single Pipe Simulation

Gorton (1978) provided simulation results for a steam turbine trip. The model consisted of a boiler drum connected to a single pipe. This pipe then feeds the steam to a steam driven turbine. At time t=0.0 the steam turbine is tripped causing the steam turbine stop valve to close. The closing time of the stop valve, represented as a linear decrease in the mass flow rate of the steam versus time, is given as 0.03 s. This defines one of the two necessary boundary conditions. The second boundary condition is given as a constant pressure in the drum of the boiler. Gorton models the pressure in the first element of the pipe as an isentropic expansion from the stagnation conditions in the boiler drum. This work will use the stagnation pressure in the drum as the static pressure in the first element of the pipe. The rest of the applicable initial conditions and model parameters are given in Table 6-1.

The assumptions employed by Gorton are the same as those employed in this work (cf. section 3.2) with two exceptions. Gorton's model employs the convective acceleration term in the momentum equation. Although this is not stated explicitly by Gorton (1978), it can be inferred from the given equations. Gorton supplies the partial differential equation form of the equations, and does not show the transformation of these equations into ordinary differential equations. The details of the method of integration of these equations are not given.

Table 6-1 Steady State Conditions and Model Parameters for Steam Turbine Trip Simulation [Gorton (1978)]

Parameter	Value
boiler drum pressure	7790 kPa
steady state steam flow	471.2 kg/s
pipe diameter	0.594 m
pipe length	45.72 m
friction factor	0.015
density of steam in the boiler drum.	40.45 kg/m^3

The second major assumption utilized by Gorton(1978) is that the flow is adiabatic. The model used in this work assumes isothermal flow. As was discussed in Chapter 2, the assumption of adiabatic flow would mean that the energy equation must be employed in the model. Consequently simulation of this system is viewed as a good test of the isothermal assumption.

A further complication in simulating the system studied by Gorton stems from the fact that no details of the wave speed calculation are given. Using the assumption of isothermal flow the wave speed was calculated from equation (3.3) to be 438 m/s. This value was assumed to remain constant throughout the duration of the simulation. It was found that while the relative magnitudes of the results were similar to those of Gorton, the propagation of the pressure waves did not track very well. An explanation for these differences can be linked to the form of the equation used to calculate the wave speed and the interval at which it was calculated. Gorton probably used the isentropic calculation of the wave speed given by equation (3-2). For a specific heat ratio of 1.3 for superheated steam [Rogers and Mayhew (1981)], the wave speed is calculated to be 500 m/s.

A second method can be used to see if this is indeed the wave speed that was used by Gorton. The dimensionless velocity (V/a) at steady state from Gorton's work was found to be 0.085. Utilizing the given steady state information of mass flow and density, the velocity at the entrance to the pipe was calculated to be 42.04 m/s. From this information the wave speed used by Gorton is calculated to be 494.56 m/s and the ratio of specific heats is calculated to be 1.27.

The isentropic wave speed calculation was used for the simulation comparisons. The results are given in Figures 6-1 to 6-6. In these figures the dimensionless pressure and the dimensionless velocity are shown as a function of time at three different locations along the pipe. Figures 6-1 and 6-2 give the results near the boiler at x/L=0.12, Figures 6-3 and 6-4 provide results near the midpoint of the pipe at x/L=0.52, and Figures 6-5 and 6-6 provide results near the stop valve at x/L=0.79.

The closing of the steam turbine stop valve causes the steam in the pipe at x/L=0.12 to be decelerated to zero velocity. This deceleration causes a pressure build up in the pipe resulting in a pressure wave travelling from the stop valve towards the boiler at a velocity equal to the wave speed. The pressure at this wave is higher than the boiler pressure; therefore, the steam starts flowing into the boiler. This negative velocity causes the pressure in the pipe to return to a value before the stop valve was closed. This causes the wave to be reflected into pipe traveling towards the stop valve.

The negative flow at the closed stop valve causes a pressure gradient that accelerates the steam flow back to zero velocity. Because of this acceleration a negative pressure wave travels back towards the boiler. The boiler pressure is higher than the pressure of the wave; the difference between the wave pressure and the boiler pressure causes the steam to accelerate and produce a positive flow back into the pipe. The pressure wave is then reflected and travels back towards the stop valve.

Agreement between this work and Gorton's work is found to be excellent at the midpoint of the pipe; however, results near the pipe boundaries are not as good. In particular the magnitude of the initial dimensionless pressure wave in Figure 6-2 and the magnitude of the dimensionless velocity profile in Figure 6-5 are not in good agreement. In both cases higher magnitudes of the dimensionless pressure and the dimensionless velocity are predicted by Gorton. Some of the discrepancies can be accounted for by the lack of resolution provided in the published figures by Gorton. Other explanations for the difference can be attributed to the adiabatic model used by Gorton versus the isothermal model used in this work. A more conclusive explanation would only be possible if the same model and boundary conditions were utilized.

The conclusion that can be drawn from the comparison of this work to the results from Gorton (1978) is that the assumption of an isothermal model and the assumption of ignoring convective acceleration is adequate for the case of transients caused by the sudden closing of the turbine stop valve.

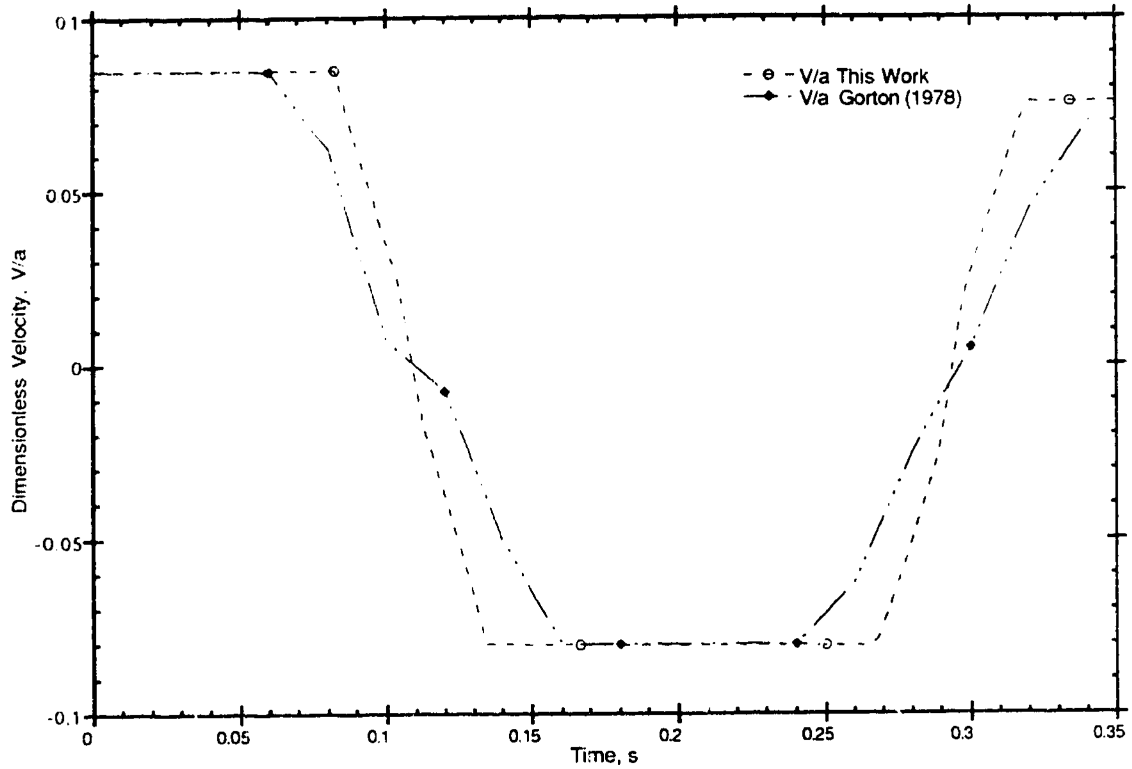

Figure 6-1 Adapted Comparison of the Velocity Response Predicted by the Simulator versus the Predicted Responses of Gorton (1978) at x/L=0.12

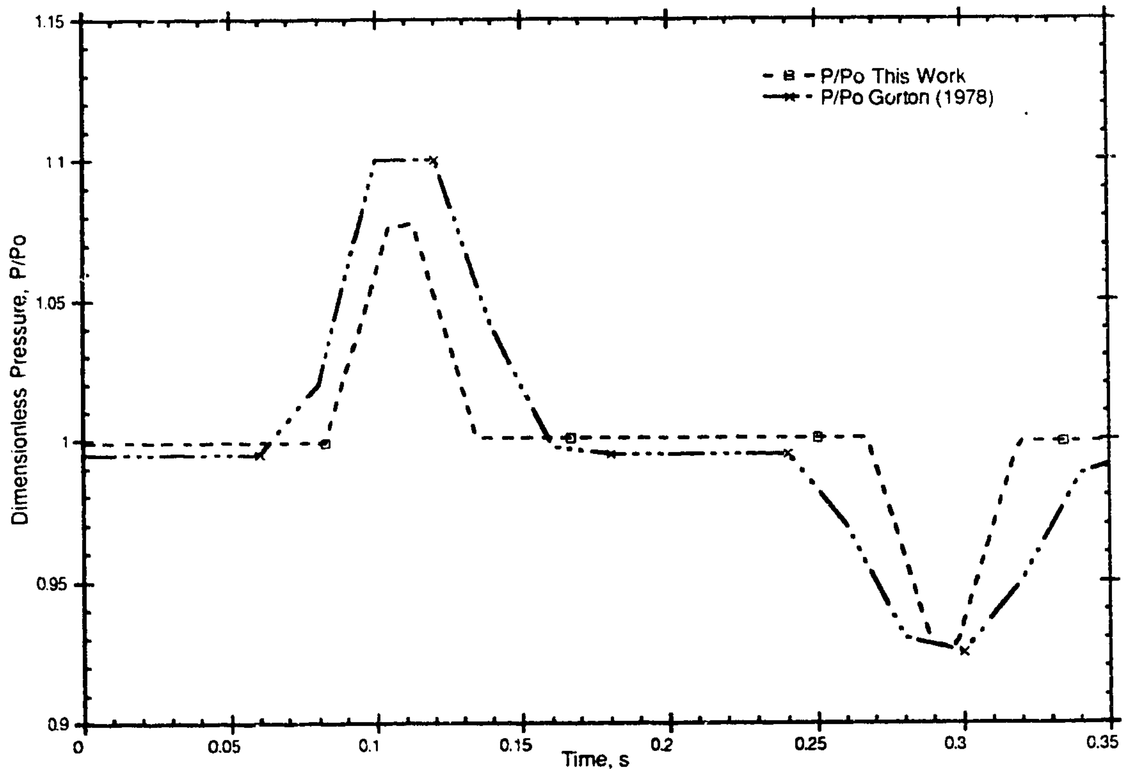

Figure 6-2 Adapted Comparison of the Pressure Response Predicted by the Simulator versus the Predicted Responses of Gorton (1978) at x/L=0.12

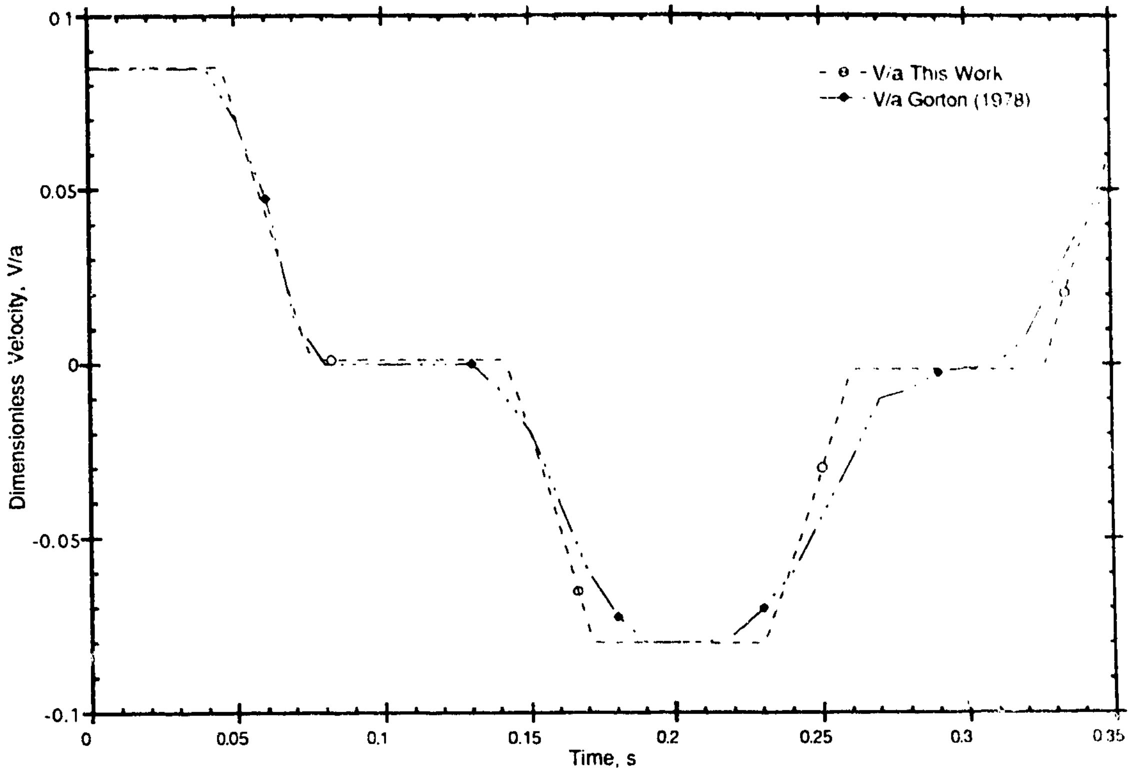

Figure 6-3 Adapted Comparison of the Velocity Response Predicted by the Simulator versus the Predicted Responses of Gorton (1978) at x/L=0.52

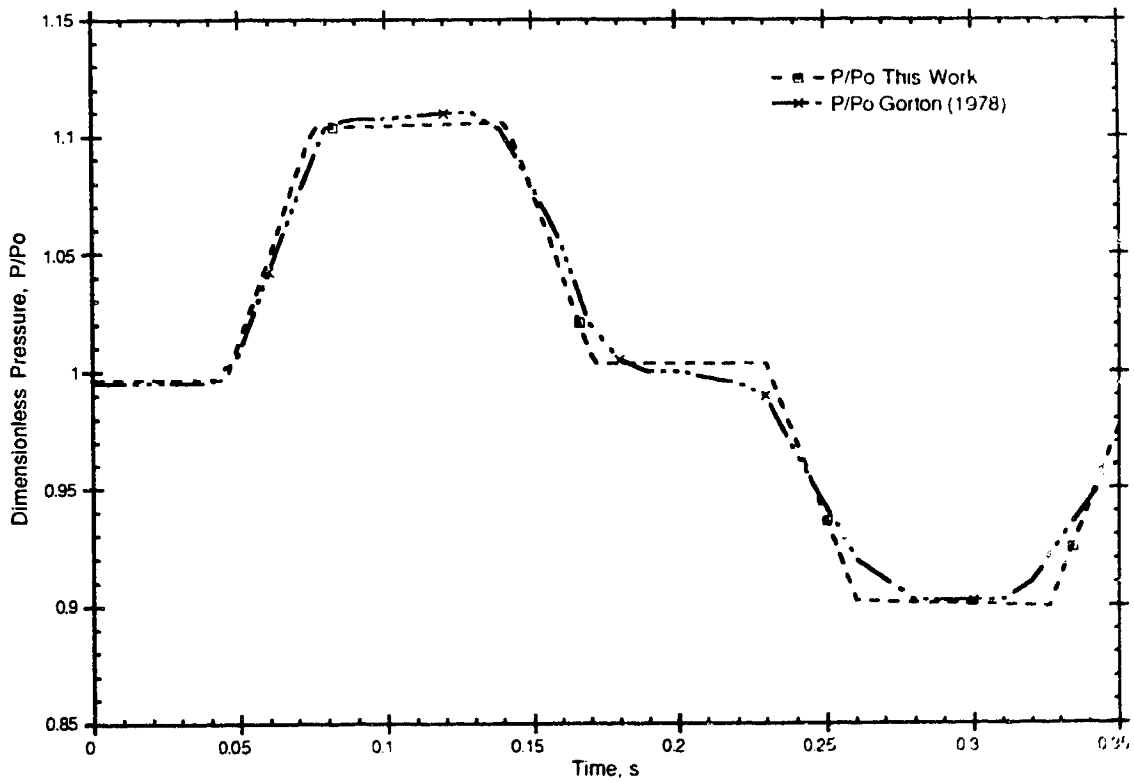

Figure 6-4 Adapted Comparison of the Pressure Response Predicted by the Simulator versus the Predicted Responses of Gorton (1978) at x/L=0.52

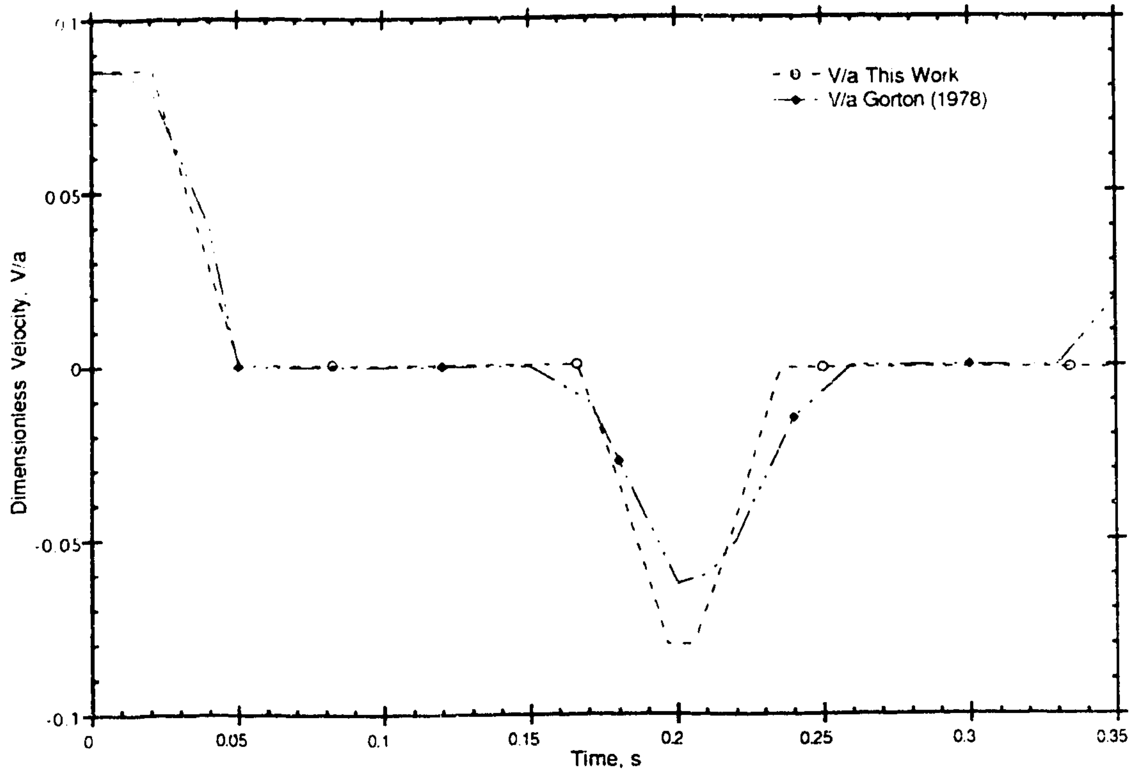

Figure 6-5 Adapted Comparison of the Velocity Response Predicted by the Simulator v .rsus the Predicted Responses of Gorton (1978) at x/L=0.79

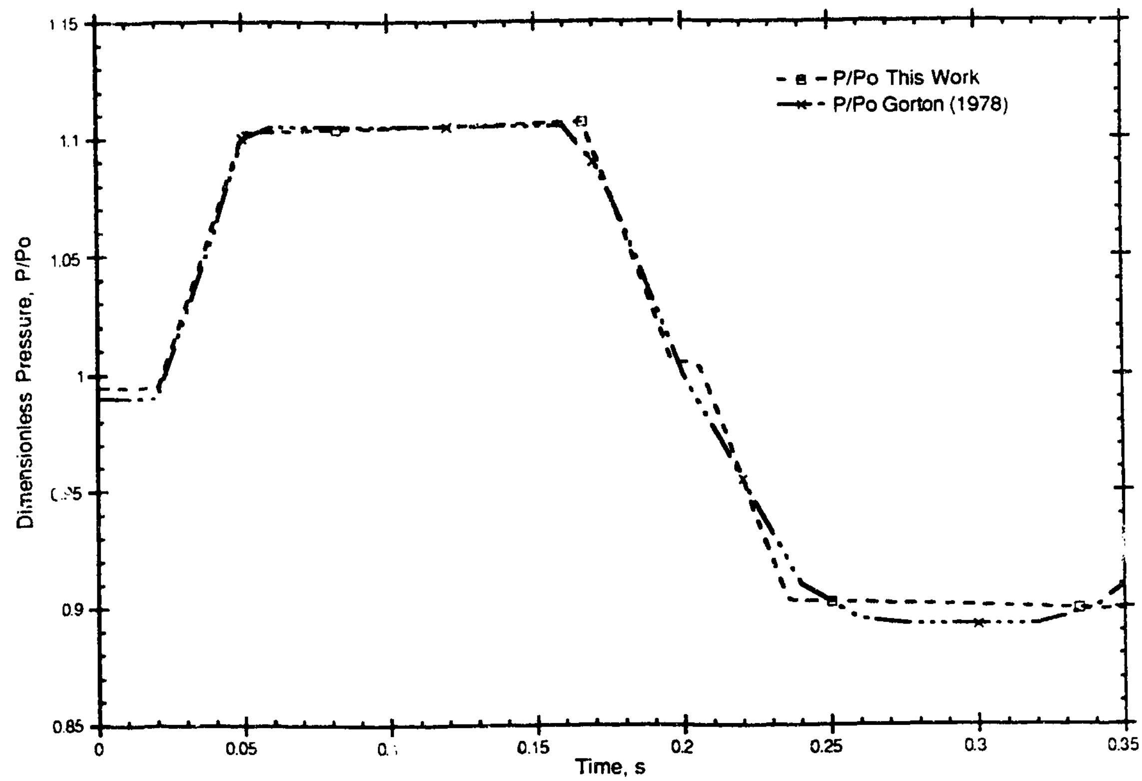

Figure 6-6 Adapted Comparison of the Pressure Response Predicted by the Simulator versus the Predicted Responses of Gorton (1978) at x/L=0.79

6.3 Network Simulation

Verification of the reliability of the dynamic responses predicted by the simulator developed in this work was evaluated by simulating the small natural gas network studied by Yow (1971). A schematic of the network along with the model parameters are illustrated in Figure 6-7. The steady state operating pressures and flow rates in each of the pipes of the network are given in Table 6-2.

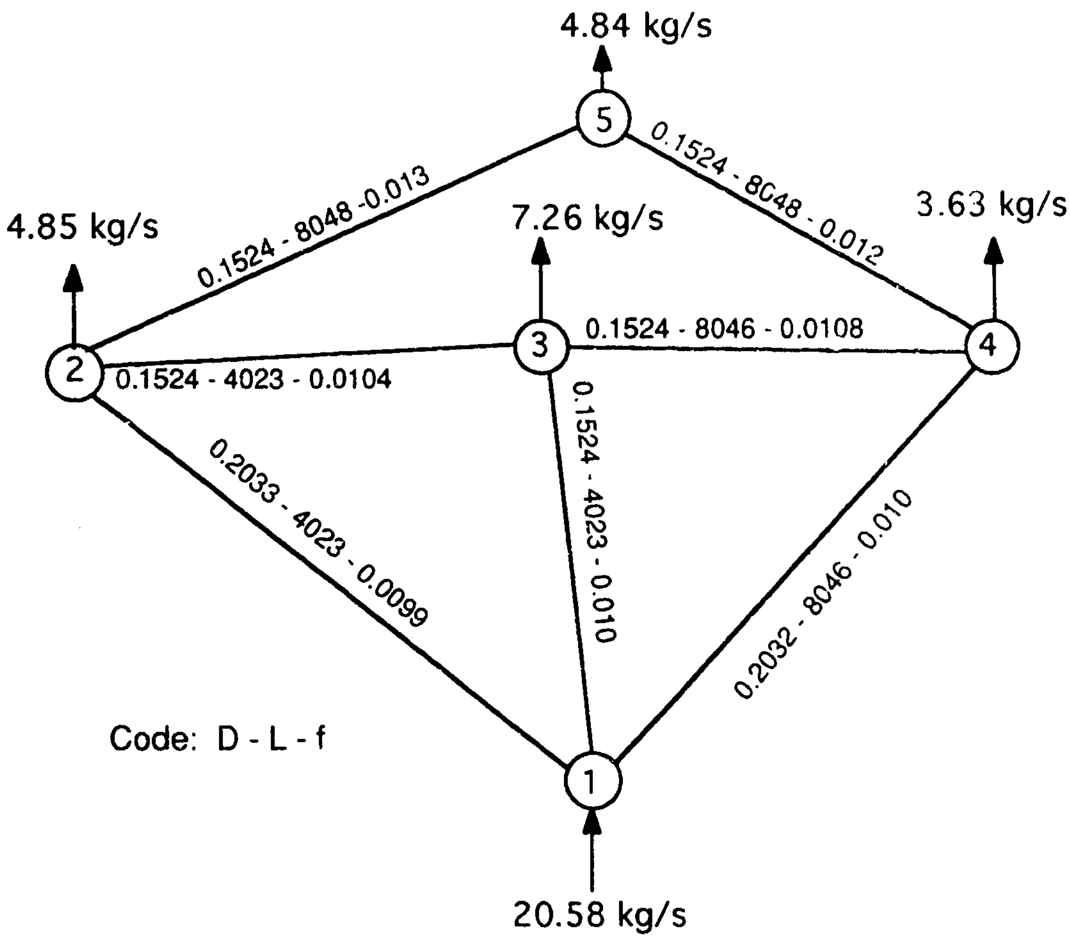

Figure 6-7 Natural Gas Network Schematic Diagram and Model Parameters for the Network Example from Yow (1971)

Table 6-2: Steady State Operating Parameters for the Network studied by Yow (1971)

FROM NODE	TO NODE	P_U(kPa)	P_D(kPa)	w (kg/s)	a (m/s)
1	2	2514.4	2113.2	8.90	355.63
1	3	2514.4	2005.6	4.83	353.40
1	4	2514.4	2027.1	6.85	354.74
2	3	2113.2	2005.6	1.94	377.95
4	3	2027.1	2005.6	0.49	461.18
2	5	2113.2	1828.4	2.11	393.50
4	5	2027.1	1828.4	2.73	352.50

The supply node, node 1, was held at a constant pressure of 2514.4 kPa with node 5 requiring a constant delivery flow of 4.84 kg/s. The rest of the nodes in the network had a required flow demand to be met as a boundary condition. The flow demands for each node are governed by the following equations:

$$w2 = 4.85 + step(t) * \frac{1.21}{3600} * t - step(t-3600) * \frac{1.21}{3600} * (t-3600) - step(t-7200) * \frac{0.61}{3600} * (t-7200) \qquad (6-1)$$

$$w3 = 7.26 + step(t) * \frac{1.21}{3600} * t - step(t-3600) * \frac{1.211}{3600} * (t-3600) \qquad (6\text{-}2)$$

$$w4 = 3.63 + step(t) * \frac{1.21}{3600} * t - step(t-3600) * \frac{1.21}{3600} * (t-3600) - step(t-3600) * \frac{1.21}{7200} * (t-3600) \qquad (6-3)$$

The wave speeds given in the last column of Table 6-2 were not provided in the work by Yow. They were calculated using equation 3-35 using the model parameters and steady state pressures and flows given by Yow. The discretization of the spatial variable for the pipe sections of the natural gas network is taken as

$$\Delta x = a\,\Delta t \qquad (3\text{-}26)$$

with the requirement that this equation must be satisfied for each pipe in the network. A more general form of equation 3-26 is given by Chaudry (1979) as

$$\Delta t_i = \frac{\Delta x_i}{a_i} = \frac{L_i}{n_i a_i} \; ; \; i = 1 \text{ to } N \tag{6-5}$$

A common time increment is needed so that the boundary conditions can be applied to the junctions of the network. The wave speed in each pipe section or the length of each pipe section must be adjusted to obtain the common time increment. Chaudry suggests adjusting the wave speed because it can not be precisely calculated; therefore, minor adjustments in its value are acceptable.

For this work the average wave speed, calculated from the values given in Table 6-2 to be 365 m/s, was held constant throughout the duration of the simulation. A time increment of 11 seconds is used by Yow. The spatial increment corresponding to this time increment and wave speed is 4000 m. The spatial increments are also rounded off to obtain an integer value for discretization of the pipe intervals.

The flow rates and pressures predicted by the simulator are compared with the predictions of Yow in figures 6-8 to 6-12. Figure 6-8 shows the predicted mass flow rate required at the supply node, node 1, to meet the boundary condition demand flows required at nodes 2 to 5 for a fixed supply pressure at node 1. Figures 6-9 to 6-12 compare the predicted pressures at nodes 2 to 5 as calculated by Yow and by the simulator developed in this work.

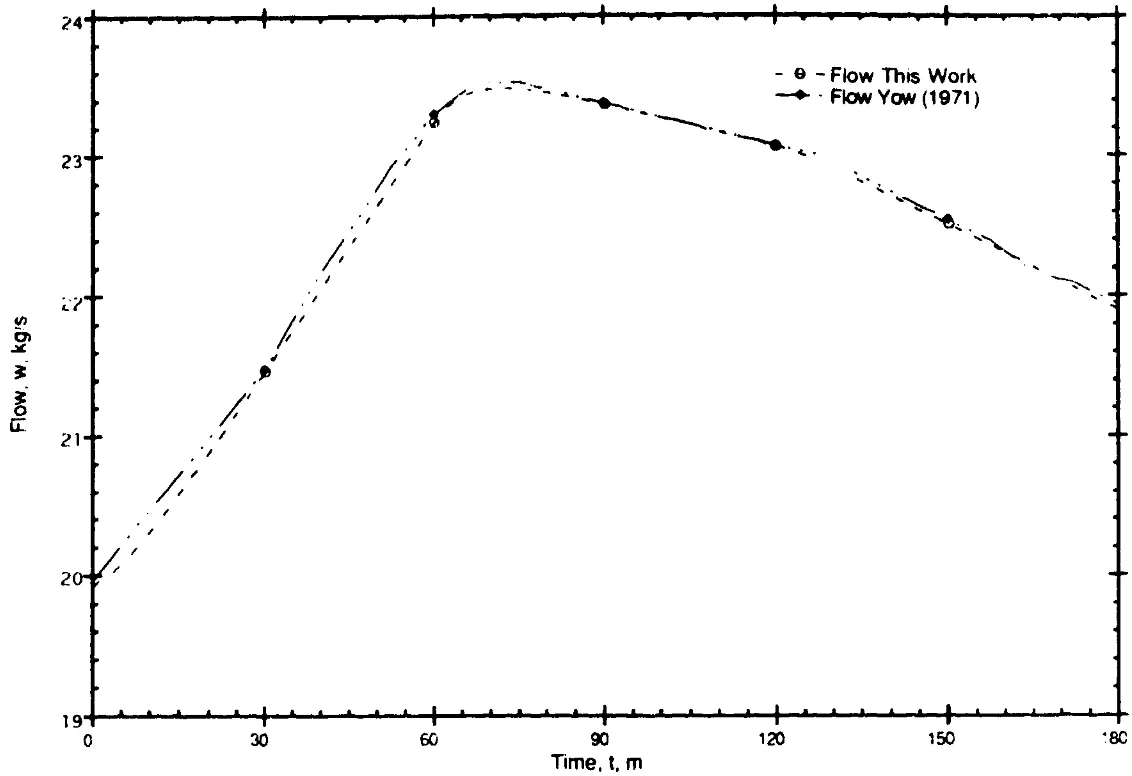

Figure 6-8 Adapted Comparison of the Mass Flow Rate Response at Node 1 Predicted by the Simulator versus the Predicted Response of Yow (1971)

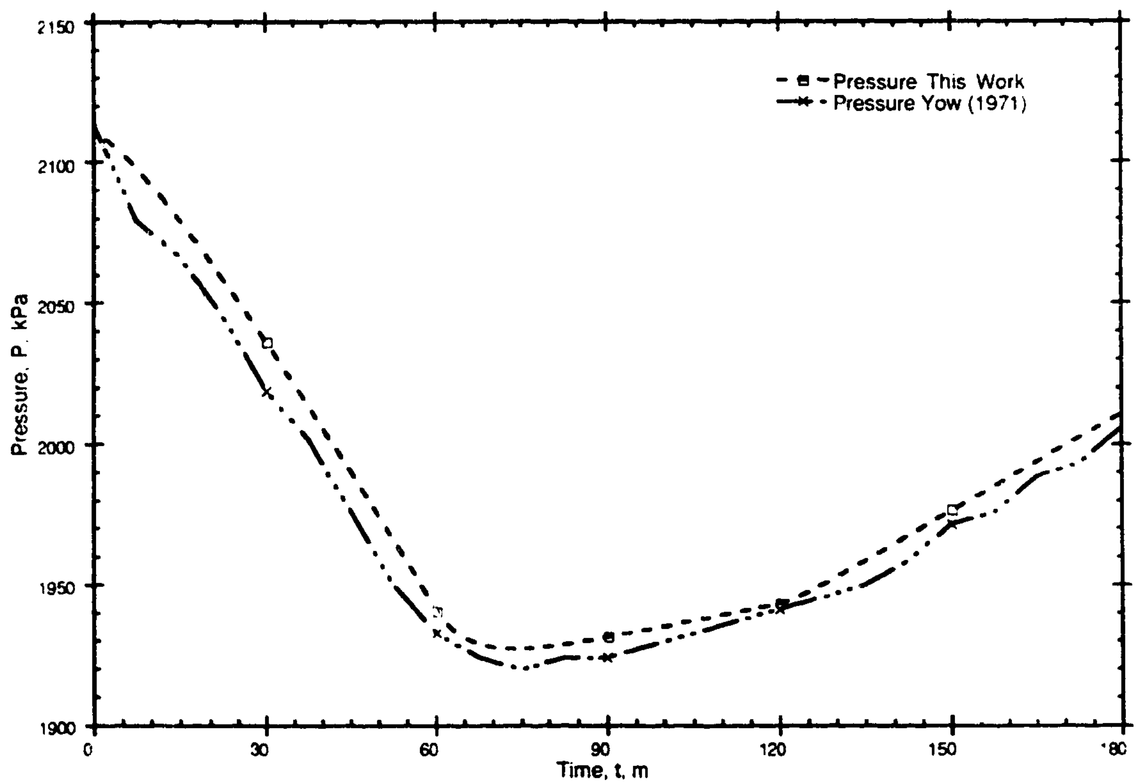

Figure 6-9 Adapted Comparison of the Pressure Response at Node 2 Predicted by the Simulator versus the Predicted Response of Yow (1971)

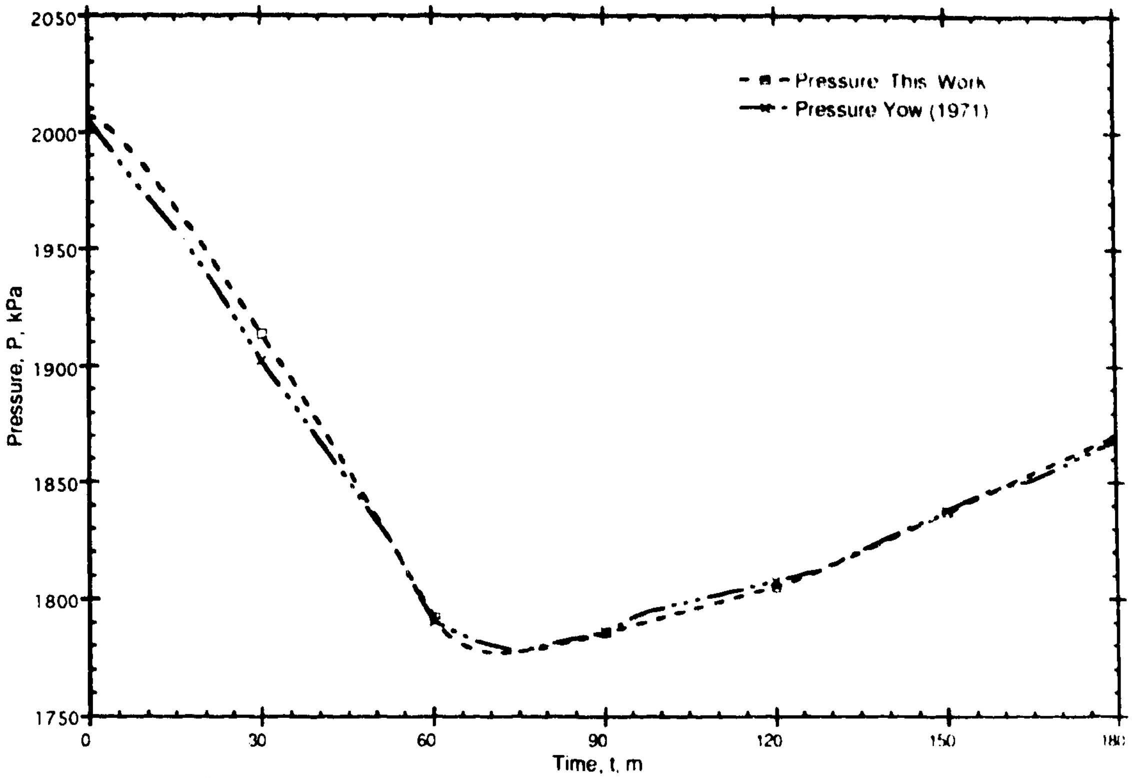

Figure 6-10 Adapted Comparison of the Pressure Response at Node 3 Predicted by the Simulator versus the Predicted Response of Yow (1971)

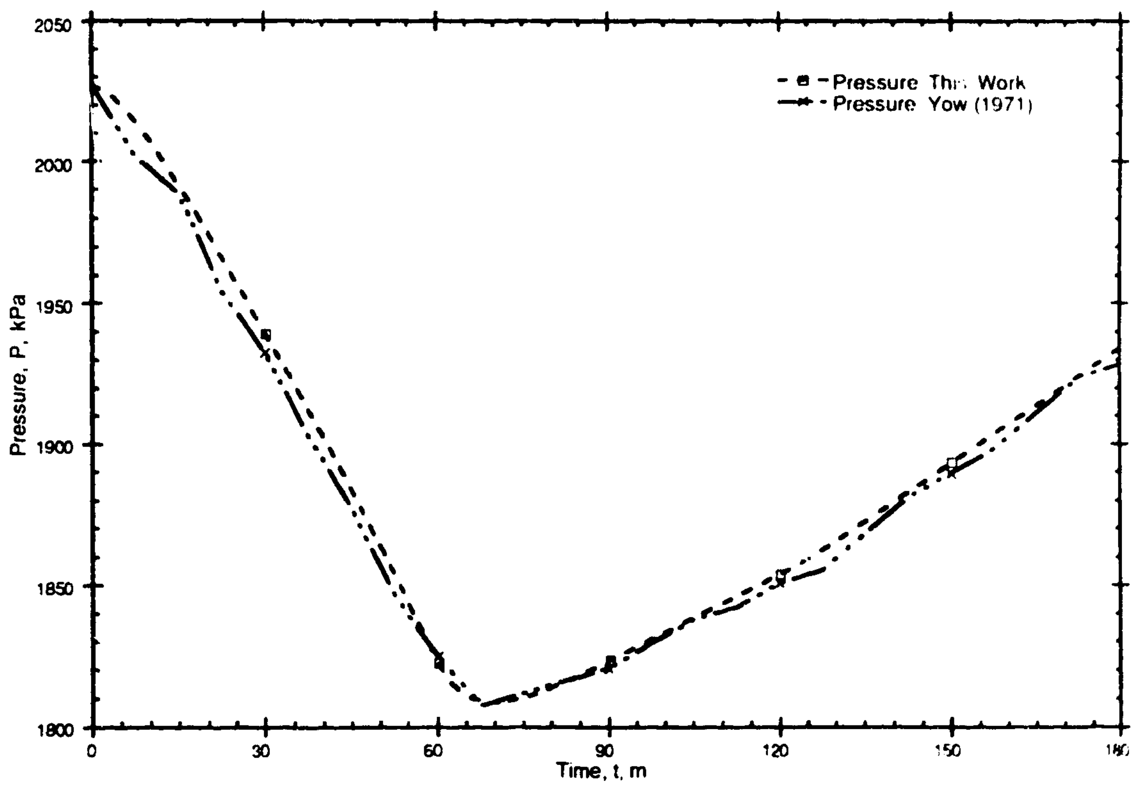

Figure 6-11 Adapted Comparison of the Pressure Response at Node 4 Predicted by the Simulator versus the Predicted Response of Yow (1971)

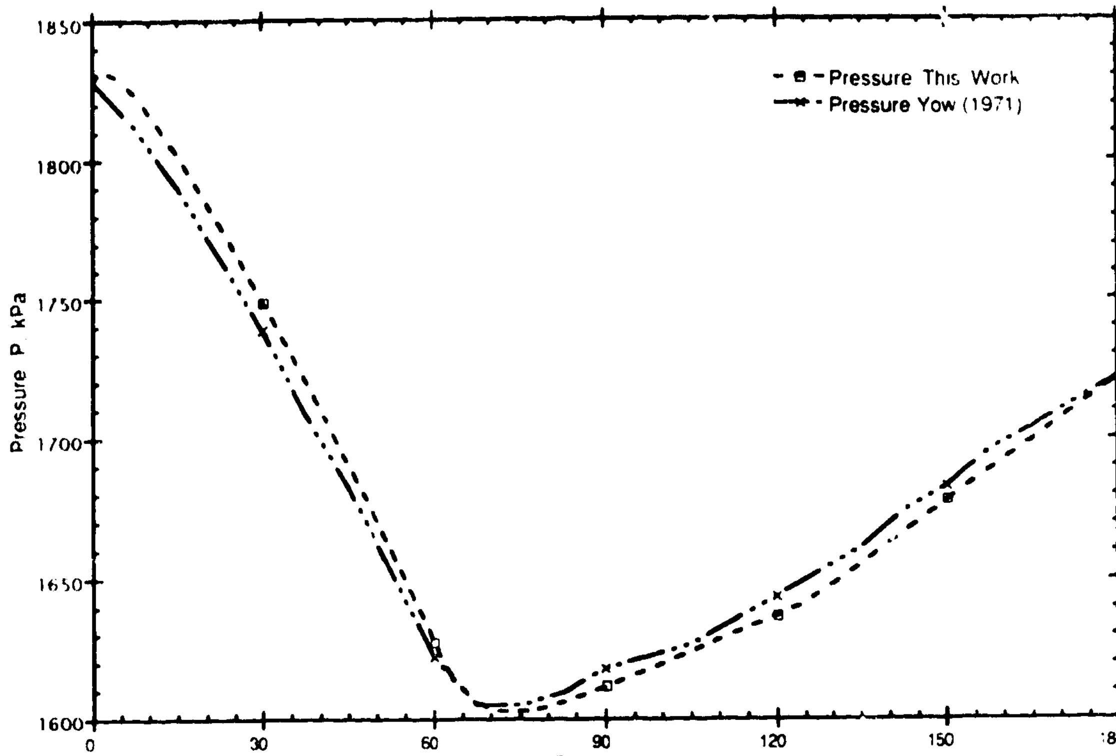

Figure 6-12 Adapted Comparison of the Pressure Response at Node 5 Predicted by the Simulator versus the Predicted Response of Yow (1971)

As can be seen from these results, the responses predicted by the simulator show very good agreement with the predicted results reported by Yow. Some of the discrepancies can be accounted for by the lack of resolution provided in the figures presented by Yow. Another source for discrepancies is that Yow does not provide complete detail concerning modeling and numerical techniques simply stating that the results imply an accurate model. For example, Yow does not state if a different wave speed was used for each pipe in the network rather than the average wave speed that was used in this work.

The results from this comparison show that the use of an average wave speed for a network analysis appears to be sufficient even with widely varying wave speeds in the different sections of the pipes.

6.4 Heating Plant Transient Data Analysis (Boiler 5 Shutdown)

To substantiate the mathematical model, flow , temperature , and pressure data were collected in the University of Alberta Heating Plant during the winter of 1992. This section will present comparisons of simulation runs against the data that were collected. The first transient data were recorded during a commissioning run of Boiler 5. Boiler 5 was operating at peak capacity when it was shut down by its safety system. The second transient data were collected when Boiler 5 was operating at approximately one third of the rated steam flow capacity. Again the boiler was tripped off-line by its safety system.

6.4.1 Transient Data Analysis of the First Boiler 5 Shutdown

The steady state operating parameters for the first case are given previously in Table 5-2. The system model parameters are located in the appendices. The comparison of the results predicted by the simulator versus the measured data are given in Figures 6-13 to 6-18. A complete description of the sequence of events that occurred during the trip is needed to fully understand the results. The reader will find for the discussion that follows, reference to the heating plant steam line layout given in Figure 5-1, the control system block diagrams given in Figures 4-2 to 4-8, and point tag locations and descriptions given in Figures 4-2 to 4-12 and Table 4-3 will be helpful.

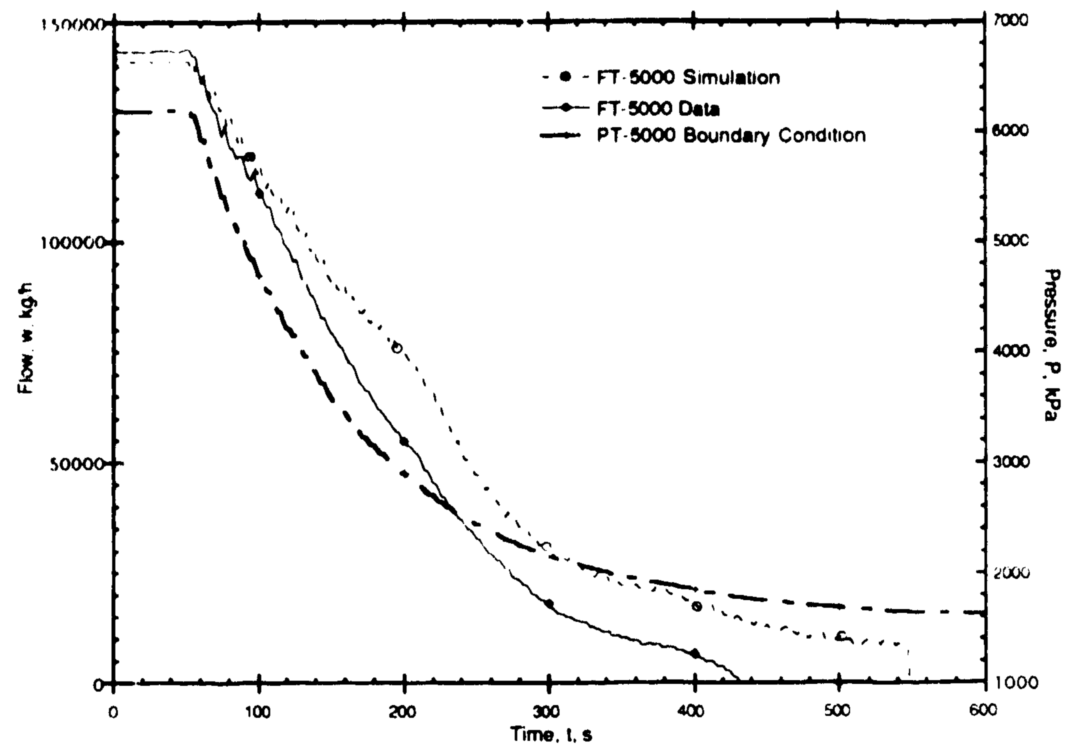

Figure 6-13 Predicted and Experimental Flow Response Comparison

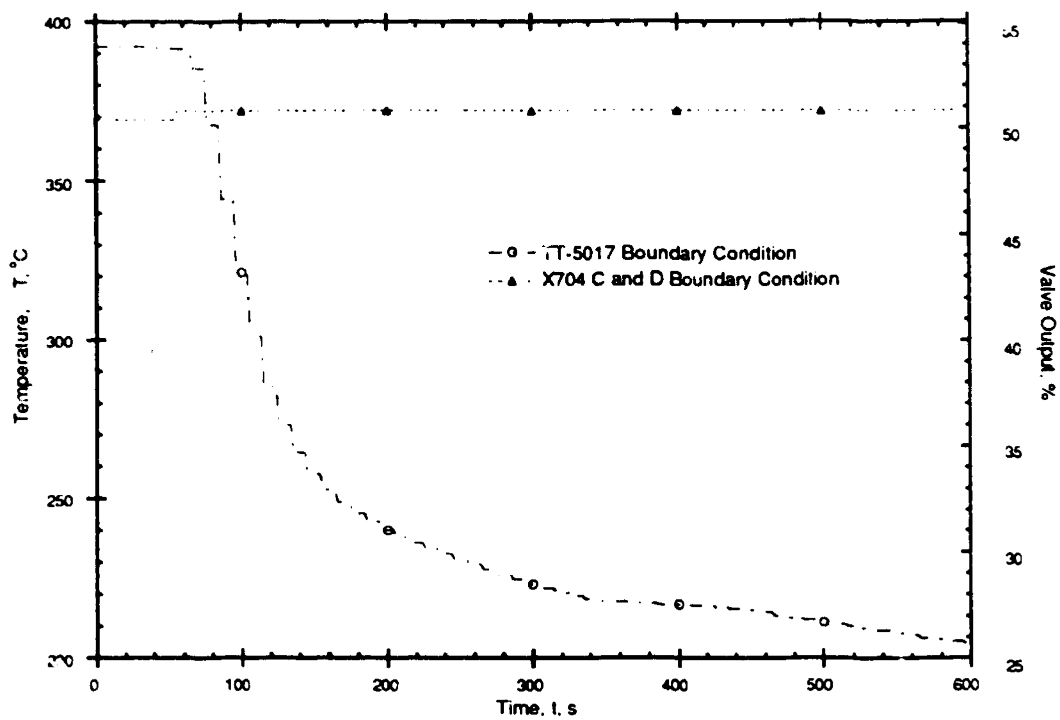

Figure 6-14 Temperature and Valve Position Boundary Conditions

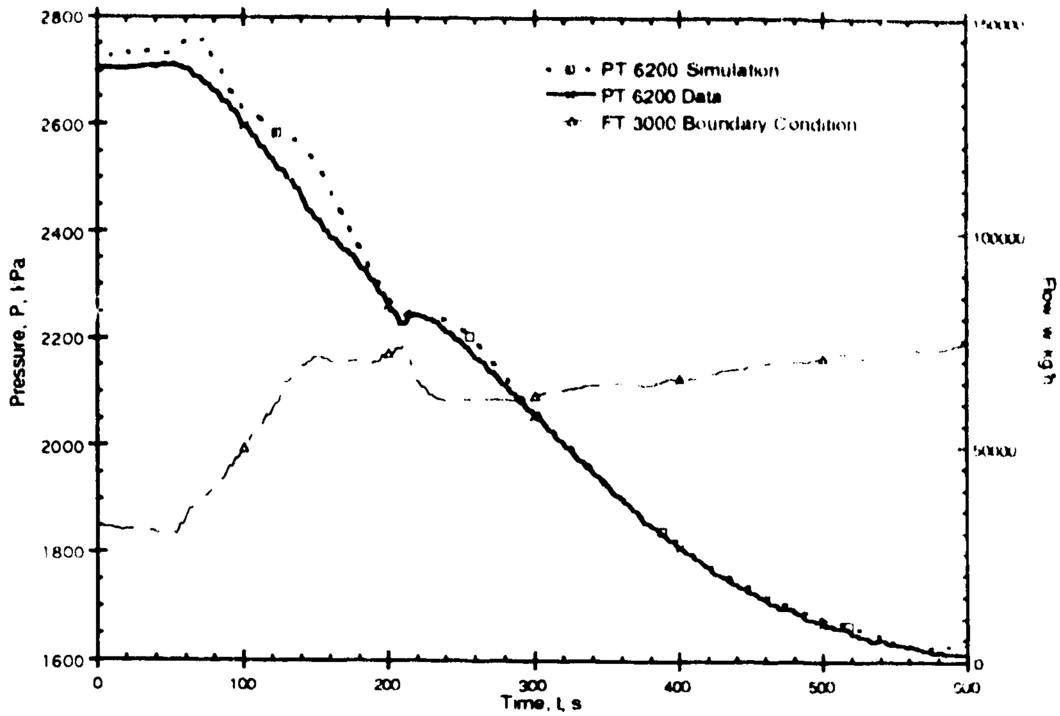

Figure 6-15 Predicted and Experimental Pressure Response Comparison

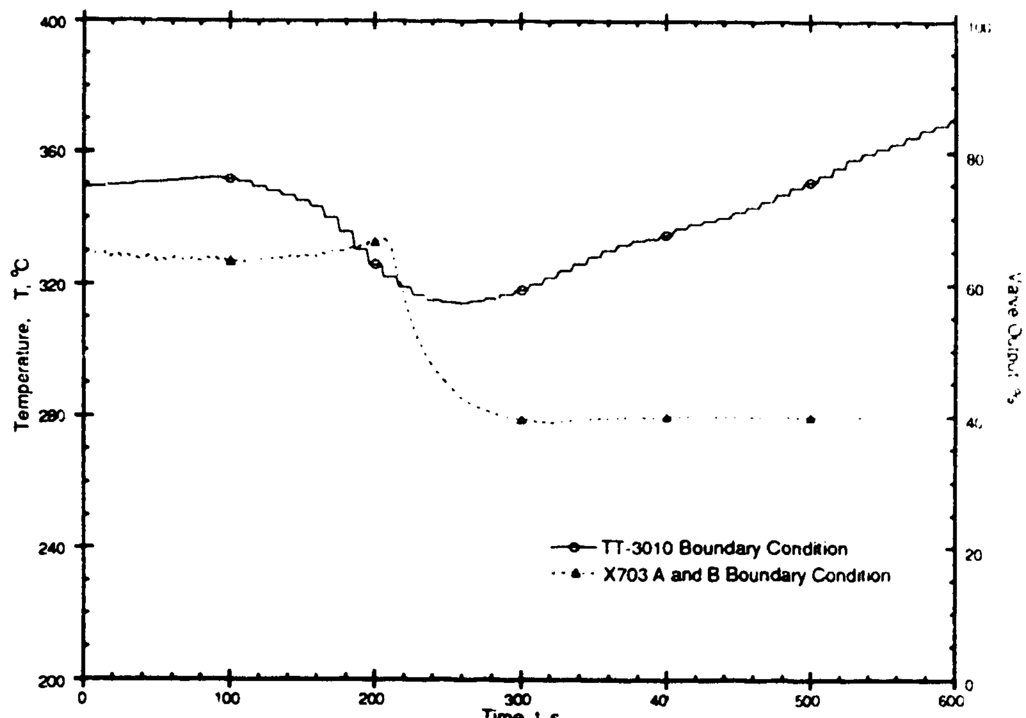

Figure 6-16 Temperature and Valve Position Boundary Conditions

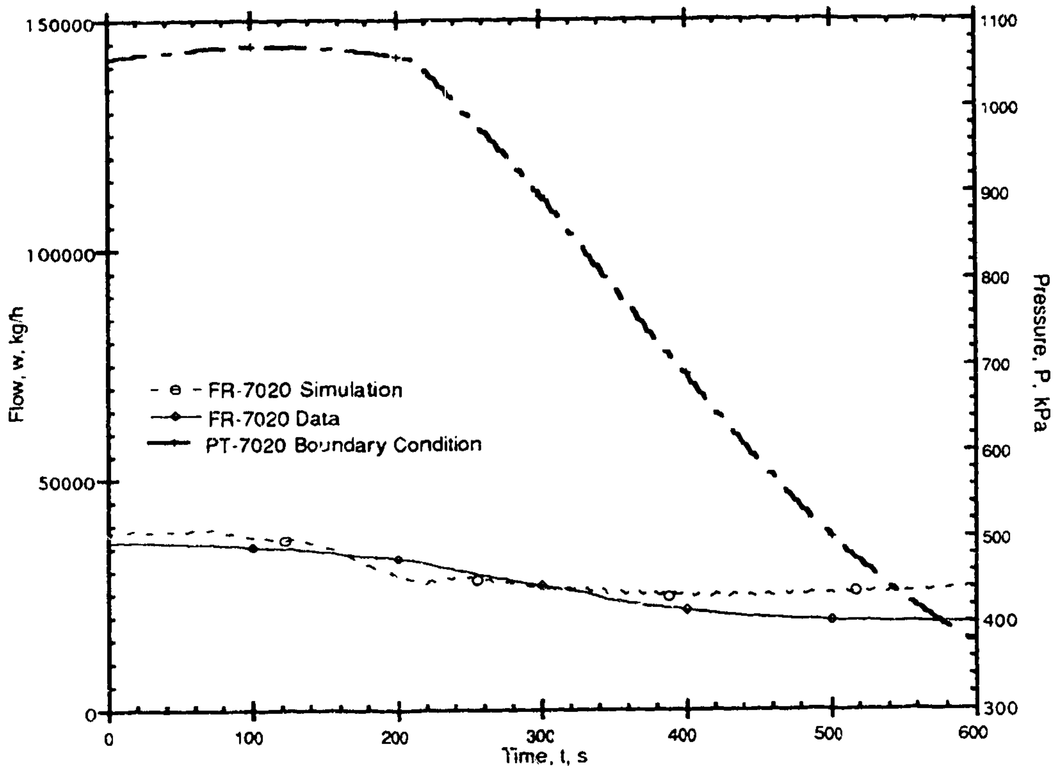

Figure 6-17 Predicted and Experimental Flow Response Comparison

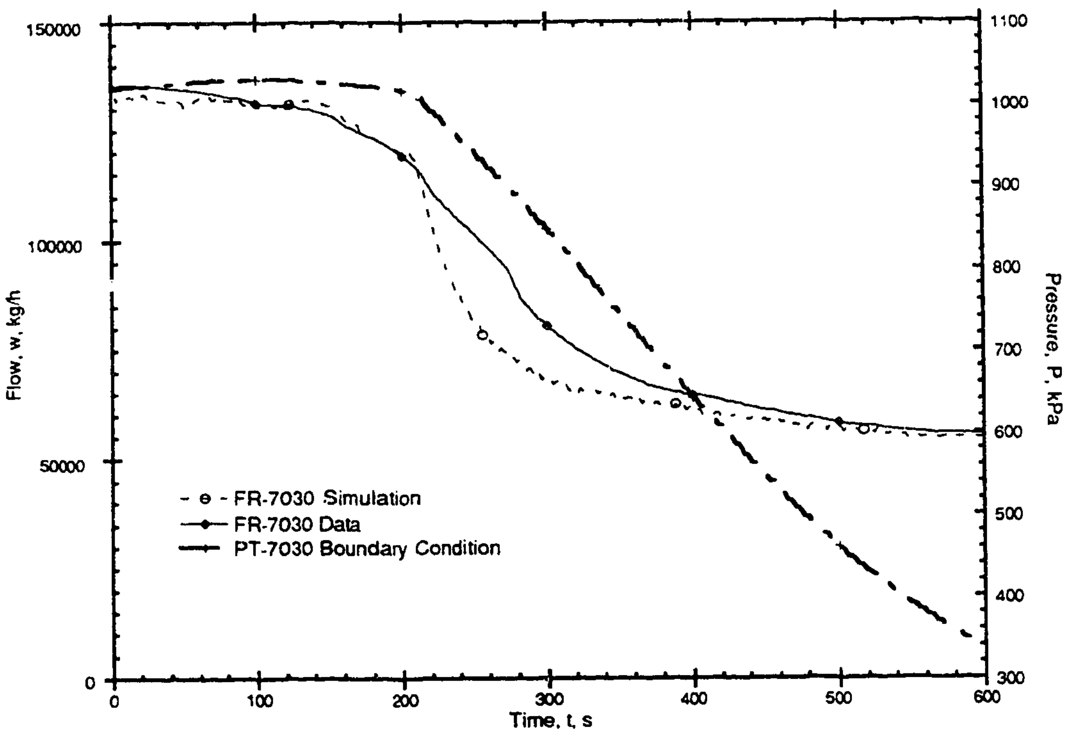

Figure 6-18 Predicted and Experimental Flow Response Comparison

Figures 6-13 and 6-14 illustrate the measured pressure (PT-5000) and temperature (TT-5017) of the steam at the exit of Boiler 5, the valve positions of both PY-7040C/D, the measured steam flow rate (FT-5000), and the simulator prediction of the flow rate at the exit of Boiler 5. The locations of these measurement points are clearly indicated in Figure 4-9 and Figure 5-1. Boiler 5 was being commissioned so its combustion controls were in the manual control mode. A block diagram of the combustion controls are given in Figure 4-2. When the controller is in the manual mode, the operator controls the signal to the final control element. In Figure 4-2 the signal that the operator will control is represented by the lines entering into the final control elements labeled as FY-5001 and FY-5002 (gas valve and air damper). The operator enters a value between 0 and 100 percent at the control computer interface. This value is transmitted to the final control element . When the control loop is in automatic control mode this 0 to 100 percent signal is calculated by the PID controllers labeled in Figure 4-2 as FRC-5001 and FRC-5002. The manual and automatic control mode convention described here will be used throughout the analysis of the Boiler 5 shutdown.

Both PY-7040C/D were in service and their master controller (PIC-7040) was in the manual mode throughout the boiler shutdown. A block diagram of this control loop is shown in Figure 4-3. These two valves were used to maintain a constant back pressure on Boiler 5 during the commissioning phase with only a slight increase in opening to both valves as shown in Figure 6-14.

The shutdown of Boiler 5 was caused by the furnace pressure exceeding safe limits. When this event occurs, the safety system immediately stops combustion in the furnace by shutting off the supply of gas and air to the boiler. This event occurred at a time of 60 seconds as illustrated in Figure 6-13. Because of the capacitance in the boiler drum and energy stored in the boiler furnace, the boiler keeps steaming even after the combustion process has stopped.

The pressure at the exit of Boiler 5 was used as one of the boundary conditions for the simulator. This pressure boundary condition is illustrated in Figure 6-13. With the pressure fixed at this entry point to the steam line network, the simulator was used to predict the steam mass flow rate at this location. The experimental and predicted flows are shown in Figure 6-13. The temperature of the steam exiting from Boiler 5, given in Figure 6-14, was used to compute the wave speed in the 6205 kPa section of the network. In this section of the network which includes the pipes labeled as P_1, P_2, and P_3, illustrated in Figure 5-1, it is assumed that a change in temperature at the boiler is immediately propagated without delay to change the temperature of the steam in a uniform fashion through all the sections of the network from Boiler 5 to the High Pressure Header No. 2. This wave speed is then combined with the wave speeds calculated in the other sections of the network to compute an average value that is used by the simulator for all sections of the network. The temperature at the exit of Boiler 5 is also used to compute the densities at valves PY-7040C/D.

As can be observed from Figure 6-13, there is close agreement between the predicted and measured steam mass flow rate in the initial portions of the response, but the difference increases with increasing elapsed time. It is significant to note that the predicted response shows the effect of the pressure disturbance caused by control valves PY-7030A/B (cf. Figure 5-1) partially being closed, as shown in Figure 6-16. The effect of this disturbance which temporarily disturbs the steady decrease in flow from Boiler 5 , which occurred at about 200 seconds of elapsed time, is also evident in the experimental data.

Most of the discrepancy between the predicted and measured rates can be attributed to a lack of detailed system information to include in the model. A check valve is installed between the exit of Boiler 5 and the entry to the steam line network. This check valve keeps steam from flowing into the boiler when the boiler is not in service. The check valve is modelled as a constant equivalent line length loss. When the steam flow is high enough this check valve will be wide open and the equivalent line length loss will be sufficient to model this component. As the steam flow starts to drop the check valve starts to close and thus provides an increasing resistance to the flow of steam. Another model error was the assumption of a constant friction factor. Both of these factors can be seen to have a large effect on the flow rate prediction towards the end of the dynamic response. As shown in Figure 6-13, the measured flow from Boiler 5 becomes zero flow at about 430 seconds while the predicted flow is still about 15,000 kg/h at 430 seconds, which does not reach zero until about 550 seconds.

Figures 6-15 and 6-16 illustrate the measured flow (FT-3000) and temperature (TT-3010) of the steam entering High Pressure Header No. 2 from Boiler 3, as well as a comparison of the prediction of the pressure (PT-6200) in High Pressure Header No. 2 with the experimental data. The valve output values for both PY-7030A/B, as mentioned previously, are shown in Figure 6-16. The locations at which the pressure, flow and temperature are measured are clearly indicated in Figure 4-10, Figure 4-12, and Figure 5-1. Boiler 3 was on line during the commissioning of Boiler 5. Its combustion control system was in the automatic control mode with the master pressure controller PIC-6200, shown in Figure 4-4, attempting to maintain the required pressure in the header and thus meet the campus steam demands. The pressure controller, PIC-7030, for the pressure reducing valves, PY-7030A/B, and the temperature controller, TIC-7030 for the desuperheater, TY-7030, were in the automatic control mode before the beginning of the transient. The pressure controller was switched to manual mode during the transient period while the desuperheating station controller remained in the automatic control mode throughout the transient period.

When the steam flow from Boiler 5 started to decrease, the pressure in the High Pressure Header No. 2, as illustrated in Figure 6-15, starts to drop so the controller, PIC-6200, then increases the flow of air and gas to Boiler 3 to increase the firing rate. This can be seen by the sharp increase in the measured steam flow from Boiler 3 during the 60 to 150 second interval as shown in Figure 6-15 before a slow increase over the remainder of the transient. This flow change occurred because the firing rate to the boiler was being increased at a faster rate than the boiler could physically handle. The feedwater supply to the boiler drum was not fast enough to maintain the water level in the drum due to the sharp increase required in steam flow. If this situation was not rectified then Boiler 3 would also shutdown because the water level in the drum would drop below a safe level. The operator stopped the increase in the firing rate to the boiler by putting the PIC-6200 controller in manual mode. By putting this controller in the manual control mode the increase in firing rate would be stopped by holding the output at the current value to the gas valve and the air vanes of Boiler 3. Once the feedwater flow to the drum and level in the drum had stabilized the operator slowly increased the firing rate to the boiler with the controller in the manual mode.

The second significant control action that had an impact on the recorded results is shown in Figure 6-16. Because of the large capacitance of the long tunnel network system and the increase in firing rate to Boiler 3, the supply pressure to the tunnel (PT-7030) illustrated in Figure 6-18 does not start dropping significantly until 200 seconds . In Figure 6-16 the valve outputs, X7030A/B, requested by the master controller (PIC-7030) start to open the control valves PY-7030A/B because the tunnel supply pressure is beginning to drop below the required pressure. The block diagram for this control loop is illustrated in Figure 4-6. Since some of the plant auxiliaries (feedwater pumps and forced draft fans) use steam turbines as their primary drivers, the operator puts the PIC-7030 controller in the manual mode and decreases the output to PY-7030A/B from approximately 65 % to 40 %. This manual control action slows the flow of steam from the plant and allows this steam to be used by the auxiliaries in the plant. The operator entered this control action as a sharp or instantaneous decrease or step change at the keyboard interface at the console computer. This request of a control signal step change is then transmitted over the data highway to the control computer. The relationship between the console and control computer is given in Section 4.5. The control computer in turn sends this step change as an electronic signal to close PY-7030A/B. The computer (CHIP computer) that collected the data used in this analysis can only record the step change given by the operator from the console computer; the data collection computer cannot record the actual position of the valve. The electronic control signal sent by the control computer is converted to a pneumatic signal by a current to pressure transducer located on the valve. The pneumatic signal then acts on an actuator connected to the valve to move the valve to the new position requested by the control computer. This current to pressure transducer and more importantly ,the actuator, have dynamics associated with them. These dynamics are associated with the force required to move the mass of the valve stem and plug, the force required to act against the stiffness of the spring inside the actuator, and the force required to act against the friction of the moving parts of the valve and the unbalanced pressure forces of the steam. These dynamics will not allow the duplication of the requested controller step input to the valve as a new valve position.

Figure 6-15 compares the predicted and measured pressure in High Pressure Header No. 2 (PT-6200). When a sharp step input was applied to the control valves PY-7030A/B with no allowance for transducer, valve, and actuator dynamics, the simulator predicted pressure fluctuation at 200 seconds was found to be much larger than the measured response. Anon (1989 A) suggests that the combination of a positioner, actuator, and a valve can be modelled as a first order system with a lag time between 5 and 30 seconds. Consequently to account for the dynamics associated with the current to pressure transducer, the actuator, and the valve, the valve closure was modelled by a first order system with a time constant of 25 seconds. The resulting valve action shown in Figure 6-16 resulted in the pressure prediction shown in Figure 6-15.

A combination of the temperature of the steam exiting Boiler 3 displayed in Figure 6-16 and the temperature of the steam exiting Boiler 5, which was assumed to undergo an adiabatic expansion across the valves PY-7040C/D, was used to calculate temperature in the 2760 kPa section of the network. An average value computed using a weighting factor provided by the steam flow from each of the boilers was used to compute the wave speed for the 2760 kPa section of the pipe network at each time step. This temperature was also used to calculate the densities needed for computation with the control valves PY-7030A/B and PY-7020A.

Figures 6-17 and 6-18 display the measured pressure at the west (PT-7020) and east (PT-7030) exit of the plant steam line network, and the predicted and measured steam flow rate at the west (FR-7020) and east (FR-7030) exit of the network. The location of the measurement points is indicated in Figures 4-11, 4-12, and 5-1. Because steam leaves the system being modelled at these two locations the pressures at these two points were selected as the boundary conditions being modelled, two boundary conditions must be provided.

The measured pressure responses in Figure 6-17 and 6-18 which show the slow fall in pressure clearly demonstrate the large capacitance of the tunnel steam supply distribution system. The tunnel system consists of approximately 13 kilometres of pipe with a diameter of 0.61 of a metre. As indicated by Figure 6-13, Boiler 5 tripped off line at approximately 60 seconds but there was no effect on the tunnel pressure until 150 seconds later or at time equal to 200 seconds. The pressure response at both exit points is approximately the same because of the connection provided by the intermediate pressure tie line illustrated in Figure 5-1. This connection will equalize the pressure at the two exit locations.

In Figure 6-17 the predicted flow to the west tunnel tracks the measured flow until about 400 seconds. After this point the deviation between the predicted and the measured values increases which is a direct result of the deviation between the predicted and measured flows from Boiler 5 presented in Figure 6-13. The higher predicted flow from Boiler 5 leads to the higher predicted flow leaving the system.

It can be observed from Figure 6-18 that the predicted flow to the east tunnel tracks the measured flow very well except for a deviation that occurs between the elapsed time from 200 to 500 seconds. The cause of this deviation can be linked to the actions of the pressure reducing control valves PY-7030A/B. As was discussed previously these control valves were closed from 65% to 40%, as illustrated from Figure 6-16, at a time of 200 seconds. As mentioned previously the closing time was simulated as being a first order with a time constant of 25 seconds relating the input sent by the control computer and the actual valve output. It was found that if the actual step change signal without the dynamics was used, the deviation between the predicted and measured steam flows in Figure 6-18 was even larger. It can be seen from Figure 6-18 that the predicted flow rate for FR-7030 almost exactly follows the control valve output X703A/B given in Figure 6-16. The simulated flow rate mirrors the response of X703A/B as a first order system with a time constant of 25 seconds while the measured flow rate for FR-7030 drops at a slower, somewhat more random manner.

The results illustrate the large effect that the valve model has on the predicted results. Both of the example comparisons given by the pressure response at 200 seconds in Figure 6-15 and the flow response at 200 seconds given Figure 6-18 show that the dynamics of the valve need to be taken into account for PY-7030A/B to more accurately model the system.

A plot of the mass balance of the system is given in Figure 6-19 to illustrate the discrepancies between the predicted and measured mass flow rates. The conservation of mass represented in Figure 6-19 is expressed as mass stored = mass entering the system - mass leaving the system

or in terms of the system in question

mass stored = (FT-1000 + FT-3000 + FT-5000) - (FR-7020 + FR-7030)

The location of these flow measurement points for developing the mass balance is shown in Figure 5-1. The measured mass balance shows that a much larger amount of steam is leaving the system during the transient than the amount of mass that is entering the system. This would coincide with the fact that one of the supply sources (Boiler 5) has been lost and the other boilers have not been able to catch up with the deficiency. The simulator predicts the same type of results, but the magnitude of the deficiency of the steam loss is much less. This is a result of the over prediction of the supply of steam from Boiler 5 by the simulator.

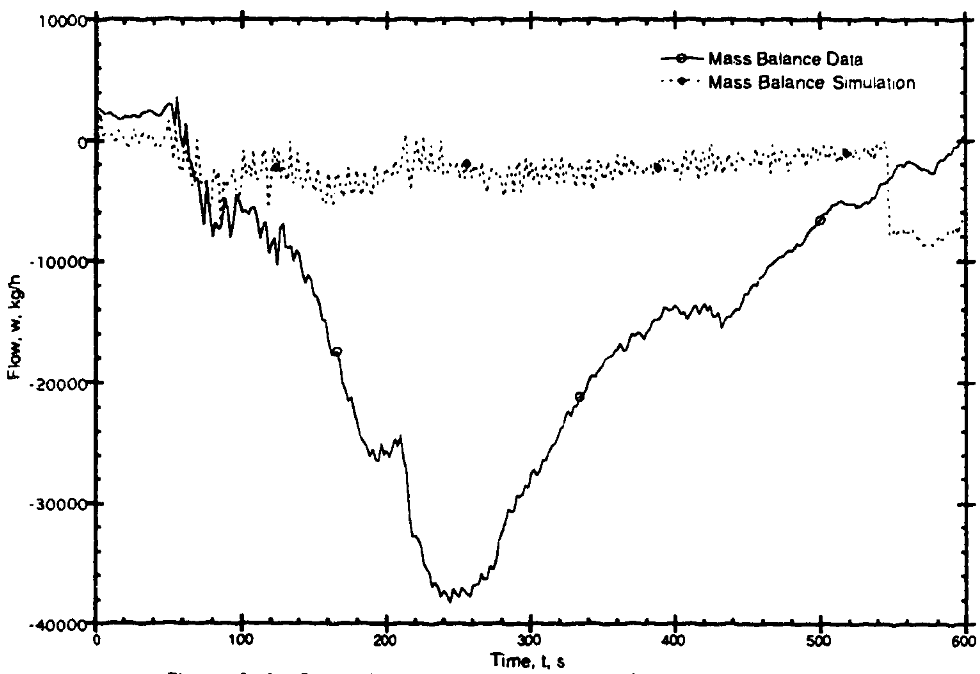

Figure 6-19 Comparison of Steam Line Network Mass Balance Predicted by the Simulator with the Measured Mass Balance

6.4.2 Transient Analysis of the Boiler 5 Shutdown: Data Set #2

The second set of experimental data, obtained with the same equipment operating except Boiler 1 was also in service, is used to assess the reliability of the simulator predicted pressure and flow rates. The steady state operating parameters for this second case are given in Table 6-3. The measured experimental data and simulated results for this shutdown of Boiler 5, caused by a faulty low combustion air signal, are shown in Figures 6-20 to 6-26.

Table 6-3: Steady State Operating Parameters for Heating Plant Transient Data Set #2

Point Tag	Steady State Value
PT-5000	6140 kPa
FT-3000	20.59 kg/s
FT-1000	4.12 kg/s
PT-7030	1030 kPa
PT-7020	1080 kPa
FT-5000	10.62 kg/s
FR-7030	25.54 kg/s
FR-7020	9.80 kg/s
CV702	150.7 (22.73 %)
CV703	109.3 (36.00%)
CV704	0.01377 (12.5%)

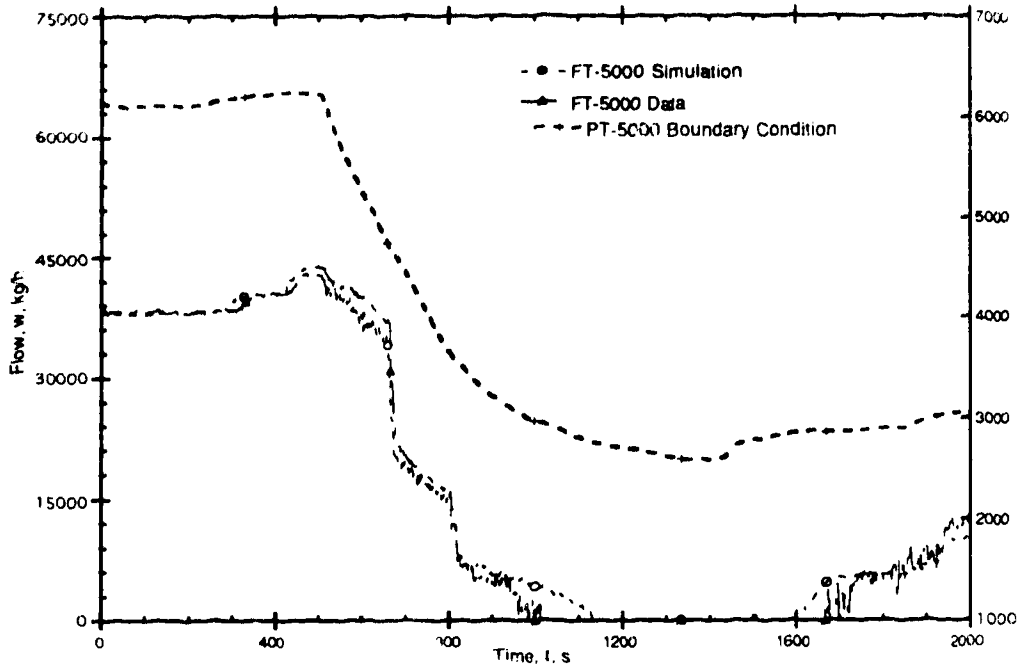

Figure 6-20 Predicted and Experimental Flow Response Comparison

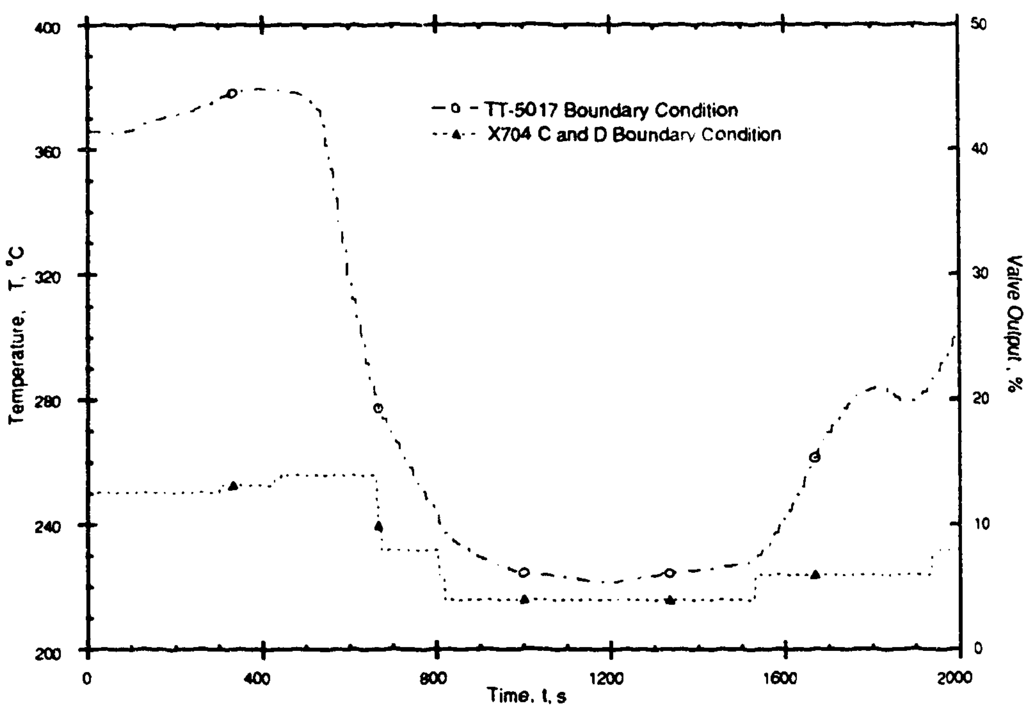

Figure 6-21 Temperature and Valve Position Boundary Conditions

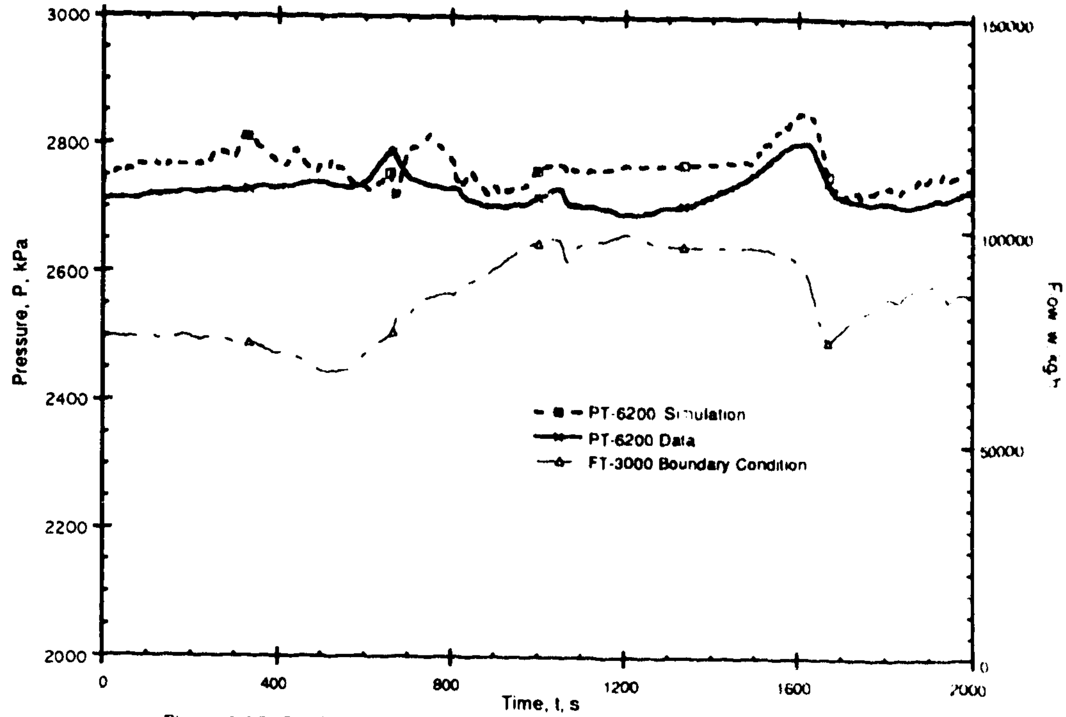

Figure 6-22 Predicted and Experimental Pressure Response Comparison

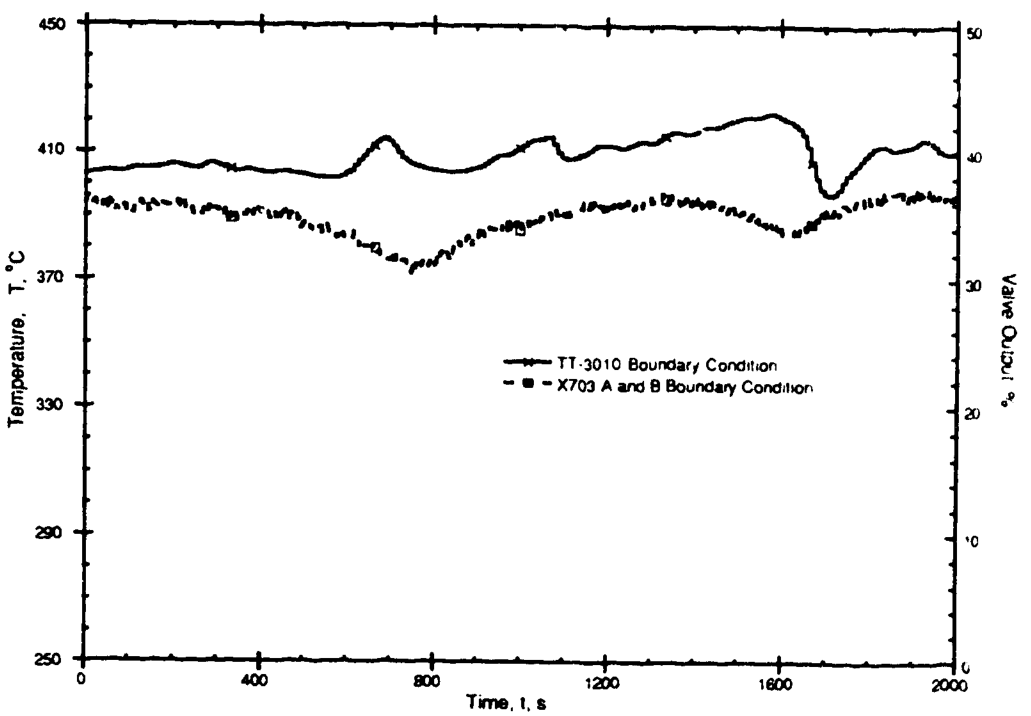

Figure 6-23 Temperature and Valve Position and Boundary Conditions

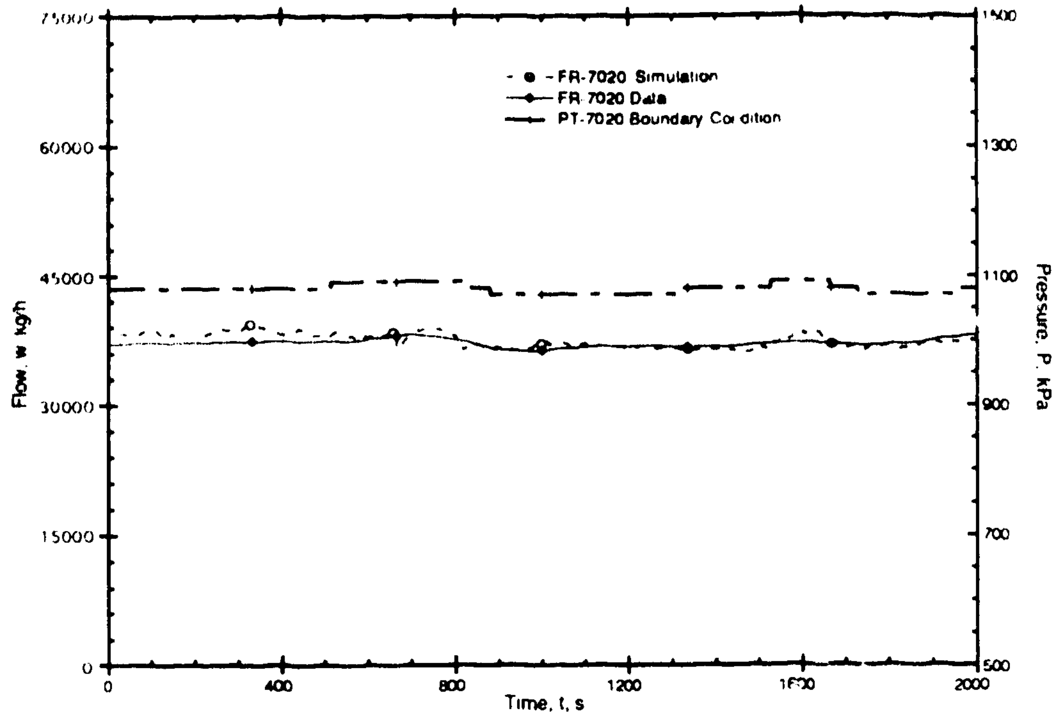

Figure 6-24 Predicted and Experimental Flow Response Comparison

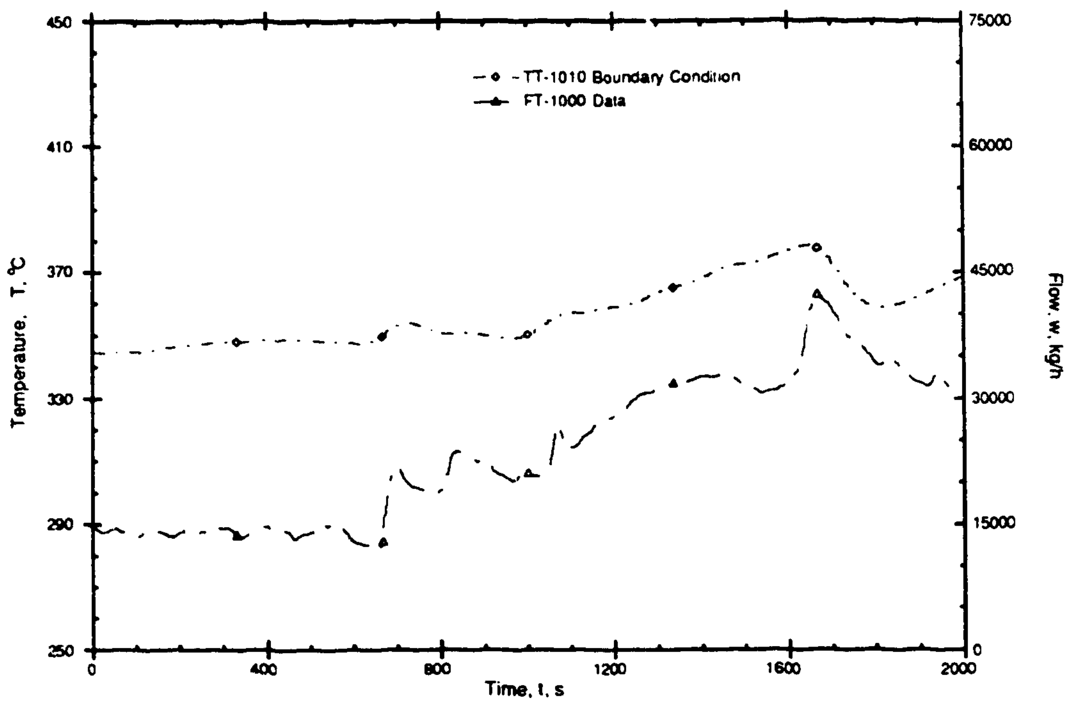

Figure 6-25 Temperature and Flow Boundary Conditions

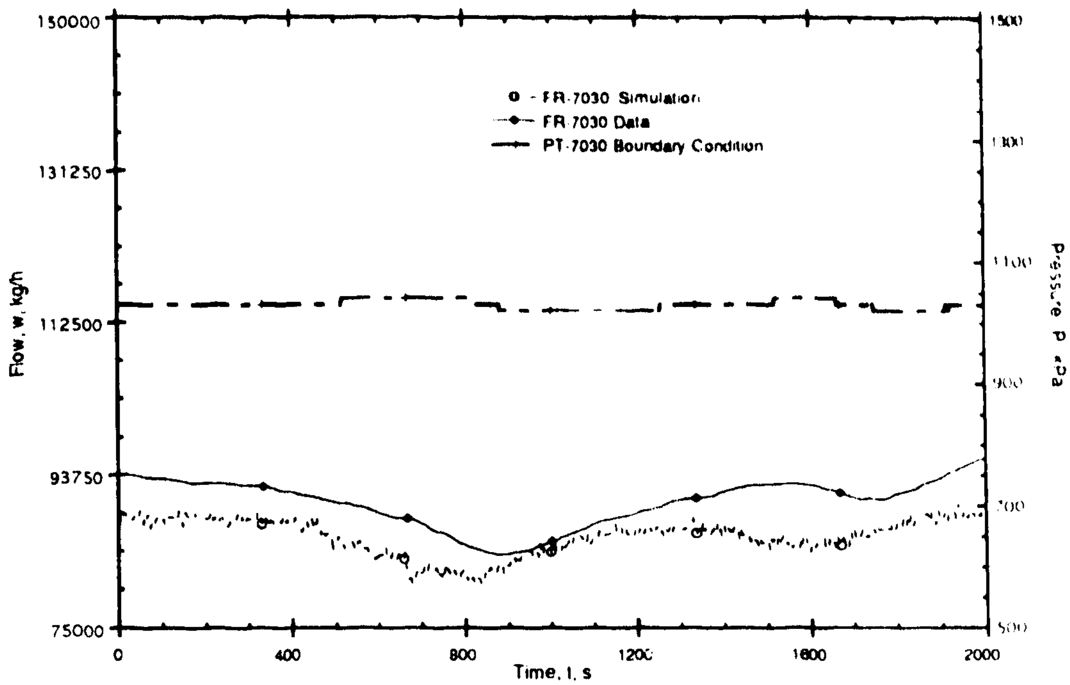

Figure 6-26 Predicted and Experimental Flow Response Comparison

Figures 6-20 and 6-21 are plots of the measured pressure (PT-5000) and temperature (TT-5017) at the exit of Boiler 5, the valve stem positions of both PY-7040C/D, as well as the predicted and measured steam flow rate (FT-5000) at the exit of Boiler 5. The locations of these measurement points are indicated in Figure 4-9 and Figure 5-1. Boiler 5 was operating at steady state with the firing control system, illustrated in Figure 4-2, in the automatic control mode. The pressure controller , PIC-7040, for the valves PY-7040C/D was in the manual control mode. The block diagram for this control loop is given in Figure 4-3. Because PIC-7040 was operating in manual mode, these valves were being held at a constant position. The pressure in the High Pressure Header No. 2 was being controlled by the master pressure controller PIC-6200.

Boiler 5 shut down at a time of about 500 seconds as illustrated in Figure 6-20. This shutdown was caused by a failure of the low combustion air flow switch which was interpreted as an unsafe condition so the boiler safety system immediately stops the flow of air and gas to the boiler which in turn stops the combustion process.

As can be seen from Figure 6-20 there is very close agreement between the predicted and measured steam flow rate at the exit of Boiler 5. The predicted results were obtained by using the measured pressure at the exit of Boiler 5 as one of the boundary conditions. The temperature of the steam at the exit of Boiler 5, shown in Figure 6-21, was used to compute the wave speed in the 6205 kPa section of the piping network and also to calculate the steam density. The valve stem position given in Figure 6-21 is used by the simulator to compute the flow coefficients for the valves PY-7040C/D which are then used with the calculated density to predict the pressure drop across the valves and the flow through the valves.

The only major deviation between the predicted and measured steam flow rates occurs just before the steam flow exiting Boiler 5 stops. This is caused by the use of a constant friction factor for the head loss in the pipes and a constant line length loss factor for the check valve between Boiler 5 and the system. The steep changes in flow rates at 650 and 800 seconds shown in Figure 6-20 correspond to the abrupt changes in the control valve output presented in Figure 6-21. It was found that neglecting the dynamics in these two control valves was a valid assumption.

This is because the actuators on the PY-7040C/D valves are of a different style to those found on the PY-7030A/B valves. The actuators on PY-7040C/D have a piston inside the actuator cylinder with an imbalance of air pressure on both sides to move the piston and thus the valve stem. This is in contrast to the actuators on the PY-7030A/B valves which have a diaphragm and a spring inside of it. Air pressure works only on one side of the actuator diaphragm against the spring force, to move the diaphragm and valve stem.

The piston type actuator is generally known to have a quicker response time. Step testing was carried out on the PY-7040C/D control valves and on control valves equipped with similar actuators to those installed on PY-7030A/B valves to compare the dynamics between these two control valves. These tests were done with the valves out of service and with equal pressure on both sides of the valve plug. A step input was provided from the controller and the resulting valve position measured as a function of time with data used to fit a first order transfer function model.

The results of these step tests verified that the in PY-7040C/D control valves do in fact have a faster response time than the other valves. The results showed that the PY-7040C/D valves had a time constant of approximately one second while the measurements done on the valves similar to PY-7030 could be modelled with a time constant of four seconds. These results justify neglecting the valve dynamics for the PY-7040 valves, but do not explain why it was necessary to add even a larger time constant to adequately characterize the dynamics of the PY-7030A/B valves, as presented in the previous section. The only explanation available is that the actual valves in service have substantially different dynamics than the valves that had the step testing performed or that actual operating conditions have a substantial effect on the dynamics of these valves.

Figure 6-22 and 6-23 display the predicted and measured (PT-6200) pressure in the High Pressure Header No. 2 in addition to the measured steam flow rate (FT-3000) and the temperature of the steam (TT-3010) at the exit of Boiler 3. Figure 6-23 also shows the control action output (X703A/B) to the PY-7030A/B valves. The locations of these measurement points are shown in Figures 4-10, 4-12, and 5-1. The master pressure controller (PIC-6200) for Boiler's 1 and 3 was operating in the automatic control mode and was being used to control the pressure in the High Pressure Header No. 2 at the time of the shut down. The block diagram for this control loop is given in Figure 4-4. This controller increases or decreases the firing rate to these boilers depending on the pressure measured by PT-6200 in the High Pressure Header No. 2. The pressure controller PIC-7030 remained in the automatic control mode throughout the duration of the transient period.

The temperature of the steam exiting Boiler 3 (TT-3010) shown in Figure 6-23 is used in the computation of the wave speed in the

2760 kPa section of the system as well as being used to calculate the density of the steam entering PY-7030A/B and PY-7020A so with the control valve action it was possible for the simulator to establish the mass flow and pressure drop across the valve.

As can be readily appreciated, the deviations in pressure in the High Pressure Header No. 2 illustrated in Figure 6-22 are not very large compared with the loss of pressure experienced in Boiler 5 shown in Figure 6-20. Obviously, the combination of Boilers 1 and 3 was large enough to accommodate the loss of steam from Boiler 5 to prevent any noticeable loss of pressure in the header. A slight deviation of approximately 50 kPa between the predicted and measured pressure curves in Figure 6-22 is too small to be explained by any physical action in the system.

Figure 6-24 shows the predicted and measured steam flow rate leaving the steam line network (FR-7020) and the recorded pressure at this point. The location of these measurement points is indicated in Figures 4-11 and 5-1. During the shut down the valve output for PY-7020A, not shown, and was kept at a constant opening of 22 %.

The pressure measured at the entrance to the West tunnel system (PT-7020) was used as a boundary condition in the simulator. Observation of the measured pressure, shown in Figure 6-24, shows even less effect from the loss of Boiler 5 than does the pressure illustrated in Figure 6-22 measured in the High Pressure Header No. 2. Consequently the variation in flow to the tunnel system is also negligible and the prediction of the flow rate by the simulator illustrated in Figure 6-24 matches this result.

Figure 6-25 provides the measured values of the steam flow (FT-1000) from Boiler 1 and the temperature of the steam (TT-1010) leaving Boiler 1 and entering High Pressure Header No. 1. The location of these measurement points is given in Figures 4-10 and 5-1. The steam flow from Boiler 1 was used as a boundary condition in the simulator. The steam temperature is averaged with the exit steam temperature from Boiler 3 and the adiabatically expanded steam temperature from Boiler 5 to compute an average steam temperature for the 2760 kPa section of the header.

Figure 6-26 shows the predicted and measured results for the steam flow (FR-7030) leaving the system. The measured pressure (PT-7030) is used as a boundary condition in the simulator. The locations of these measurement points is illustrated in Figures 4-12 and 5-1.

As was found at the other exit to the tunnel steam supply system, the pressure at this exit point did not feel the effect of the shut down to Boiler 5. This result is also reflected in the measured steam flow at this point. The predicted result deviates from the measured result by 5%. This value varies throughout the interval of interest. Again the magnitudes of the variations and the deviations between the predicted and measured results are not large enough to be attributed to any single physical part of the steam line network system.

6.5 Simulation of the Shut Down of a Steam Turbine

A steam driven turbine to be used for cogeneration will be installed and integrated into the heating plant steam line network. The commissioning of this machinery should be complete by January of 1994. A model of the steam line network including the addition of a steam driven turbine will enable the Utilities Department to analyze and develop a control strategy for the addition of this unit.

Figure 6-27 illustrates the addition of the turbine generator to the steam line network. Preliminary drawings have been provided by the design engineers to indicate the relative position of the turbine within the network and the dimensions of the piping associated with the unit. To simplify the analysis only one possible operating scenario will be examined in this work.

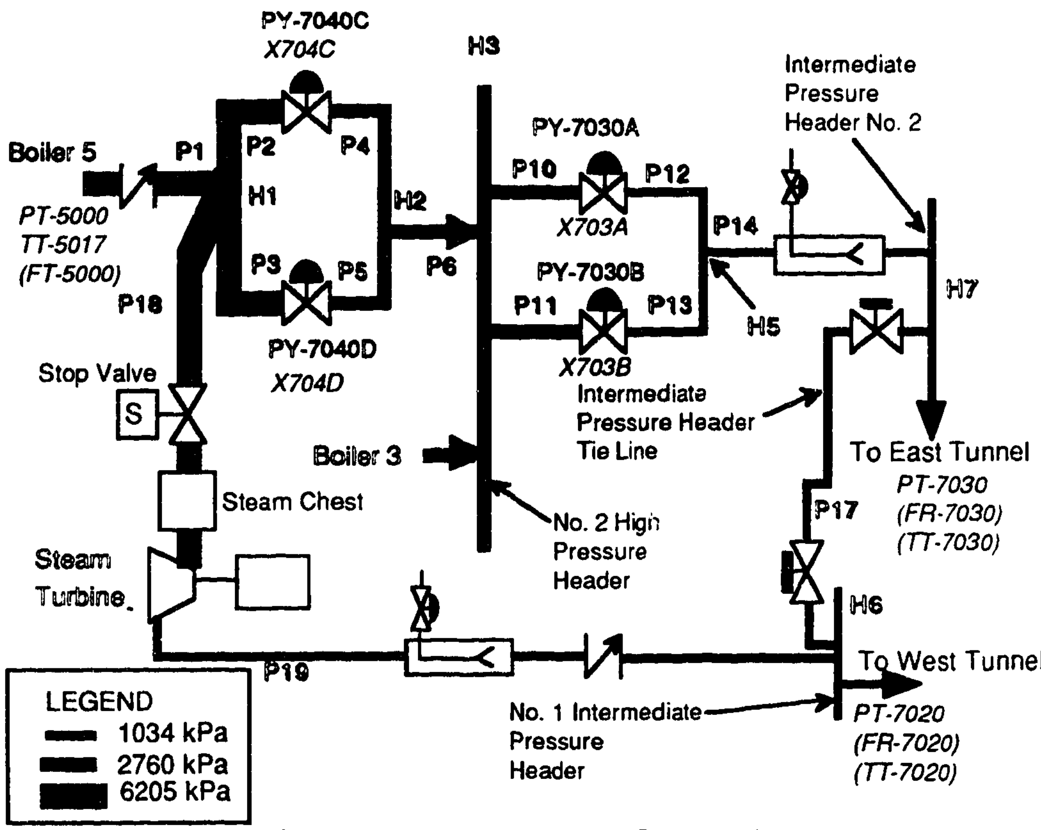

Figure 6-27 Simplified Heating Plant Steam Line Network with Steam Driven Turbine for Cogeneration

It is envisaged that only Boiler 5 will be operating to feed steam to the steam line network. The majority of the steam flow will be passing through the steam turbine to generate the maximum amount of electricity within the constraints of the amount of 1035 kPag steam required for use by the customers on the University campus. The balance of the steam will pass through PY-7040C/D and PY-7030A/B.

The control of the turbine can be defined using two separate sections: process control and safety control. The process control requires that the speed of the turbine be kept constant so that electrical power can be generated. This speed is kept constant through the use of a governor control system. The governor regulates the steam supply to the turbine through the use of the steam chest and control valves. The steam chest, illustrated in

Figure 6-27, is a finite volume located in the steam turbine housing. In this steam chest are located 5 control valves. These valves, used by the governor to control the flow of steam to the turbine, not unlike a typical process control valve which can be modulated between 0 and 100 % are either open or closed. This type of action minimizes the pressure let down across these valves so the energy is used by the turbine and not lost in a pressure drop across the valves.

The turbine is designed and operated as a back pressure turbine. In this configuration the turbine will be used similar to the PY-7030A/B and PY-7020A/B/C control valves in that the unit can be used to maintain the operating pressure at 1035 kPag in Intermediate Pressure Header No. 1. Two possible control strategies for operation with the steam turbine using the presently installed control valves are considered based on the configuration of equipment shown in Figure 6-27. Both of the control strategies will be implemented through the use of a digital turbine governor controller. This controller will make use of the feedback information provided by the shaft speed, generator load (power output), and exhaust pressure of the steam turbine to calculate the control action to the control valves and the generator set. The calculation of the control action will depend on the control strategy selected.

One control strategy would be based on the steam turbine maintaining a certain load (the amount of power produced by the generator) on the turbine with the exit pressure of the turbine not a concern. This exit or back pressure would be controlled utilizing both PY-7040C/D and PY-7030A/B. Both of the controllers for these valves would be in the automatic control mode maintaining the exit pressure in Intermediate Pressure Headers No. 1 and 2 at a nominal value of 1035 kPag. This type of arrangement is suggested by Liptak and Venczel (1988).

An alternative control strategy would be to use the pressure measurement from Intermediate Pressure Header No. 1 to the turbine governor controller (1989 B). The manufacturer of the turbine governor supplies an input to the governor controller which allows the steam turbine to maintain both a constant back pressure at the exit of the turbine as well as a constant rotational speed of the turbine. In this instance the controller for the 7040C/D valves will be in the automatic control mode while the controller for the 7030A/B valves will be in the manual control mode.

The safety system of the turbine provides the same function as the safety system of the boilers, to protect the turbine against damage that might occur to the turbine or injury to personnel because of unsafe operating conditions. Typical hazardous operating conditions for the turbine include overspeed of the turbine shaft, low oil pressure supply to the turbine bearings, high temperature in the turbine bearings, and excessive vibration of the turbine unit. When any of these conditions indicate a possible problem, the turbine stop valve shown in Figure 6-27 closes almost immediately to stop the flow of steam to the turbine. Of particular interest to the safe operation of the plant is the effect of the pressure transient that will result from the rapid closure of the steam turbine stop valve. To analyze the effect of this transient a steam turbine component was added to the steam line network model tested in the previous two sections. The assumptions given in Chapter 3 will apply to this system along with the additional assumptions

1. The boiler boundary condition will be assumed to be an infinite reservoir or mass source with a constant pressure.

2. The volume of the steam chest and thus the dynamics of the steam chest will be ignored.

3. The pressure drop across the steam turbine will be modelled as a control valve with an equivalent flow coefficient (CVTUR) used to relate the percentage turbine loading to the pressure drop and flow rate obtained through the turbine.

4. The closing of the steam turbine stop valve will be assumed to be linear.

5. The temperature at the exit of the turbine will be obtained from a steady state energy balance across the turbine utilizing the generator load, generator efficiency, and steam turbine efficiency provided by the manufacturer.

Modeling the boiler as a constant pressure source is typical of case studies found in the literature [Gorton (1978), Lee and Muldoon (1978), Luk (1975), Strong (1978), Ying and Shah (1978)]. This simplification is justified by Strong (1978) because the pressure in the steam generator changes very slowly compared with the speed at which the pressure transient takes place. In most studies the interest is in obtaining the maximum positive pressure transient to analyze the forces on the piping structures. This maximum pressure rise will occur before the pressure in the boiler rises significantly. Ying and Shah (1978) compares the constant pressure source condition at the boiler with modelling the boiler as a finite volume with an assumed amount of heat addition during the transient period. Predictions utilizing the latter boundary condition was found to show better agreement with measured. The comparison showed that the assumption of a constant pressure source boundary condition at the boiler under predicted the maximum pressure transient.

The volume of the turbine steam chest which will be installed is small in comparison with the pipe lengths and can be ignored. If the volume of the steam chest were to be considered large enough to be incorporated into the model this could be done. The approach of Luk (1975) studied the effect of a steam chest on the analysis of steam hammer for a nuclear piping system.

Assumption 3 will allow the use of the existing valve subroutine of the simulator to be included into the model. A fictitious valve coefficient was employed to describe a linear relationship between the percent turbine loading to the valve coefficient and thus the pressure drop and flow across the turbine. The assumption of a linear relationship is common for the closing of these stop valves. This relationship was then used as an input to simulate the closing of the steam turbine stop valves.

Simulation results for 3 different case studies are presented to compare the maximum pressure transients recorded near the exit of Boiler 5 and at the steam turbine stop valve. Each case examines a different loading of the turbine with the same steady state initial condition steam load from Boiler 5 (100% boiler loading). In each case it is assumed that the steam turbine will be controlling the exit pressure from the turbine at 1035 kPag. In this case PY-7040C/D would be in the automatic control mode to maintain the pressure of 2760 kPag in the high pressure headers, but for simplicity it will be assumed that the controller (PIC-7040) for the control valves will be in the manual control mode. The controller (PIC-7030) for PY-7030A/B valves will be in the manual mode and will be base loaded at a certain valve opening. The valve opening of PY-7030A/B will determine the loading of the turbine.

The steady state operating conditions for the three cases studied using the simulator are provided in Table 6-4. Case number 1 represents a loading of 73.17% of the maximum turbine load, case number 2 represents a steady state loading of 85.36% of the maximum turbine load, and case number 3 represents a steady state loading of 92.6% of the maximum turbine output. Prediction of the pressures near the exit of the Boiler and at the turbine stop valve for the 3 case studies are given in Figures 6-28 to 6-30. The closing time for the steam turbine stop valve is considered to be 0.2 seconds.

Table 6-4: Steady State Operating for Analysis of a Steam Turbine Shut Down

Point Tag	Steady State Value		
	Case 1	Case 2	Case 3
PT-5000 (kPa)	6205.0	6205.0	6205.0
PT-7030 (kPa)	1027.0	1027.0	1027.0
PT-7020 (kPa)	1076.0	1076.0	1076.0
FT-5000 (kg/h)	144000.0	144000.0	144000.0
FR-7030 (kg/h)	49350.0	31350.0	20550.0
FR-7020 (kg/h)	94650.0	112650.0	123450.0
CVTUR (Turbine Load)	0.0646 (73.17 %)	0.0755 (85.36 %)	0.0822 (92.6 %)
CV703 (Valve Position)	51.53 (20.22 %)	25.70 (11.00 %)	10.28 (3.78 %)
CV704 (Valve Position)	0.0130 (11.96 %)	0.0065 (5.97 %)	0.0026 (2.38 %)

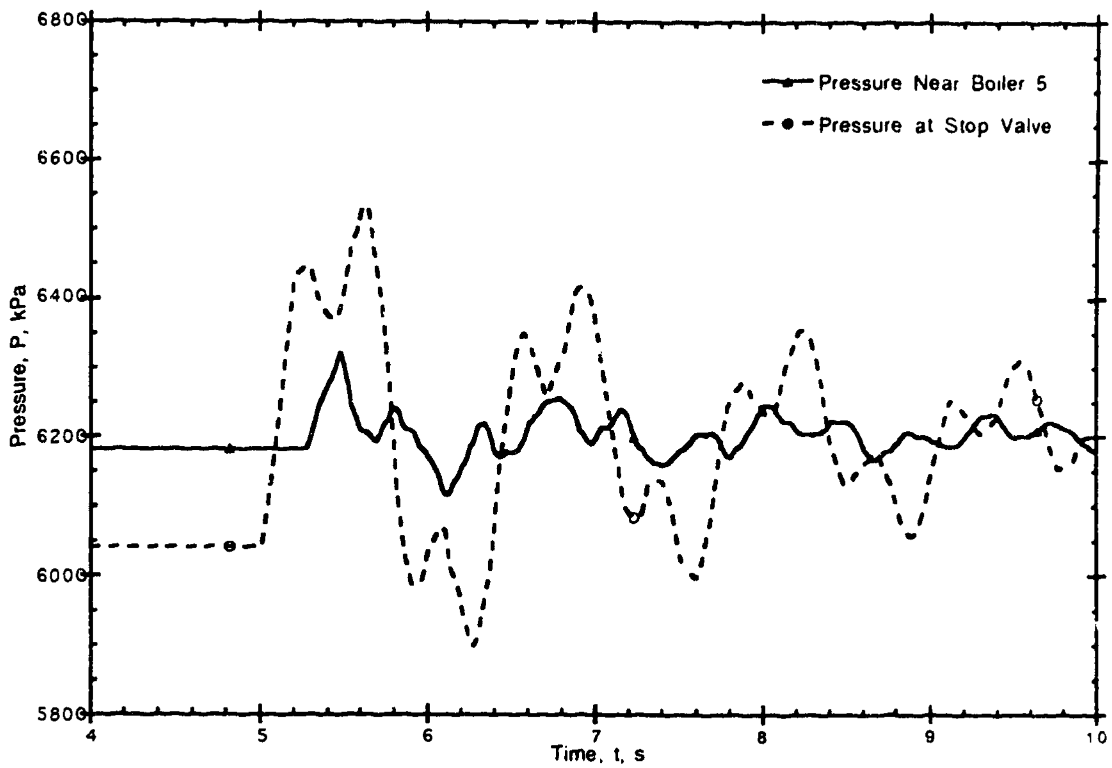

Figure 6-28 Predicted Transient Pressure Response to Turbine Trip at 73 % Turbine Operating Capacity

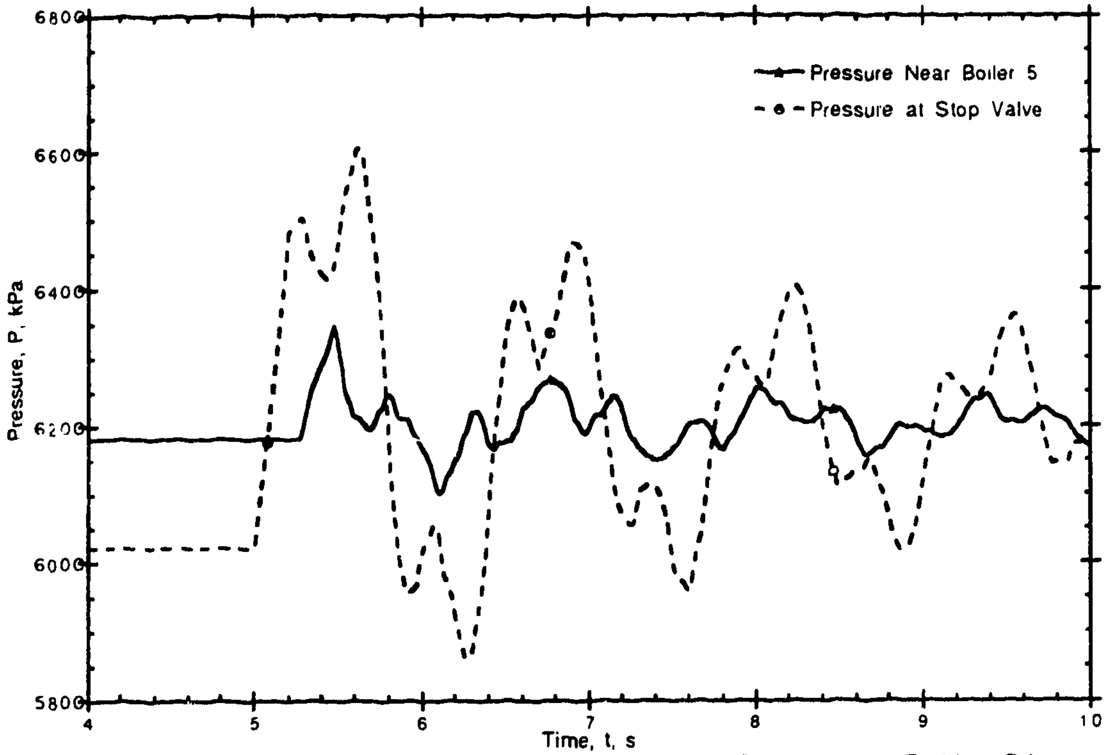

Figure 6-29 Predicted Transient Pressure Response to Turbine Trip at 85% Turbine Operating Capacity

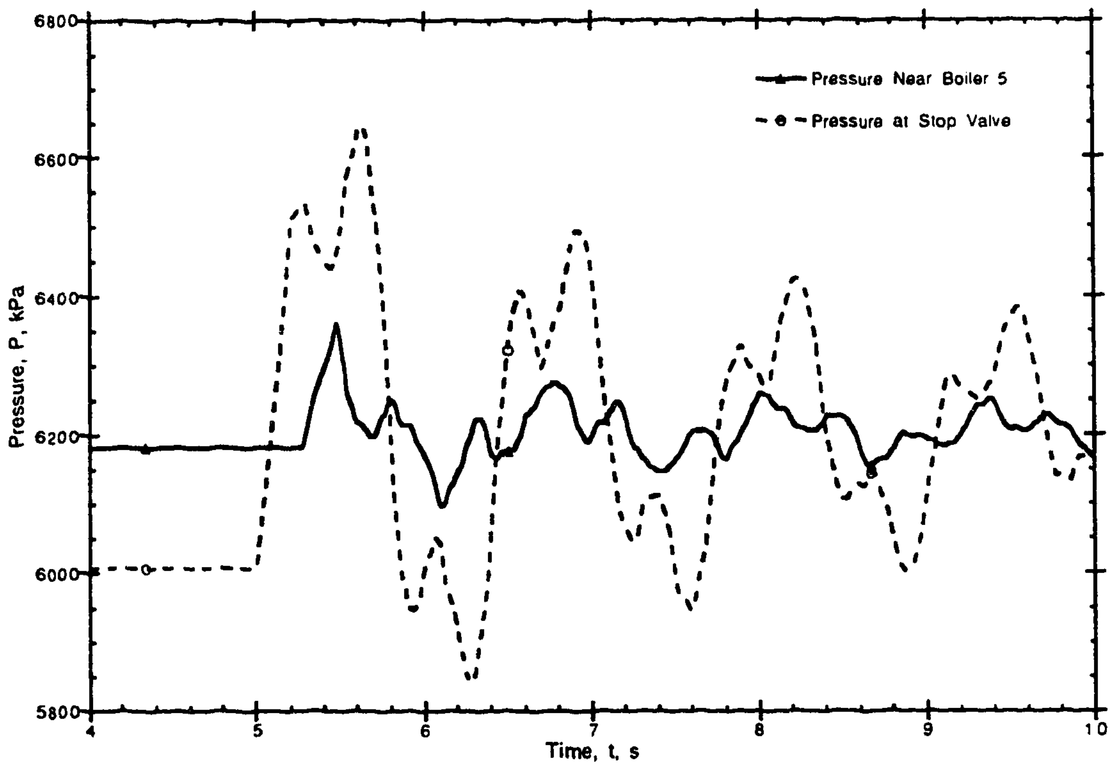

Figure 6-30 Predicted Transient Pressure Response to Turbine Trip at 92% Turbine Operating Capacity

From these simulation results, it can be seen that transients caused by different turbine loading due to different openings of the control valves PY-7040C/D and PY-7030A/B form a similar pressure wave propagation pattern. The different loading of the turbine only affect the maximum peak of the transient pressure wave. The maximum predicted transient pressures are given in Table 6-5.

Table 6-5 Maximum Positive Predicted Pressure Transient

Steady State Turbine Loading (%)	Near Boiler 5 (kPa)	At Turbine Stop Valve (kPa)
73.17	6322.0	6530.0
85.36	6343.0	6606.0
92.60	6364.0	6643.0

The steam flow is decelerated as the turbine stop valve starts to close. This deceleration of the steam causes the pressure to rise at the stop valve. A pressure wave is then transmitted upstream of this stop valve towards the header, H1. The pressure wave then splits at the header and travels towards Boiler 5 and towards PY-7040C/D. From these three points the pressure wave is then reflected back towards the stop valve. This oscillatory process will repeat itself until the wave motion is dissipated by the friction forces. The theoretical period of oscillation for this pressure wave is given by [Lee and Muldoon (1978)]

$$\theta = \frac{4 * L}{a} \tag{6-1}$$

Using the distance from the turbine stop valve and the calculated average wave speed of the system of 593 m/s the period is calculated to be 1.18 seconds. The period measured from the predicted results is 1.29 seconds, which deviates about 8.5 % from the theoretical value.

To investigate the effect of the closing time of the steam turbine stop valve, the response of system pressure was simulated, at a steady state steam turbine operating condition of 73.17% of maximum for the closing time of the stop valve was increased to 0.4

seconds. The simulation results for these conditions are given in Figure 6-31. These values compare to 6322 kPag and 6530 kPag predicted for a valve closing time of 0.2 seconds as was shown in Figure 6-28.

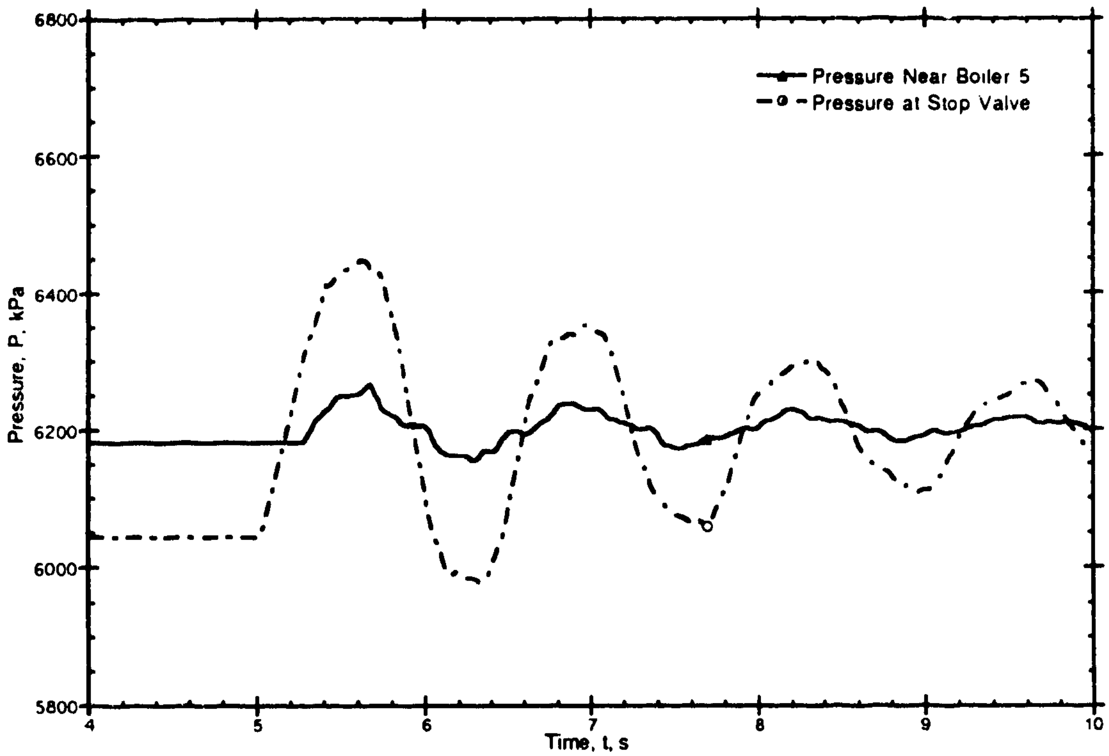

Figure 6-31 Predicted Transient Pressure Response to Turbine Trip with Stop Valve Closing Time of 0.4 seconds

Comparison of the results in this Figure with those in Figure 6-28 show that increasing the closing time of the stop valve of the steam turbine not only influences the wave shape, it also influences the magnitude of the pressure transients. The maximum positive peak pressure near Boiler 5 predicted to be 6267.0 kPag while the maximum positive peak pressure experienced at the stop valve was found to be 6449.0 kPag. These results correspond to observations made by Lee and Muldoon (1978) who has discussed the importance of the stop valve closing time on the resulting pressure transients. Moody (1990) provides a simple relationship to predict the stop valve closure time to minimize pressure surges in liquid systems while Elansary and Contractor (1990) provides a study to minimize stress in liquid piping systems for sudden closure of valves.

Chapter 7 Conclusions

In this thesis a dynamic mathematical model of a steam distribution network has been developed and implemented in a FORTRAN language simulator. The reliability of the model has been validated by successfully simulating pressures and flow rates occurring in the University of Alberta Heating Plant steam distribution network. This network consists of 5 boiler steam supply sources, three separate sections characterized by different nominal operating pressures (6205, 2760, and 1035 kPag), and two distribution nodes. Steam conditioning in the network is performed through the use of nine pressure reducing valves and four desuperheaters. Nineteen separate pipe sections are included in the model with pipe sizes ranging from 0.2 metres to 0.6 metres and equivalent pipe lengths from 12 metres to 290 metres.

The pipe mathematical model consists of two hyperbolic partial differential equations describing the isothermal flow of a compressible fluid. The simulator is composed of a steady state and a dynamic component. The validity of the assumptions used in the model development and the simulator operation have been checked against data collected from the University of Alberta Heating Plant steam distribution network and against published results. The simulator was then used to predict the pressure transients, caused by the sudden closing of a large steam turbine stop valve, that could occur in the Heating Plant.

The following points provide a more detailed explanation of the work and results provided by this thesis. These results are presented in chronological order of their development within this work.

1. Dynamic Mathematical Model

The dynamic mathematical model, developed to simulate the pressures and mass flow rates in a steam plant distribution network, consists of a pipe, a valve, a header where two or more pipes of different diameters meet, and pipe end boundary conditions. The pipe component, which was the main building block of the model, utilized the assumption of isothermal flow and thus this part of the model was described using two first order partial differential equations. The method of characteristics was used to convert the model partial differential equations into a set of four ordinary differential equations. A second order finite difference technique was applied to these equations to integrate them to obtain a solution.

Other major assumptions used in this work included use of a constant friction factor for all transient calculations, no holdup in the header sections, the properties of the compressible fluid being transported can be modelled using the ideal gas law, and an average value of the wave speed was used for every pipe in the network being modelled.

2. Steady State Solution

To obtain a dynamic solution of this mathematical model, a steady state solution of the hydraulic gradeline and the flow rates in all the pipes was needed. This solution was needed because the method of characteristics solution converges very slowly to a steady state solution . A technique to develop this steady state solution was developed. This technique utilized a spreadsheet to obtain good starting values for the solution. These starting values were then further refined by a subroutine in the simulator code. This subroutine utilized a simultaneous solution of the nonlinear steady state momentum and continuity equations and employed small movements of the pressure control valves located in the network to obtain an exact steady state solution for use by the dynamic portion of the simulator.

3. Comparison with Published Results

Simulation results obtained using the dynamic mathematical model were compared with published results. The first comparison was for published simulation results of pressure and flow transients occurring in a pipe connecting a boiler, operating at a constant pressure, to a steam turbine. A turbine stop valve, located at the entry to the steam turbine, was closed causing the transient in the system. The model in the published results consisted of a system of three partial differential equations with the main assumption of adiabatic flow conditions. The dynamic model developed in this work using the main assumption of isothermal flow under predicted the initial pressure transients in the pipe at a location near the boiler by about 3 %. Consequently, this result demonstrates that the simpler second order model used in this work was sufficient to model a transient of this severity.

Also although an isothermal model was used in this work, the wave speed was calculated using the assumption of isentropic conditions.

The model and simulator developed in this work provided a good correlation with published simulation results for transient pressures and flows occurring in a small natural gas pipeline network. The natural gas pipeline network had a constant pressure at the supply point to the system. A slowly varying delivery flow rate was required at the supply nodes of the system. With these boundary conditions, the supply flow rate and the demand pressures were predicted.

The main result from this comparison showed that utilizing an average wave speed, obtained by averaging the wave speeds from each different section of the network, in the solution of the pressure and flow rates over a network is a good assumption even when the wave speeds vary widely over the different sections of the network.

4. Comparison of Predicted Results with Data Collected in the University of Alberta Heating Plant steam line Network

The distributed control system was utilized to collect data from the University of Alberta Heating Plant. Software was written on a specialized mini computer, associated with the distributed control system, to obtain the data at predefined periodic intervals. This data were then stored in ASCII files for use in this work.

Transient pressures and flow rates predicted by the dynamic model developed in this work were compared with the data. From this comparison it was found that the dominant component of the model was the pressure reducing valves. The dynamics of the I/P transducer and the actuator for PY-7030A/B valves need to be included in the model; the dynamics of the actuator components for PY-7040C/D valves did not need to be included in the model. The reason for this lies in the different construction of the actuators for the two sets of valves. The actuator for the PY-7040C/D valves is a piston type of construction while the actuator for the PY-7030A/B valves is a diaphragm type of construction. The piston actuator has air pressure operating on both sides of the piston while the diaphragm actuator has air acting on only one side of the diaphragm. Field tests performed in this work verified that the piston type actuators have a faster response time than the diaphragm actuators when subjected to a change in input signal.

5. **Steam Turbine Shut Down Pressure Transient Predictions**

A large steam driven turbine to be used for cogeneration purposes will be added to the Heating Plant steam line network. This turbine has a stop valve that can close in 0.2 seconds should an unsafe condition at the turbine occur. Pressure transients, for different turbine loadings with a constant load from Boiler 5, that could be caused by the closing of this stop valve were predicted by the simulator.

Higher turbine loading was found to cause a higher maximum transient pressure at locations in the pipe near both the turbine and the boiler. A study of the effect of the closing time of the turbine stop valve on the pressure transients showed that slower closing resulted in smaller peak values of the pressure. These results showed that the simulator is capable of handling the severe transients caused by this type of action.

7.1 Recommendations

1. The importance of the dynamics associated with the pressure reducing valves in this network requires a more rigorous modelling approach for the valves. The actuator and valve could be modelled as a mechanical system with mass, spring, and damper components, or an empirical model could be used with step tests required to determine the model parameters.

2. The desuperheaters, located in the network, add water to the steam to drop the steam temperature before the steam leaves the Heating Plant. This work made the assumption that the mass addition of the desuperheating water was negligible. Subsequent investigations into plant logs show that addition of the desuperheating water results in 10 to

15 % extra steam production per month. This indicates that subsequent work on a system of this size can not ignore the effect of the desuperheaters.

Preliminary testing done on the system indicate that the desuperheating station can be modelled by a simple first order plus time delay transfer function.

3. The simulator should model the complete control loop including the control algorithm for any of the controllers that were operating in the automatic control mode. Included in the data collection were the control signals calculated by the controllers. This data were then used in the simulator to determine the position of the final control elements (valves). A more realistic simulation would be to have the control algorithms built into the simulator and completely simulate the automatic mode of operation of the control loop. This would increase the usefulness of the simulator for the purpose of control studies.

4. A more thorough simulation investigation needs to be undertaken directed towards minimizing the effects of the pressure transients caused by the turbine trip. Included in this investigation would be

a) Development of a control strategy that would minimize the pressure transients utilizing the existing pressure reducing valves.

b) Improve the boiler boundary condition by modelling the boiler as a finite volume with heat addition rather than a constant pressure source with infinite mass supply.

Bibliography

Ames, W. F., 1977. Numerical Methods for Partial Differential Equations (Second Edition), Academic Press, Inc., New York, New York.

Anon (1978), "Control Valve Flow Capacity Sizing", Valtek Engineering Data, pp. 1-1 - 1-8.

Anon (1980), Flow of Fluids through Valves, Fittings, and Pipe, Crane Canada Inc., Montreal, Quebec. Publication 410M (Metric Edition).

Anon (1989 A), Protuner Instruction Manual Version 3.0, Techmation Inc.

Anon (1989 B), "Digital Governors Woodward 505/505E Series: Rev 7-23-89", Woodward Governor Company.

Avallone, E. A., Baumeister III, T., (ed.), 1986. Marks' Standard Handbook for Mechanical Engineers (Ninth Edition), McGraw Hill Book Company, New York, New York.

Brown, T. D. , 1987. "Waterhammer Formulation for Pipe Networks with Check Valves", Forum on Unsteady Flow - 1987, (Rothe, P. H. , Moody, F. J. , ed.), Presented at the Winter Annual Meeting of the American Society of Mechanical Engineers, Boston, Massachusetts. FED v. 63, PVP v. 131, pp. 31 - 33.

Carver , M. B., 1980. "Pseudo Characteristic Method of Lines Solution of the Conservation Equations", Journal of Computational Physics, v. 35, pp. 57 - 76.

Carver , M. B., 1981. "Method of Lines Solution of Differential Equations Fundamental Principles and Recent Extensions", Foundations of Computer-Aided Chemical Process Design, v. 1, pp. 369 - 402.

Cheng, L. C., Bowyer, J. M., 1978. "TUBE - Transient Compressible Flow Code", Fluid Transients and Acoustics in the Power Industry, (Papadakes, C. , Scarton, H. S. , ed.), Presented at The Winter Annual Meeting of The American Society of Mechanical Engineers, San Francisco, California. pp. 31 - 35.

Elansary, A. S., Contractor, D. N., 1990. "Minimization of Stresses and Pressure Surges". ASME Journal of Pressure Vessel Technology, v. 112 pp. 311 - 316.

Fisher Controls, 1977. Control Valve Handbook (Second Edition), Fisher Controls, Marshalltown, Iowa.

Flatt, R., 1985. "A Singly-Iterative Second-Order Method of Characteristics for Unsteady Compressible One-Dimensional Flows", Communications in Applied Numerical Methods, v. 1, pp. 269 - 274.

Fox, J. A. , 1989. Transient Flow in Pipes, Open Channels and Sewers, John Wiley and Sons, New York, New York

Gorton, R. L. , 1978. "Application of Finite Difference Methods to Transient Steam Flow Problems in Power Plant Piping Systems", Fluid Transients and Acoustics in the Power Industry, (Papadakes, C. , Scarton, H. S. , ed.), Presented at the Winter Annual Meeting of the American Society of Mechanical Engineers, San Francisco, California. pp. 25 - 30.

Hancox, W. T. , Banerjee, S. , 1977. "Numerical Standards for Flow-Boiling Analysis", Nuclear Science and Engineering, 1977 ,v. 64, pp. 106 - 123.

Hindmarsh, A. C., 1974. GEAR: Ordinary Differential Equation System Solver, Lawrence Livermore National Laboratory Report UCID-30001, Rev. 3.

Hindmarsh, A. C., 1982. ODEPACK, A Systemized Collection of ODE Solvers, Lawrence Livermore National Laboratory Report UCRL-88007.

Lee, M. Z., Muldoon, J. B. , 1978. "Recorded Pressure Surges After Turbine Trips", Fluid Transients and Acoustics in the Power Industry, (Papadakes, C. , Scarton, H. S., ed.), Presented at the Winter Annual Meeting of the American Society of Mechanical Engineers, San Francisco, California. pp. 17 - 23.

Liptak, B. G., Venczel, K. (ed.), 1985. Instrument Engineers' Handbook (Revised Edition), Chilton Book Company, Radnor, Pennsylvania.

Luk, C. , 1975. "Effects of the Steam Chest on Steamhammer Analysis for Nuclear Piping Systems", ASME Paper No. 75 - PVP - 61.

IMSL, 1989. IMSL Math/Library, User's Manual v1.1, IMSL, Inc. Houston, Texas.

Instrument Society of America, 1985. ISA-S75.01 Flow Equations for Sizing Control Valves, Instrument Society of America, Research Triangle Park, North Carolina.

Miner, E. W., Skop, R. A., 1982. "Application of Two-Step Integration Procedures for Hyperbolic Equations", Presented at The 10th IMACS World Congress on System Simulation and Scientific Computation, August, pp. 85 - 88.

Moody, F. J., 1973. "Time - Dependent Pipe Forces Caused by Blowdown and Flow Stoppage", Journal of Fluids Engineering, Transactions of the ASME, 1990, pp. 422 - 428.

Moody, F. J., 1990. "Unsteady Fluid Mechanics Examples from Reactor and Containment Systems", Winter Annual Meeting of ASME, pp. 9 - 13.

Modisette, J. L., Nicholas, R. E., Whaley, R. S. Jr., 1984 "A Comparison of Transient Pipeline Flow Models and Features", Pipeline Simulation Interest Group Annual Meeting , October 18 - 19.

Nicholas, R. E. , 1990. "Leak Detection on Pipelines in Unsteady Flow", Forum on Unsteady Flow, American Society of Mechanical

Engineers, Fluids Engineering Division (Publication) FED. v 102 New York pp. 23 - 25.

Niessner, H. , 1980. "Comparison of Different Numerical Methods for Calculating One-Dimensional Unsteady Flows", Lecture No. 16 of Unsteady One-Dimensional Flows in Complex Networks and Pressurized Vessels, Lecture Series 190-81, Von Karman Institute for Fluid Dynamics, Belgium.

Perry, R. H., Green, D. W., Maloney, J. O., (ed.), 1984. Perry's Chemical Engineers' Handbook (Sixth Edition), McGraw Hill Book Company, New York, New York.

Payne, R. L. , 1989. "A Model that Predicts Steady-State Hydraulic Profiles in Flare/Relief Discharge Piping", Pipeline Dynamics and Valves - 1989, American Society of Mechanical Engineers, Pressure Vessels and Piping Conference, pp. 95 - 106.

Picard, D. J., Bishnoi, P. R. , 1988. "The Importance of Real-Fluid Behavior and Nonisentropic Effects in Modeling Decompression Characteristics of Pipeline Fluids for Application in Ductile Fracture Propagation Analysis", The Canadian Journal of Chemical Engineering, v66 February, 1988, p 3 - 12.

Richtmeyer, R. D. , Morton, K. W. , 1967. Difference Methods For Initial-Value Problems (Second Edition), Interscience Publishers, New York, New York.

Rogers, G. F. C. , Mayhew, Y. R., (ed.), 1981. Thermodynamic and Transport Properties of Fluids (Third Edition), Basil Blackwell Publisher, Great Britain.

Safwat, H. H., 1976. "Analysis of the Safety Relief Valve Discharge Transients of a Boiling Water Reactor", 2nd International Conference on Pressure Surges, BHRA Fluid Engr.

Samra, R. S. , 1978. "Pressure Surges in Power Plant Hydraulic Systems", Fluid Transients and Acoustics in the Power Industry, (Papadakes, C. , Scarton, H. S. , ed.), Presented at the Winter Annual Meeting of the American Society of Mechanical Engineers, San Francisco, California. pp. 37 - 43.

Sod, G. A., 1978. "A survey of Several Finite Difference Methods for Systems of Nonlinear Hyperbolic Conservation Laws", Journal of Computational Physics, v. 27, pp. 1 - 31.

Strong, B. R. , 1978. "Fluid Transient Load Generation for Dynamic Analysis of Power Plant Piping Systems", Fluid Transients and Acoustics in the Power Industry, (Papadakes, C. , Scarton, H. S. , ed.), Presented at the Winter Annual Meeting of the American Society of Mechanical Engineers, San Francisco, California. pp. 149 - 160.

Wang , Y. , 1987. Extension of the Pseudo Characteristic Method of Lines to Simulation of Multiphase Flow in Pipes and Pipe Networks, Ph. D. Thesis, Lehigh University.

Watton, J. , 1983. "The Simulation of Transmission Line Dynamics in Non-Linear Electrohydraulic Systems", Fluid Transmission Line Dynamics 1983, (Frank, M. E. , Drzewiecki, T. M. , ed.), Presented at the Winter Annual Meeting of the American Society of Mechanical Engineers, Boston, Massachusetts. pp. 98 - 112.

Wylie, E. B. , Streeter, V. L. , 1983. Fluid Transients, FEB Press, Ann Arbor, Michigan.

Ying, S. P., Shah, V. J., 1978. "Transient Pressure in Boiler Steam Lines", Fluid Transients and Acoustics in the Power Industry, (Papadakes, C. , Scarton, H. S. , ed.), Presented at the Winter Annual Meeting of the American Society of Mechanical Engineers, San Francisco, California. pp. 13 - 16.

Yow , W. , 1971. Analysis and Control of Transient Flow in Natural Gas Piping Systems, Ph. D. Thesis, Lehigh University.

Zucrow, M. J.. , Hoffman, J. D. , 1976. Gas Dynamics, v. 1 and 2, John Wiley and Sons, Inc., New York, New York.

Appendix A Method of Characteristics Solution

In order to gain some insight into some of the problems involved in obtaining a numerical solution of the model hyperbolic partial differential equations, an understanding of the nature or "characteristics" of these equations is needed. Partial differential equations that occur in engineering and science can be generally be classified into two categories. The first category being an equilibrium or boundary value problem. These are steady state problems where the solution of a differential equation is sought. Generally boundary values are supplied around the domain of interest and the interior points are allowed to reach steady state. The governing differential equations for these types of problems are elliptical.

The other main category of partial differential equations are the propagation problems. In these problems all the initial conditions are supplied. Alongside these initial conditions boundary values are supplied on either side. These boundary values then serve to march or guide the solution forward from the initial condition. The governing partial differential equations for this type of problem are either parabolic or hyperbolic in nature.

We identify the type of partial differential equations through the use of characteristics or eigenvalues. For a first order partial differential equation the value of the characteristic determines the type of partial differential equation. If the characteristics are imaginary, real and equal, or real and distinct, the equations are classified as elliptical, parabolic, or hyperbolic respectively.

If the partial differential equations are hyperbolic the method of characteristics can be employed to obtain a numerical solution. Good description of the method of characteristics are provided by Zucrow and Hoffman (1976), Wang (1987), Ames (1977), Hancox and Banjeree (1977), and Wylie and Streeter (1983). Physically, characteristics represent the path of propagation of information of a physical disturbance. Along these characteristics the derivatives of certain physical properties are discontinuous while the properties themselves are continuous. It is this discontinuous nature of the solution that gives rise to difficulties when standard numerical techniques are employed.

From a mathematical standpoint, characteristics represent curves along which the governing partial differential equations can be represented by ordinary differential equations. These ordinary differential equations are valid only along the characteristic curves.

To obtain a mathematical representation of the method of characteristics, we consider a function y(x,t) given by the following first order partial differential equation of the form

$$a\frac{\partial y}{\partial t}+b\frac{\partial y}{\partial x}=c \tag{A-1}$$

where the coefficients a and b and the term c may be functions of the independent variables x and t and the dependent variable y. We rearrange equation (A-1) to obtain

$$a\left(\frac{\partial y}{\partial t}+\frac{b}{a}\frac{\partial y}{\partial x}\right)=c \quad . \tag{A-2}$$

Since y is a function of both x and t and assuming y is a continuous function we may write the following total differential dy as

$$dy=\frac{\partial y}{\partial t}dt+\frac{\partial y}{\partial x}dx \ . \tag{A-3}$$

Rearranging equation (A-3) we obtain

$$\frac{dy}{dt}=\left(\frac{\partial y}{\partial t}+\frac{\partial y}{\partial x}\frac{dx}{dt}\right) \quad . \tag{A-4}$$

comparing the terms in brackets in equations (A-2) and (A-4), we can obtain the following equation

$$\frac{dx}{dt} = \frac{b}{a} = \lambda \tag{A-5}$$

We then define equation (A-5) as the characteristic equation (characteristic for short) which has a slope that is a function of x, t, and y because a and b are functions of these same variables. These characteristics are also known as the eigenvalues of the equation.

If we then replace the bracketed term in equation (A-2) by the left hand side of equation (A-4) we obtain the following ordinary differential equation

$$a\frac{dy}{dt} = c\ . \tag{A-6}$$

Equation (A-6) is commonly known as the compatibility equation. Because of the definition given by equation (A-5), equation (A-6) is only valid along the characteristic given by equation (A-5).

Because a, b, and c are usually complicated functions of x, t, and y, a numerical solution of equations (A-5) and (A-6) is needed. Initial values of y must first be obtained and then the solution is marched forward in time using a finite difference form of the characteristic and compatibility equations.

The isothermal model for compressible transient fluid flow is given by equations (3-5) and (3-21). Wylie and Streeter (1983), Fox (1989), Yow (1971), and Zucrow and Hoffman (1976)all contain a good methodology for converting a second order system of hyperbolic equations to a set of ordinary differential equations. To begin an auxiliary function is created from equations (3-5) and (3-21) through the use of an unknown multiplier λ . This function is given by

$$\lambda\left(\frac{\partial P}{\partial t}+\frac{a^2}{A}\frac{\partial w}{\partial x}\right)+\frac{1}{A}\frac{\partial w}{\partial t}+\frac{\partial P}{\partial x}+\frac{f\,w^2\,a^2}{2\,P\,D\,A^2}=0 \tag{A-7}$$

Rearranging equation (A-7) we obtain

$$\frac{1}{A}\left(\lambda\, a^2 \frac{\partial w}{\partial x} + \frac{\partial w}{\partial t}\right) + \lambda \left(\frac{\partial P}{\partial t} + \frac{1}{\lambda}\frac{\partial P}{\partial x}\right) + \frac{f\, w^2\, a^2}{2\, P\, D\, A^2} = 0 \qquad \text{(A-8)}$$

Following the procedure outlined above, the total differential for both the mass flow rate and the pressure can be written as

$$\frac{dw}{dt} = \frac{\partial w}{\partial x}\frac{dx}{dt} + \frac{\partial w}{\partial t} \qquad \text{(A-9)}$$

$$\frac{dP}{dt} = \frac{\partial P}{\partial x}\frac{dx}{dt} + \frac{\partial P}{\partial t} \qquad \text{(A-10)}$$

The following definition is made

$$\frac{dx}{dt} = \lambda\, a^2 = \frac{1}{\lambda} \qquad \text{(A-11)}$$

therefore

$$\lambda = \pm\frac{1}{a} \qquad \text{(A-12)}$$

With this definition ,the first term in brackets in equation (A-8) corresponds to equation (A-9) and the second term in brackets in equation (A-8) corresponds to equation (A-10). The following ordinary differential equation can then be written

$$\frac{1}{A}\frac{dw}{dt} + \lambda\frac{dP}{dt} + \frac{f\, w^2\, a^2}{2\, P\, D\, A^2} = 0 \qquad \text{(A-13)}$$

subject to the constraint that

$$\frac{dx}{dt} = \pm\, a \qquad \text{(A-14)}$$

Equation (A-14) defines the characteristic lines along which the ordinary differential equations or compatibility equations given by equation (A-13) are true. For the positive value of "a" equation (A-

14), the positive characteristic and compatibility equations are defined as C^+

$$\frac{1}{A}\frac{dw}{dt} + \frac{1}{a}\frac{dP}{dt} + \frac{f\,w^2\,a^2}{2\,P\,D\,A^2} = 0 \qquad \text{(A-15)}$$

$$dx = +\,a\,dt \qquad \text{(A-16)}$$

and for the negative value of "a" from equation (A-14), the negative characteristic and compatibility equations are formed and defined as C^-

$$\frac{1}{A}\frac{dw}{dt} - \frac{1}{a}\frac{dP}{dt} + \frac{f\,w^2\,a^2}{2\,P\,D\,A^2} = 0 \qquad \text{(A-17)}$$

$$dx = -\,a\,dt \qquad \text{(A-18)}$$

Appendix B Valve Model Parameters

The valve coefficient is the main parameter in the valve model. It relates the valve stem position to the pressure drop and the flow through the control valve. This valve coefficient can be obtained from the valve supplier or it can be established from steady state plant data. In this work both sources were used to obtain these coefficients. The valve coefficients vs. valve stem position for PY-7030A/B, shown in Figure 5-1, were obtained from **Fisher Controls** and are given in Table B-1. These coefficients are used for the valve coefficient in equation 3-37. The valve coefficient vs. valve stem position for PY-7040C/D were obtained from steady state operating data and are given in Table A-2. These valve coefficients are used with equation 3-38.

The valve flow characteristic describes the change in the valve stem position to a change in the flow across the valve with a constant pressure drop across the valve. Typical flow characteristics include quick opening, linear, and equal percentage [Fisher Controls (1977)]. All of the valve flow characteristics in the heating plant steam line network are linear. For a constant pressure drop across the valve, the flow rate is directly proportional to the valve stem position.

Table B-1 Valve Coefficients for PY-7030A/B

Valve Opening (% of Maximum Valve Travel)	10	20	30	40	50
C_V	23.2	51.0	80.6	111.0	141.0

Valve Opening (% of Maximum Valve Travel)	60	70	80	90	100
C_V	173.0	211.0	254.0	299.0	340.0

Table B-2 Valve Coefficients for PY-7040C/D

Valve Opening (% of Maximum Valve Travel)	10.0	11.0	12.6	34.0
Cvm	0.01097	0.01168	0.01409	0.03702

Valve Opening (% of Maximum Valve Travel)	39.4	42.0	45.5	47.5
Cvm	0.04367	0.04657	0.05006	0.05173

Valve Opening (% of Maximum Valve Travel)	48.3	49.4	50.4
Cvm	0.05245	0.05338	0.05485

Appendix C Equivalent Lengths for the Main Pipes in the Heating Plant Steam Line Network

To allow for the static pressure drop caused by various restrictions to flow in the line, an equivalent steady state factor (L/D) is used. This factor is the equivalent length of the pipe expressed in pipe diameters of straight pipe that causes the same pressure drop as the restriction [Anon (1980)]. The equivalent length factors representing the restrictions occurring in the Heating Plant steam line network are given in Table C-1 [Baumeister, (1986)].

Table C-1 Equivalent Lengths in Pipe Diameters for Various Valves and Fittings

Device	L/D
Gate Valve	13
Swing Check Valve	135
90 degree Elbow	30
45 degree Elbow	16
Flow Thru Run Tee	20
Flow Thru Branch Tee	60
Flow Nozzle	135
Orifice Plate	150
Sudden Enlargement *	10
Sudden Contraction **	20

*: Based on an enlargement of 0.2 to 0.25 metre and a friction factor of 0.015.

**: Based on a contraction of 0.25 to 0.2 metre and a friction factor of 0.015.

The apparent line lengths (actual line lengths plus equivalent lengths for restrictions) for the pipes in the Heating Plant are given in Table C-2.

Table C-2 Apparent Line Lengths for Pipes in the Heating Plant Steam Line Network

Pipe #	1		2		3		4	
	Number	Equivalent Length, m	Number	Equivalent Length, m	Number	Equivalent Length, m	Number	Equivalent Length, m
Physical Length, m	14.7	14.7	1.7	1.7	2.8	2.8	2.8	2.8
Diameter, m	0.2	-	0.2	-	0.2	-	0.2	-
Elbows (90 degree)	3	18	0	0	1	6	1	6
Elbows (45 degree)	0	0	0	0	0	0	0	0
Gate Valves	2	5.2	1	2.6	1	2.6	1	2.6
Tee (Flow Through Run)	0	0	1	4	0	0	0	0
Tee (Flow Through Branch)	0	0	0	0	1	12	1	12
Check Valves	1	27	0	0	0	0	0	0
Flow Nozzles	1	27	0	0	0	0	0	0
Orifice Plates	0	0	0	0	0	0	0	0
Contractions	1	4	2	8	2	8	2	8
Enlargements	0	0	0	0	0	0	0	0
Apparent Length, m	-	**95.9**	-	**16.3**	-	**31.4**	-	**31.4**

Table C-2 (Continued) Apparent Line Lengths for Pipes in the Heating Plant Steam Line Network

Pipe #	5		6		7		8	
	Number	Equivalent Length, m	Number	Equivalent Length, m	Number	Equivalent Length, m	Number	Equivalent Length, m
Physical Length, m	1.7	1.7	56.3	56.3	29	29	53.9	53.9
Diameter, m	0.2	-	0.3	-	0.3	-	0.25	-
Elbows (90 degree)	0	0	11	99	8	72	5	37.5
Elbows (45 degree)	0	0	2	9.6	0	0	0	0
Gate Valves	1	2.6	1	3.9	2	7.8	2	6.5
Tee (Flow Through Run)	1	4	0	0	0	0	0	0
Tee (Flow Through Branch)	0	0	1	18	1	18	2	30
Check Valves	0	0	0	0	1	40.5	0	0
Flow Nozzles	0	0	0	0	0	0	0	0
Orifice Plates	0	0	0	0	1	45	0	0
Contractions	0	0	0	0	0	0	0	0
Enlargements	2	4	1	3	0	0	0	0
Apparent Length, m	-	**12.3**	-	**189.8**	-	**212.3**	-	**127.9**

Table C-2 (Continued) Apparent Line Lengths for Pipes in the Heating Plant Steam Line Network

Pipe #	9		10		11		12	
	Number	Equivalent Length, m	Number	Equivalent Length, m	Number	Equivalent Length, m	Number	Equivalent Length, m
Physical Length, m	53.9	53.9	3.8	3.8	3.8	3.8	1	1
Diameter, m	0.4	-	0.2	-	0.2	0	0.2	-
Elbows (90 degree)	5	60	1	6	1	6	0	0
Elbows (45 degree)	0	0	2	6.4	2	6.4	0	0
Gate Valves	2	10.4	1	2.6	1	2.6	1	2.6
Tee (Flow Through Run)	1	8	0	0	0	0	0	0
Tee (Flow Through Branch)	0	0	1	12	1	12	1	12
Check Valves	0	0	0	0	0	0	0	0
Flow Nozzles	0	0	0	0	0	0	0	0
Orifice Plates	0	0	0	0	0	0	0	0
Contractions	1	20.8	0	0	0	0	0	0
Enlargements	1	26.4	0	0	0	0	0	0
Apparent Length, m	-	**179.5**	-	**30.8**	-	**31.8**		**15.6**

Table C-2 (Continued) Apparent Line Lengths for Pipes in the Heating Plant Steam Line Network

Pipe #	13		14		15		16	
	Number	Equivalent Length, m	Number	Equivalent Length, m	Number	Equivalent Length, m	Number	Equivalent Length, m
Physical Length, m	1	1	28	28	12	12	24.4	24.4
Diameter, m	0.2	-	0.6	-	0.2	-	0.3	-
Elbows (90 degree)	0	0	0	0	1	6	4	36
Elbows (45 degree)	0	0	3	28.8	0	0	0	0
Gate Valves	1	2.6	1	7.8	1	2.6	2	7.8
Tee (Flow Through Run)	0	0	2	24	0	0	0	0
Tee (Flow Through Branch)	1	12	0	0	1	12	1	18
Check Valves	0	0	0	0	0	0	0	0
Flow Nozzles	0	0	0	0	0	0	0	0
Orifice Plates	0	0	0	0	0	0	0	0
Contractions	0	0	0	0	0	0	0	0
Enlargements	0	0	0	0	0	0	0	0
Apparent Length, m	**-**	**15.6**	**-**	**88.6**	**-**	**32.6**	**-**	**86.2**

Table C-2 (Continued) Apparent Line Lengths for Pipes in the Heating Plant Steam Line Network

Pipe #	17		18		19	
	Number	Equivalent Length, m	Number	Equivalent Length, m	Number	Equivalent Length, m
Physical Length, m	1	1	28	28	12	12
Diameter, m	0.2	-	0.6	-	0.2	-
Elbows (90 degree)	0	0	0	0	1	6
Elbows (45 degree)	0	0	3	28.8	0	0
Gate Valves	1	2.6	1	7.8	1	2.6
Tee (Flow Through Run)	0	0	2	24	0	0
Tee (Flow Through Branch)	1	12	0	0	1	12
Check Valves	0	0	0	0	0	0
Flow Nozzles	0	0	0	0	0	0
Orifice Plates	0	0	0	0	0	0
Contractions	0	0	0	0	0	0
Enlargements	0	0	0	0	0	0
Apparent Length, m	-	**15.6**	-	**88.6**	-	**32.6**